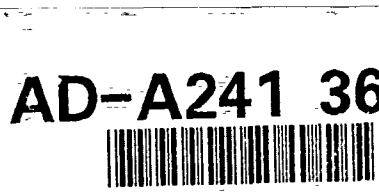

NAVAL POSTGRADUATE SCHOOL
Monterey, California

THESIS

OCEANOGRAPHIC AND ACOUSTICAL SURVEY OF THE EAST IONIAN SEA

by

Radamanthis P. Fountoulakis

September 1990

Co-Advisor Robert H. Bourke
Co-Advisor Alan B. Coppens

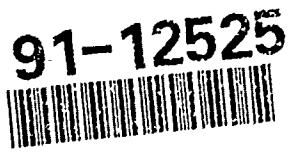

REPORT DOCUMENTATION PAGE

1a Report Security Classification: Unclassified			1b Restrictive Markings
2a Security Classification Authority			3 Distribution/Availability of Report: Approved for public release; distribution is unlimited.
2b Declassification/Downgrading Schedule			
4 Performing Organization Report Number(s)			5 Monitoring Organization Report Number(s)
6a Name of Performing Organization: Naval Postgraduate School	6b Office Symbol (if applicable): 33		7a Name of Monitoring Organization: Naval Postgraduate School
6c Address (city, state, and ZIP code): Monterey, CA 93943-5000			7b Address (city, state, and ZIP code): Monterey, CA 93943-5000
8a Name of Funding/Sponsoring Organization	8b Office Symbol (if applicable)		9 Procurement Instrument Identification Number
8c Address (city, state, and ZIP code)			10 Source of Funding Numbers: Program Element No / Project No / Task No / Work Unit Accession No

11 Title (Include security classification): OCEANOGRAPHIC AND ACOUSTICAL SURVEY OF THE EAST IONIAN SEA

12 Personal Author(s): Radamanthis P. Fountoulakis

13a Type of Report	13b Time Covered	14 Date of Report (year, month, day)	15 Page Count
Master's Thesis	From To	September 1990	98

16 Supplementary Notation: The views expressed in this thesis are those of the author and do not reflect the official policy or position of the Department of Defense or the U.S. Government.

17 Cosati Codes			18 Subject Terms (continue on reverse if necessary and identify by block number)
Field	Group	Subgroup	Oceanographic, Acoustic Survey, East Ionian Sea, PEmodel

19 Abstract (continue on reverse if necessary and identify by block number)

A study was conducted in an area off the Hellenic west coast to examine the spatial and time variability of various oceanic parameters, with special emphasis on those effecting ASW operations. Propagation loss runs were conducted using PE and RAYMODE models. The reactions of both models to different bottom morphology and sound speed profiles (seasons) were examined. Between the two models, the PE model was found to be closer to reality than RAYMODE. Results suggest that the application of these models can improve the understanding of sound propagation in the Hellenic seas. The bottom modeling program, BLUG, appears to need improvement.

20 Distribution/Availability of Abstract	21 Abstract Security Classification	
☒ unclassified unlimited ☐ same as report ☐ DTIC users	Unclassified	
22a Name of Responsible Individual: Robert H. Bourke	22b Telephone (include Area code): (408) 646-3270	22c Office Symbol: OCBf

DD FORM 1473,84 MAR 83 APR edition may be used until exhausted
All other editions are obsolete

Approved for public release; distribution is unlimited.

Oceanographic and Acoustical Survey of the East Ionian Sea

by

Radamanthis P. Fountoulakis
Lieutenant, Hellenic Navy
B.S., Hellenic Naval Academy

Submitted in partial fulfillment of the
requirements for the degree of

MASTER OF SCIENCE IN ENGINEERING ACOUSTICS

from the

NAVAL POSTGRADUATE SCHOOL
September 1990

Author: 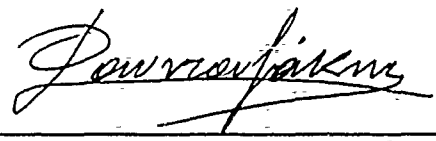

Radamanthis P. Fountoulakis

Approved by: 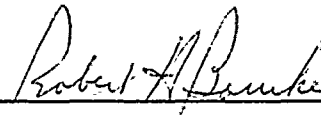

Robert H. Bourke, Co-Advisor

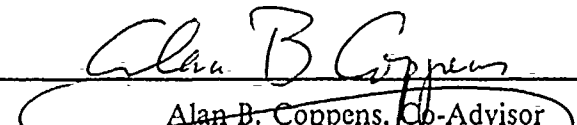

Alan B. Coppens, Co-Advisor

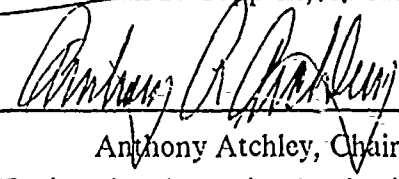

Anthony Atchley, Chairman,
Engineering Acoustics Academic Committee

ABSTRACT

A study was conducted in an area off the Hellenic west coast to examine the spatial and time variability of various oceanic parameters, with special emphasis on those effecting ASW operations. Propagation loss runs were conducted using PE and RAYMODE models. The reactions of both models to different bottom morphology and sound speed profiles (seasons) were examined. Between the two models, the PE model was found to be closer to reality than RAYMODE. Results suggest that the application of these models can improve the understanding of sound propagation in the Hellenic seas. The bottom modeling program, BLUG, appears to need improvement.

TABLE OF CONTENTS

LIST OF FIGURES

I. INTRODUCTION

A. GENERAL

The Hellenic Navy (H.N.) recently established an underwater laboratory in order to perform tests for underwater acoustical devices. A number of areas were examined in the region of Eastern Mediterranean and some of them were found to comply with the requisite specifications for low environmental noise and a smooth shallow sea bottom. In the present study one of these areas was selected for examination of its acoustic propagation characteristics. The study area is located in the Ionian Sea , specifically the region north of 37° 00'N, a restriction to avoid the sea lanes in the southern Ionian Sea which cross the area in an east-west direction. A partition of the Ionian Sea into smaller sectors, each with similar characteristics, was made according to Chart No 30 published by the Hydrographic Service of the Hellenic Navy (H.S.H.N., 1988a). This study covers only the eastern sectors close to the west coast of Hellas (Greece), namely areas Alpha, Bravo and Golf, names that will be used in the study hereafter.

B. OBJECTIVES

The principal objective of this study is to examine the spatial and temporal variations of the oceanic factors that affect underwater sound propagation in order that an acoustic analysis and understanding of the sound propagation in the Ionian Sea can be performed. In addition, an evaluation of the acoustic computer models used by the United States Navy is performed to examine their application to this unique region of the Ionian Sea and the Eastern Mediterranean in general.

C. AREA DESCRIPTION

The Ionian Sea is that part of the Mediterranean Sea lying to the west of Hellas. The geography and partitioning of the Mediterranean Sea into regional basins is shown in Figure 1. This study covers that part of the southeast Ionian Sea from 37° 00'N to 38° 30'N and 19° 30'E to 21° 00'E. The total area is 20000 km² and is bounded to the east by the Hellenic Peninsula (Fig. 2). The area can be separated into the coastal waters lying between the mainland and the offshore islands and the pelagic waters of the Ionian Sea. The mainland is divided into two parts, the main Hellenic Peninsula and the smaller Peloponnesos Peninsula. Between the two there is a sea lane of about 10 km in width and 165 km long which connects the Ionian Sea to the Aegean archipelagos via the

Strait of Corinthos. Area Alpha is located in the shallow waters between the mainland and offshore islands of Kefallonia and Zakynthos (Fig. 3). It has an overall area of 1880 km² and a smooth sea floor with an average depth of around 120 m. The other two areas, Bravo and Golf, are located west of the above islands with Bravo to the north of Golf. The area of Bravo is 4116 km² and has bottom depth which extends to 100 m over the continental shelf and then falls sharply to 1500 m, eventually reaching depths in excess of 2000 m. Area Golf is 15000 km² in extent and has bottom features similar to that of Bravo but has deeper depths which extend to 3000-3300 m.

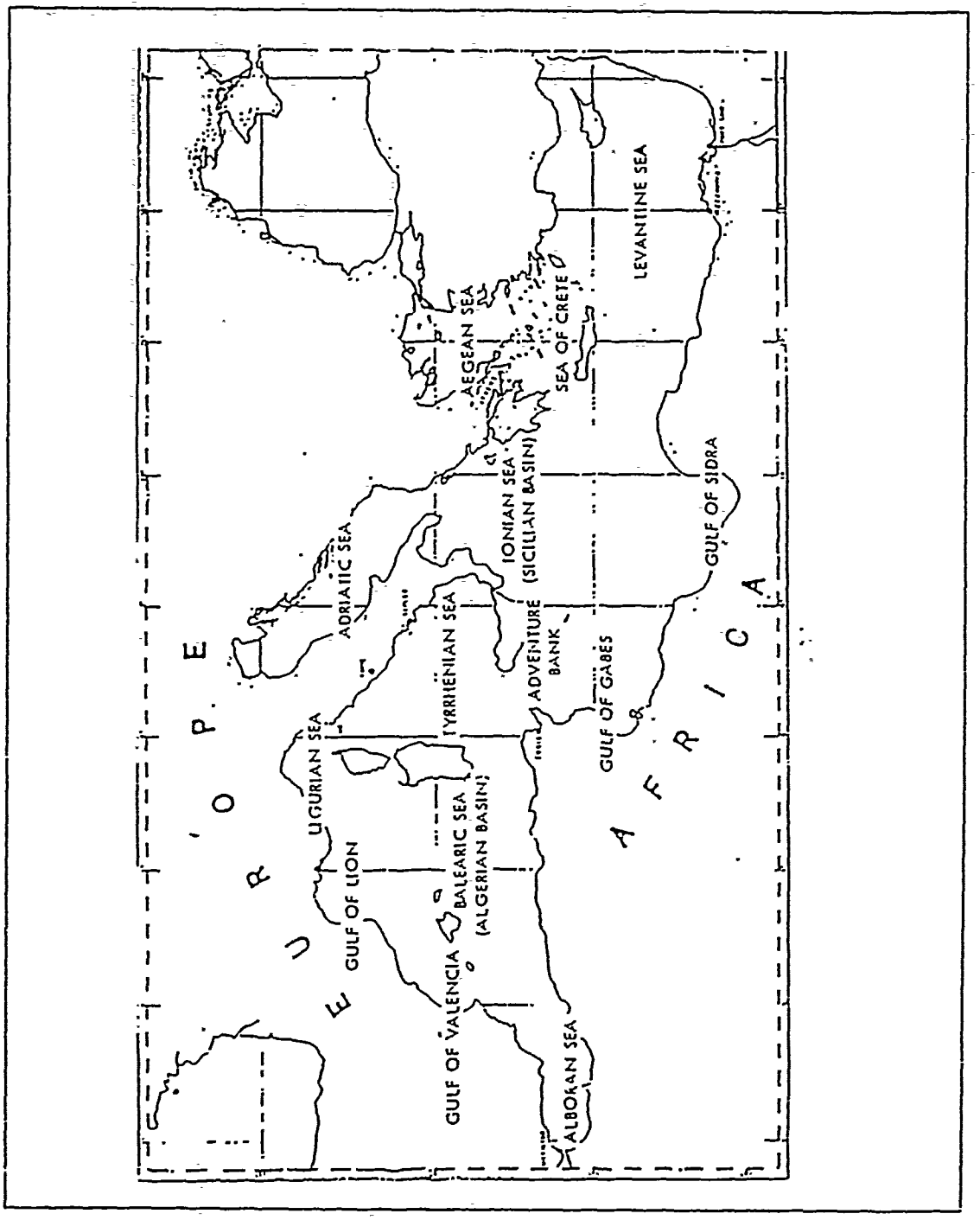

Figure 1. Local seas and basins of the Mediterranean Sea: The eastern part is comprised of the Ionian, Aegean and Levantine Seas (from Maury Center for Ocean Science, 1974).

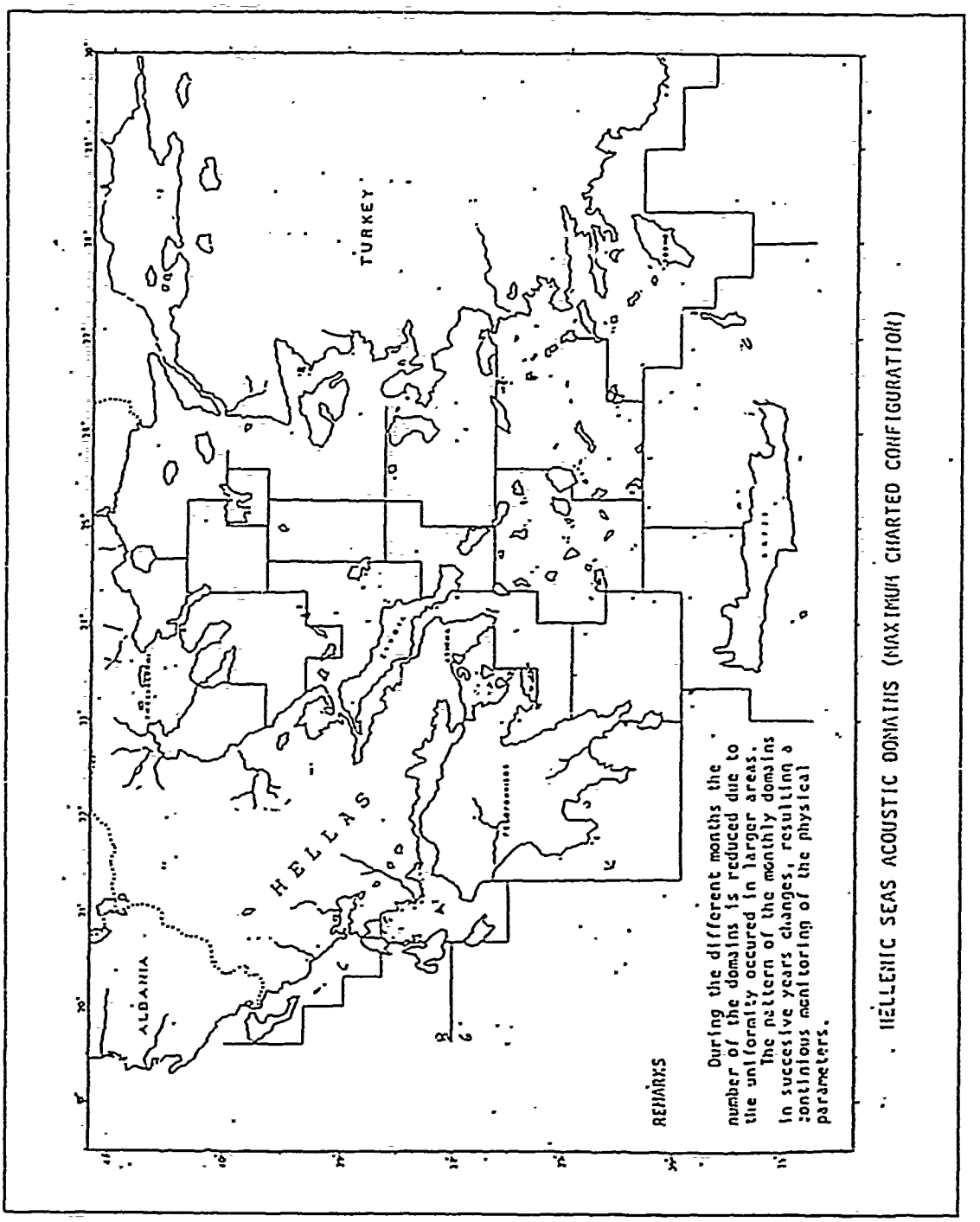

Figure 2. The location of ASW prediction areas: According to the Hydrographic Service of the Hellenic Navy (from HSHN, 1988a).

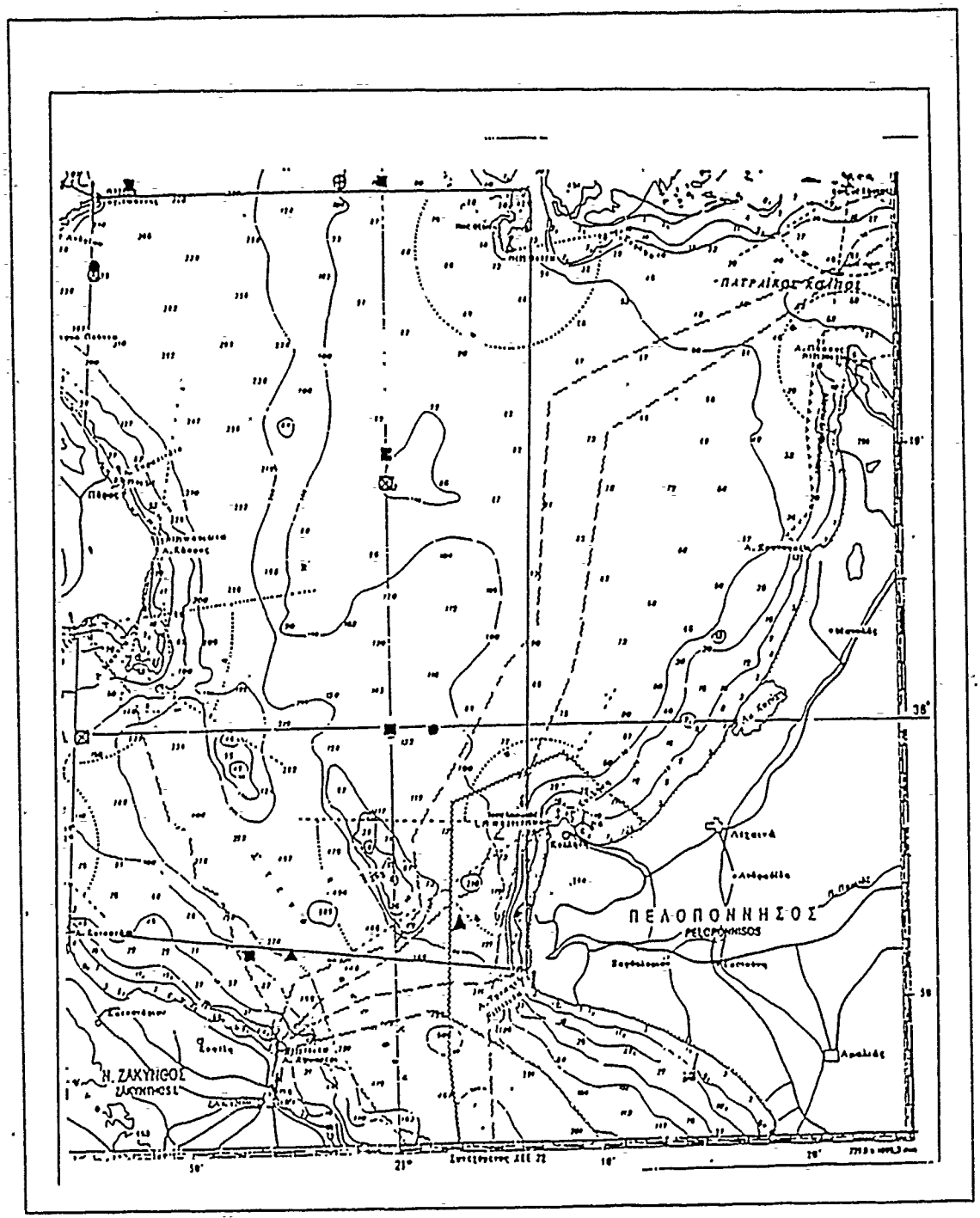

Figure 3. Detail of coastal area Alpha: Bathymetry and location of the stations used in this study are shown (from HSHN, 1982).

II. OCEANOGRAPHY

A. WATER MASSES

Oceanographic conditions in the study area are effected by the circulation of the three major water masses present in the Eastern Mediterranean Sea. These masses, Atlantic, Levantine and Deep Water, are separated by different depths which vary as they move from their places of formation towards other areas, being mixed by other waters along their paths. A number of authors such as Lacombe and Tchernia (1958), Wust (1961), Ovchinnikov (1978) and others have studied the water masses and the circulation characteristics of the Mediterranean Sea. In general, the Mediterranean can be divided into a western and an eastern basin, the latter being defined as the sea eastwards of the Straits of Sicily. Malanotte-Rizzoli and Hecht (1988) state that the physical mechanisms that determine the circulation patterns in the Mediterranean are still uncertain. They, as well as El-Gindy and El-Din (1986), have reported on a number of studies that have been done or are still under execution such as the POEM (Physical Oceanography of the Eastern Mediterranean) cooperative program (UNESCO reports 30, 35 and 44). Part of the uncertainty is due to the complexity of the land barriers to the circulation modeling, coupled with sometimes conflicting reports which have appeared since 1945.

The major water inflow comes from the Atlantic Ocean. This flow pattern results from the fact that the Mediterranean is a concentration basin wherein evaporation exceeds precipitation and runoff. Hence, Atlantic Water (AW) flows into the Mediterranean in order to preserve mass conservation (Bethoux, 1979 and 1980). It flows eastward extending from the surface to 200 m and enters the Eastern Mediterranean by the Straits of Sicily. In the vicinity of Gibraltar, AW has a temperature of 15°C and a salinity of 36.15 psu (Lacombe and Richez, 1982). At the entrance to the eastern Mediterranean the salinity has increased to 38.6 and continues to increase eastwards until at the coast of Israel it is 38.7. In the winter the lower evaporation rate and vigorous mixing destroy the upper layer quickly so the identification of AW is difficult. Frassetto (1965) reports that in wintertime some evidence of AW was observed in the Straits of Sicily so the assumption that this water penetrates as far east as the Ionian Sea holds. Based upon geostrophic calculations (Nielsen, 1912), a cyclonic gyre is observed to the west of Crete (Fig. 4) which carries the AW northwards into the Ionian

Sea. The identification of AW in summer is easier as the high insolation and evaporation rate, coupled with limited wind action, create a buoyant warm and saline layer at the surface which preserves the low salinity influx water found just beneath the surface.

Beneath the AW is Levantine Intermediate Water (LIW). This water is formed in the Levantine basin (Wust, 1961; Bryden and Stommel, 1982) at depths between 200-600 m and is present in the Levantine Basin throughout the year. This water flows westward (Wust, 1961) and upon reaching Gibraltar enters the Atlantic Ocean where it sinks to 1,000 m. It can be traced to the east coast of the American continent by its salinity maximum (Lacombe and Tchernia, 1960). LIW also penetrates into the Ionian and Adriatic Seas. LIW is formed mostly in the winter and can be identified in the Levantine Basin by its salinity maximum (39.1) and a temperature of 15°C (Fig. 5). As it moves towards Crete, the salinity decreases to 38.9 and continues to reduce due to mixing as it progresses westward. The salinity of LIW at the Straits of Sicily is 38.7; upon exiting the Mediterranean at Gibraltar it a has value of 38.4.

The Deep Waters in the Eastern Mediterranean are thought to be formed in the North Adriatic Sea (Pollack, 1951; Pickard and Emery, 1982; Roether et al., 1983), the latter basing their hypothesis on the results of tritium tracer studies. These waters flow to the bottom of the Ionian Sea and then into the Levantine Basin (Fig. 6). Some of these bottom waters can also be formed in the Aegean Sea but no evidence of flow into the Ionian via the Kythera Straits has been identified (Lacombe et al., 1958). These waters are characterized by a temperature of 13.6°C and a salinity of 38.7.

B. CURRENTS

Observations of the currents in the Eastern Mediterranean Sea have lead to conflicting results. A number of measurements and models has been published (Malanotte-Rizzoli and Hecht, 1988; El-Gindy and El-Din, 1986) but no coherent picture of the general circulation can be drawn. This is in part because the wind stress in the Eastern Mediterranean exhibits such strong seasonal variability (Fig. 7). The wind driven currents are expected to form a cyclonic gyre in the Ionian Basin which reverses in summer (Moslalenko, 1974), a feature which has been confirmed by numerical experiments carried out by Malanotte-Rizzoli and Bergamasso (1988). The Pilot of the Hellenic Seas (HSHN, 1979) describes a relatively steady northward surface flow, with no seasonal variability, along the coastal margin of the study area (Fig. 8). More current measure-

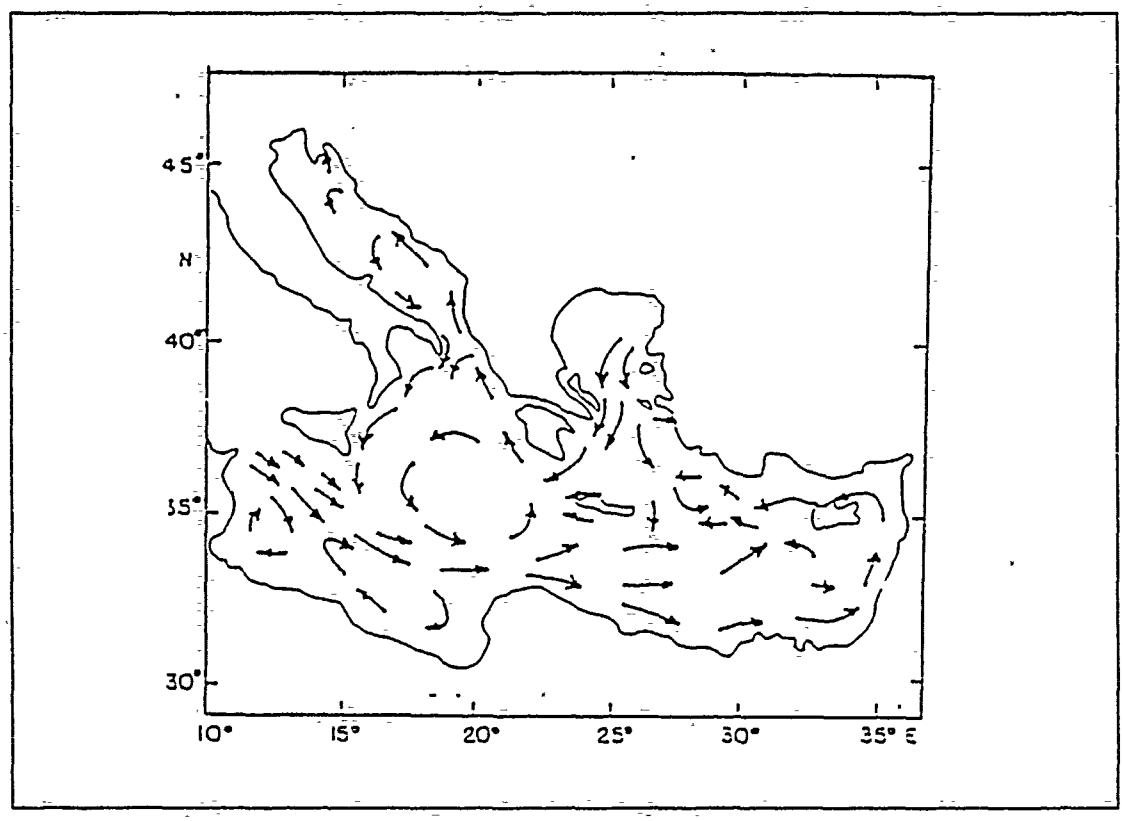

Figure 4. General circulation of the surface waters in the Eastern Mediterranean (from Nielsen, 1912).

ments made by the Hellenic Navy (HSHN, 1989) confirm the northward direction at the surface and at 200 m with no significant seasonal variations (Fig. 9).

The Ionian Sea and its neighbor to the north, the Adriatic Sea, have relatively high surface evaporation rates both in winter, due to dry strong winds from Europe, and in summer, due to high insolation. Assuming that the deep water, formed from the excess evaporation flows southward, then mass conservation requires a surface replacement inflow from the south (Atlantic and Levantine types). Thus a two-layer circulation pattern of opposing currents is formed.

No frontal regions are located in the study area. The Maltese Oceanic Frontal Zone (Johannessen, Stobel and Gehin, 1971), located east of Malta in the region between 36° 00′N 17° 00′E is far to the west and does not affect the study area.

The above water masses and their circulation produce the temperature and salinity profiles seen in Figure 10 typical of the Ionian Sea.

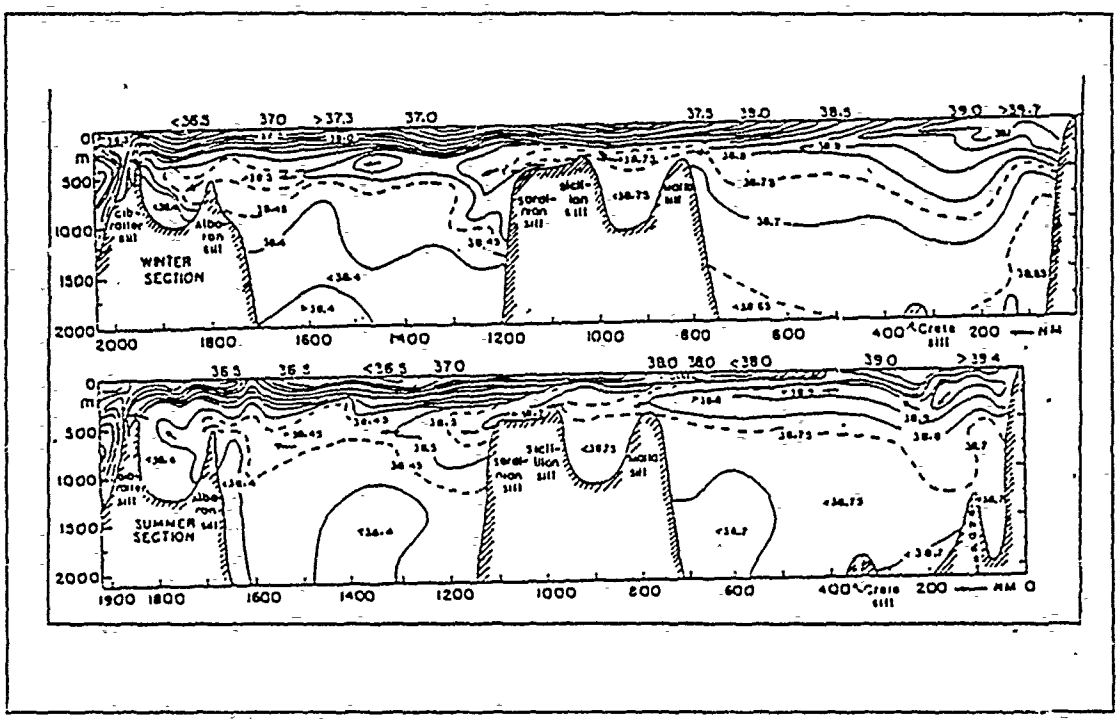

Figure 5. Transverse cross section of salinity: Both seasons, winter (top) and summer (bottom), illustrate the presence of near surface Atlantic Water, high salinity Levantine Intermediate Water at mid depth, and Deep Water below (from Wust, 1961).

C. TEMPERATURE DISTRIBUTION

The temperature profiles found in the study area exhibit a strong seasonal variation. This variability is constrained to the surface waters as profiles below 300 m show negligible seasonal variability (Podeszwa, 1971). The annual sea surface temperature (SST) distribution in the Mediterranean is shown in Figure 11 for four representative months. The SST during the winter (February) is about 14.5°C (58°F) while in summer (August) it warms to 25.5°C (78°F). In winter a mixed layer exists from the surface to about 30 m depth. The temperature slowly decreases from 15°C at the bottom of the mixed layer to 13°C in the deep waters (Podeszwa, 1971; El-Gindy and El-Din, 1986). Summer conditions are characterized by a very hot sea surface (25.5)°C where insolation and the absence of mixing prohibit the formation of a mixed layer. A sharp temperature decrease then follows to a depth of 150 m (15° C) followed by a slower decrease. Between 200 and 600 m (LIW) the temperature is about 15°C; in the deep water it is close

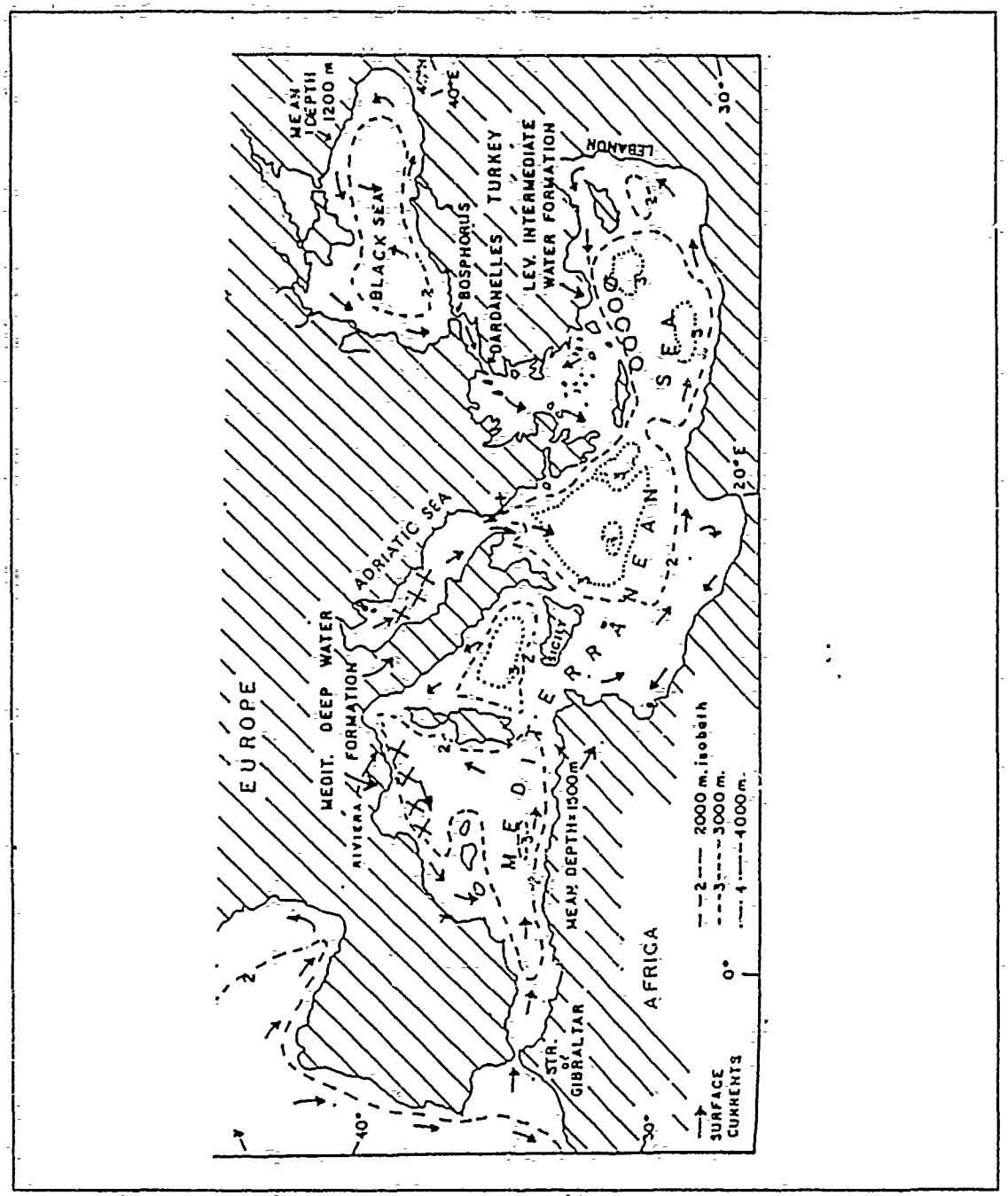

Figure 6. The formation areas of the Deep Waters in the Mediterranean (denoted by XXX): The Adriatic Sea for the Eastern Mediterranean and off the coast of the French Riviera for the Western Mediterranean (from Pickard and Emery, 1982).

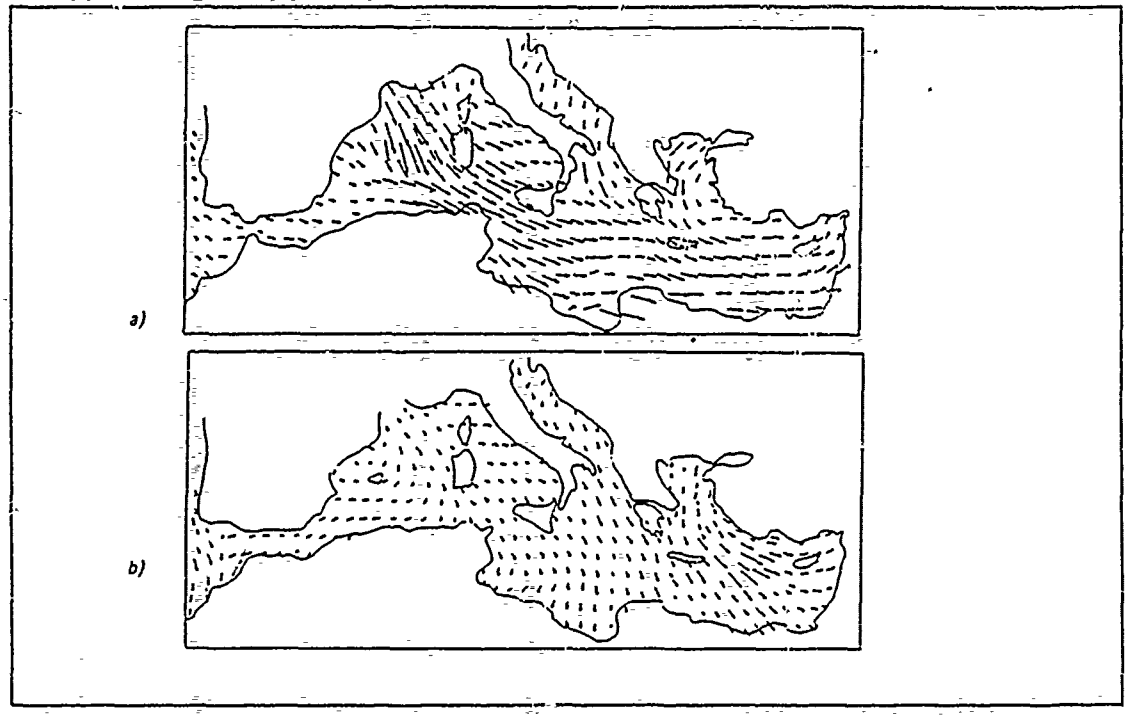

Figure 7. Wind stress over the Mediterranean Sea: a). January mean, b). August mean (from Malanotte - Rizzoli, and Hecht, 1988).

to isothermal at 13.5°C. The difference between summer and winter temperature profiles becomes negligible for depths greater than 400 m (Fig. 10).

The transitions between these two seasons is observed mainly in the depth of the mixed layer, 10 m in spring and about 25 m in the fall. Acoustic conditions during these transition seasons are not examined in this study, instead preferring to concentrate on the two extreme seasonal conditions.

In addition to being influenced by the above large-scale properties of the Mediterranean circulation, the local temperature and salinity profiles can be affected by meso or small scale activities like eddies (Malanotte - Rizzoli and Hecht, 1988). For example, El-Gindy and El-Din (1986) cite the possibility of deep warm eddies in the central Ionian Sea. Also a satellite image of the Ionian Sea (Fig. 12) shows the presence of warm eddies in the area under investigation.

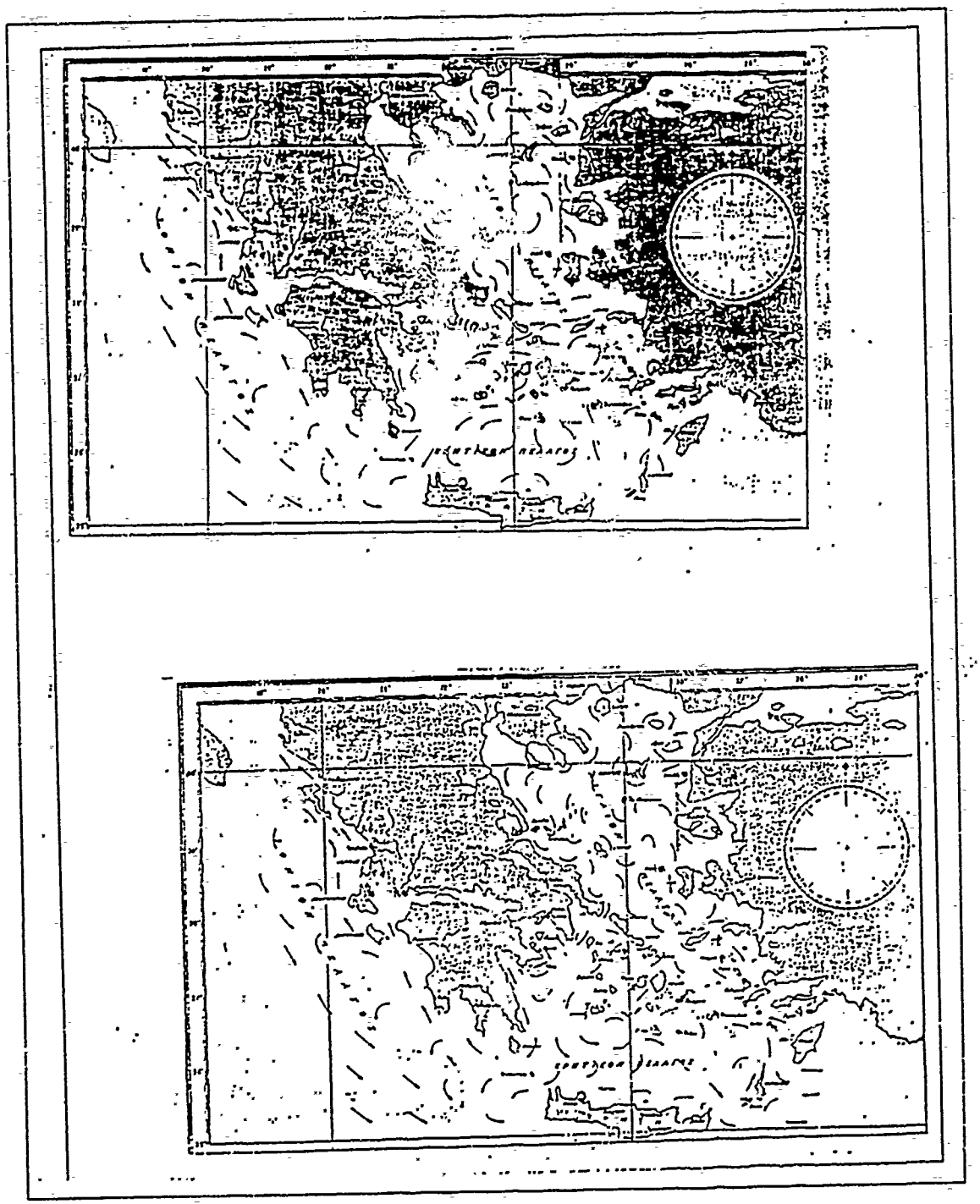

Figure 8. Surface currents in the Hellenic Seas: top: winter mean, bottom: summer mean. Both seasons have a northward direction along the west coast of Hellas with a speed of 0.2 to 0.5 Kts (from HSHN, 1979).

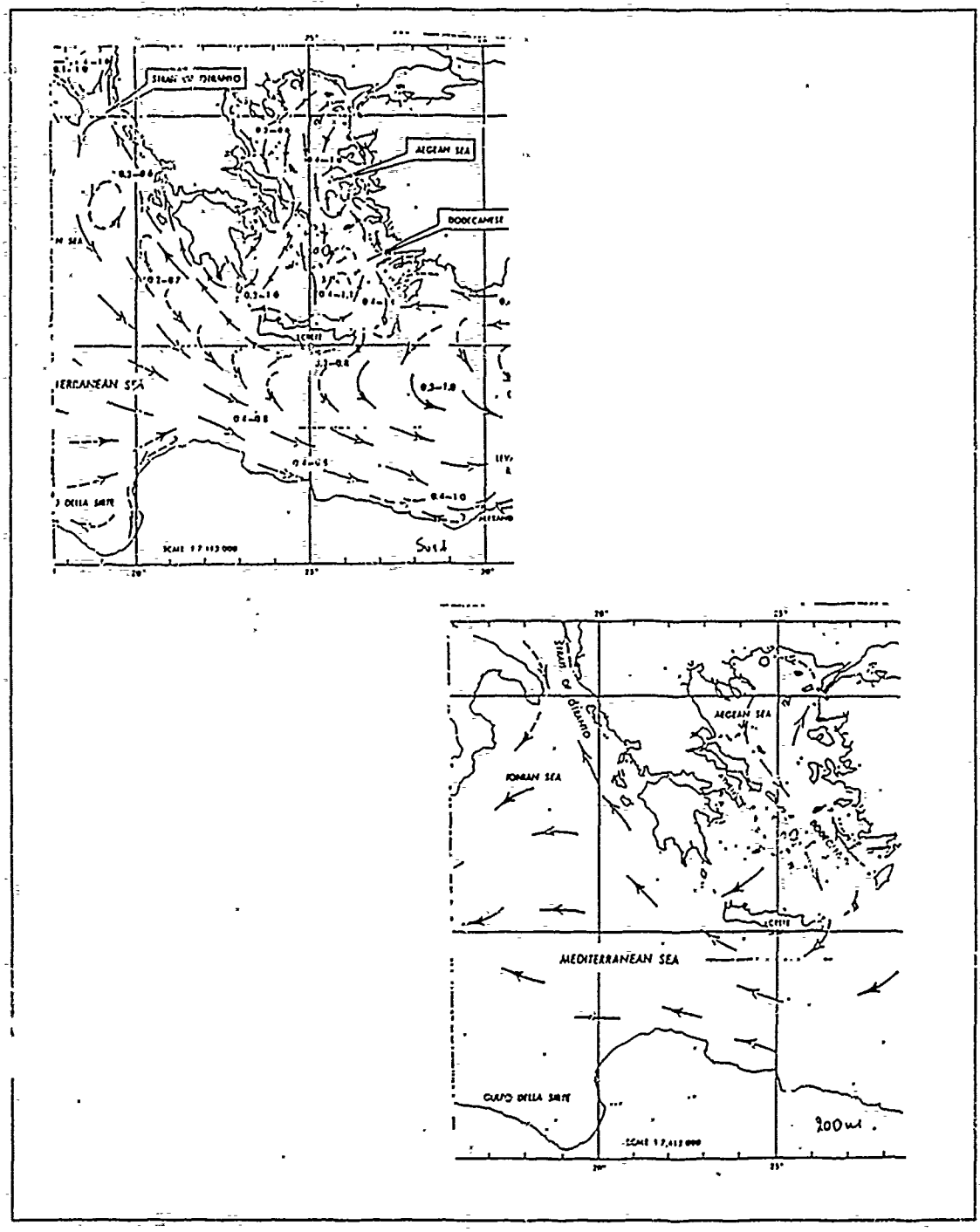

Figure 9. Currents at the surface and at 200 m depth: Recent measurements from HSHN show very little directional variability throughout the seasons (from HSHN, 1989).

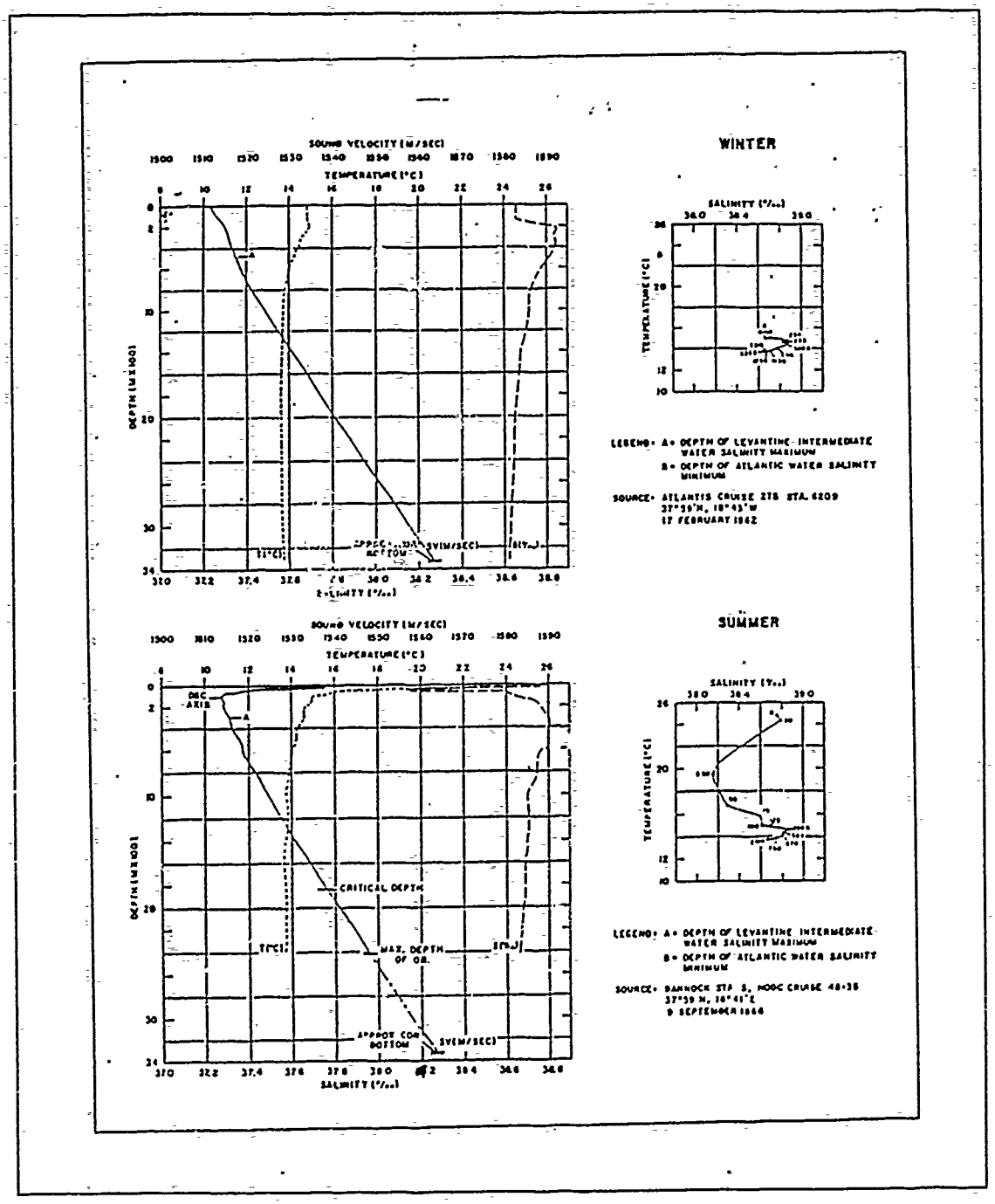

Figure 10. Seasonal Temperature, salinity and SSP in the Ionian Sea: Both seasons show the presence of the three different water masses (AW, LIW, DW) in the Eastern Mediterranean (from Maury Center for Ocean Science, 1974).

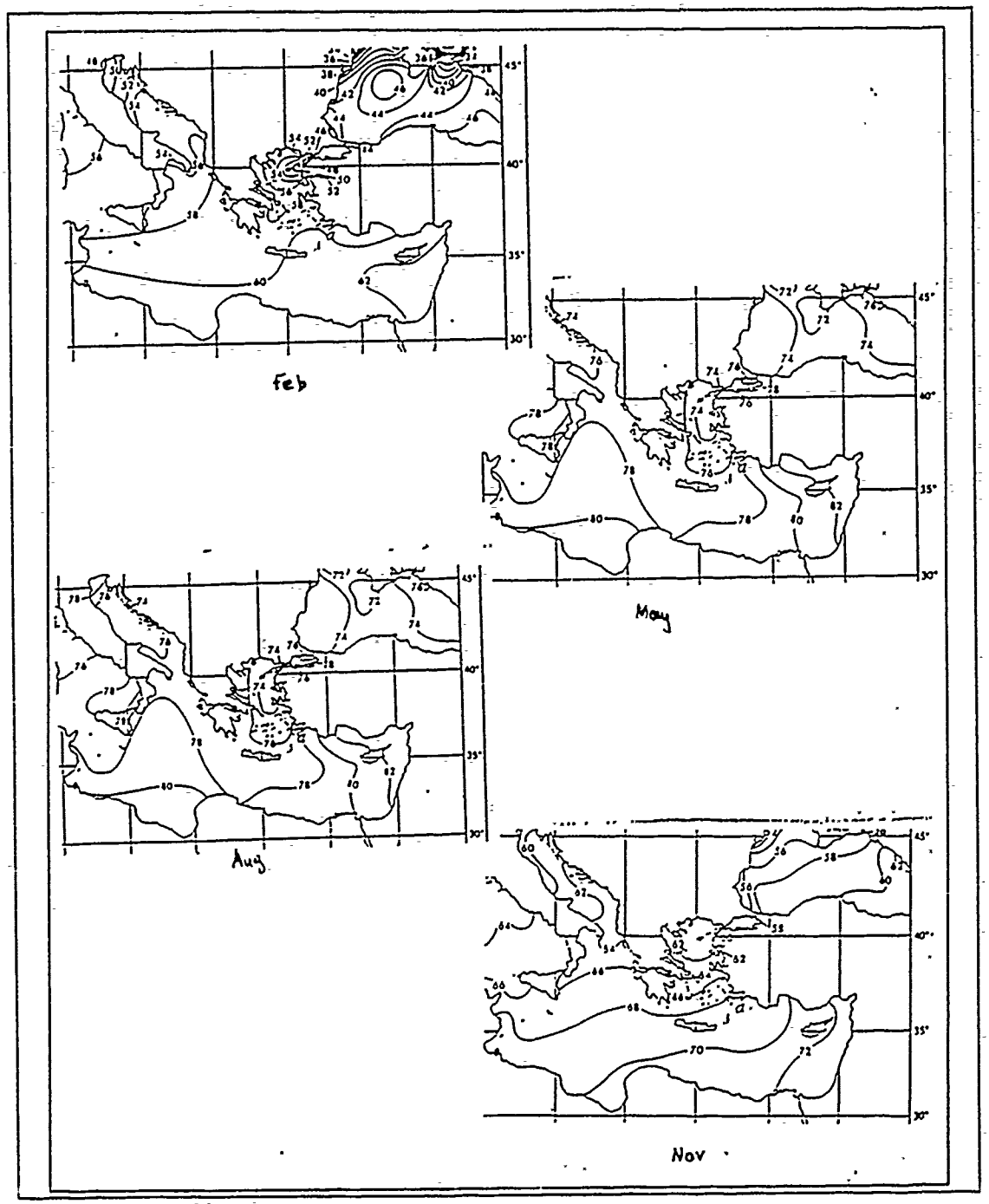

Figure 11. Distribution of sea surface temperature (°F), (a) February, (b) May, (c) August and (d) November (from Maury Center for Ocean Science, 1974).

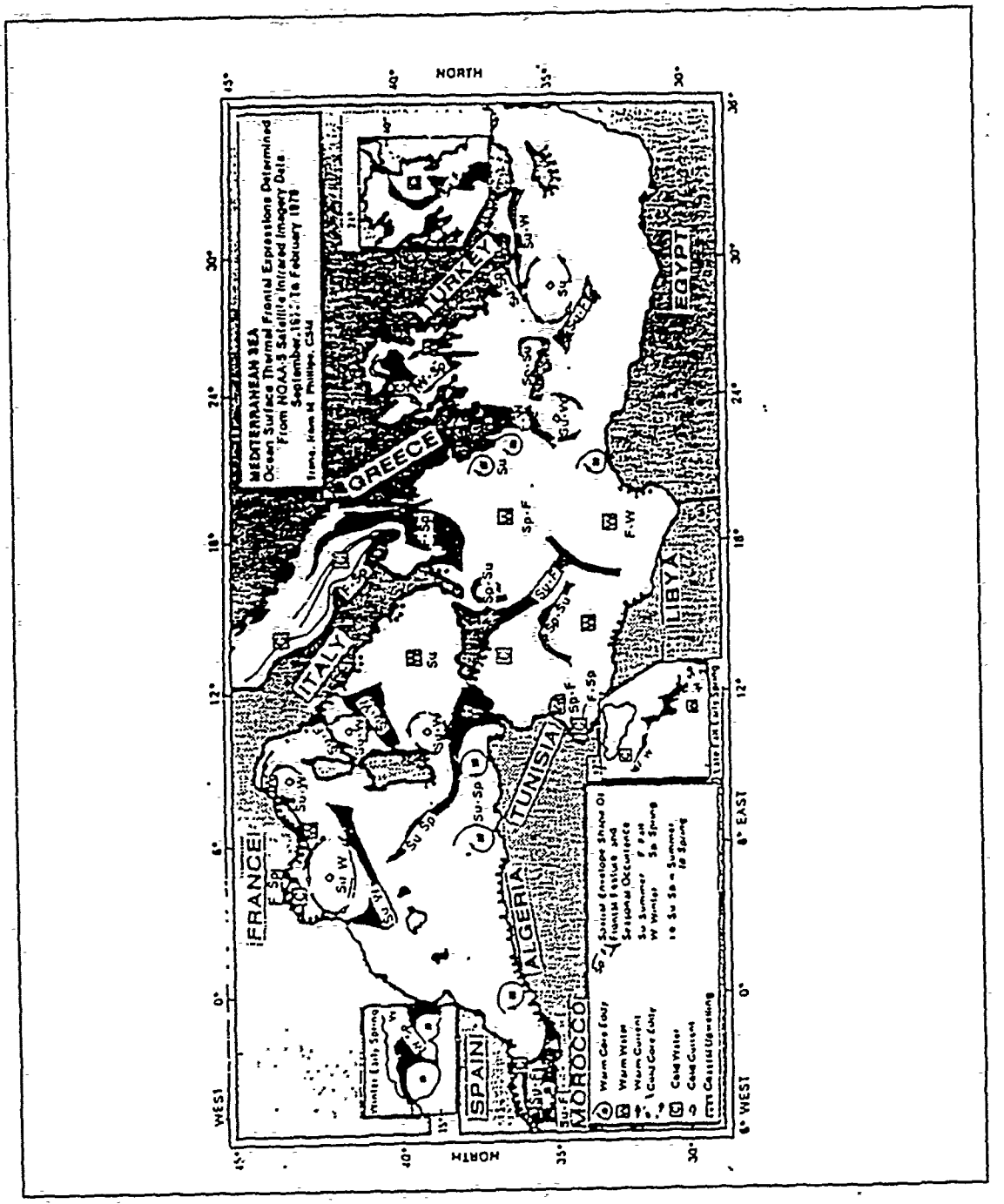

Figure 12. Thermal surface features of the Mediterranean Sea: The presence of warm eddies in the eastern Ionian Sea are shown in this plot derived from satellite I.R. data from Sept. 1977 to from Feb. 1979 (Robinson, 1985).

D. SUMMARY OF OCEANOGRAPHY

A summary of the preceding hydrographic analysis is presented below describing conditions present in the study area during the two principal seasons. Typical profiles for the Ionian Sea are shown in Figure 10.

1. Winter season

The winter season, January through March, is in general characterized by strong wind mixing and convection which produces a well-mixed surface layer to 200 m ($T \cong 14.0°$ C, $S \cong 38.2$). Beneath this layer and extending to 600 m is LIW which flows northward along the west coast of Hellas. The Deep Water from the Adriatic fills the depths from 600 m to the bottom ($T \cong 13.5°C$, $S \cong 38.7$). The mean temperature, salinity and sound speed profiles of Figure 10 appear to be representative of the entire region of the Ionian Sea. Small variations from these profiles are expected due to local influence and year to year fluctuations.

2. Summer season

The summer season, July, August and first days of September, are characterized by high insolation and limited wind mixing. This produces a hot and saline lid at the surface($T \cong 25°C$, $S \cong 38.8$) which overlies the low-salinity Atlantic Waters below. The AW is identified by its lower temperatures and salinity minimum ($T \cong 14°C$, $S \cong 38.2$) at a depth of 20 m to 200 m. Little or no seasonal effects are expected below this depth of 200 m.

III. DATA ANALYSIS

A. SOURCES OF DATA

1. Hydrographic data (Temp., Sal., SSP vs Depth)

Two sources of hydrographic station data were used; from the National Oceanographic Data Center (NODC) at Washington DC (1989) and from the Hydrographic Service of the Hellenic Navy (HSHN) at Athens, HELLAS (1988b, 1989). Historical sound speed profiles compiled by Podeszwa (1980) for the Ionian Sea were also used for comparison, as they include more than 6000 records in this area. From the NODC data file a total of 192 observations (Nansen and CTD) were extracted. The majority of them (180 records) represent synoptic data collected in areas Bravo and Golf in November 1980 while the rest are mostly single records taken from various sources in the study areas between 1970 and 1983. The Hellenic Navy data included 15 CTD stations in the coastal area, Alpha. Additionally the Hellenic Navy provided groups of three to four synoptic records covering the entire area Alpha and representing all four seasons. These records were used for spatial investigation of each group inherently and for seasonal variation analysis, averaging records of the same group. The time interval covered by the data from all these sources starts in 1970 and ends in 1983 and the observations are distributed over all the interested areas and seasons of the year (Fig. 13).

Sound speed profiles were calculated from these temperature and salinity data using the Chen - Millero (1977) equation. In selecting a typical SSP, more attention was given to the upper 600 m as this was the depth range exhibiting most of the seasonal variability. Records having some data points lying outside the normal standard variation were corrected by interpolation. If the number of bad data points was significant, then the whole record was discarded. Plots and graphs were expanded to 350 m for the shallow area (Alpha) and to 3000 m for deep ones, Bravo and Golf. The range 0-600 m is also used to increase the resolution of the upper water strata.

2. Bottom Characteristics

The bottom depth in the area of interest varies such that it can be divided into two regions. The coastal region is a part of the continental self with depths less than 200 m. The Ionian Basin is significantly deeper having depths between 200 m and 3000 m and in some areas exceeding 3000 m. A representation of the bottom morphology can been seen from three transects which pass over the continental shelf into deep water

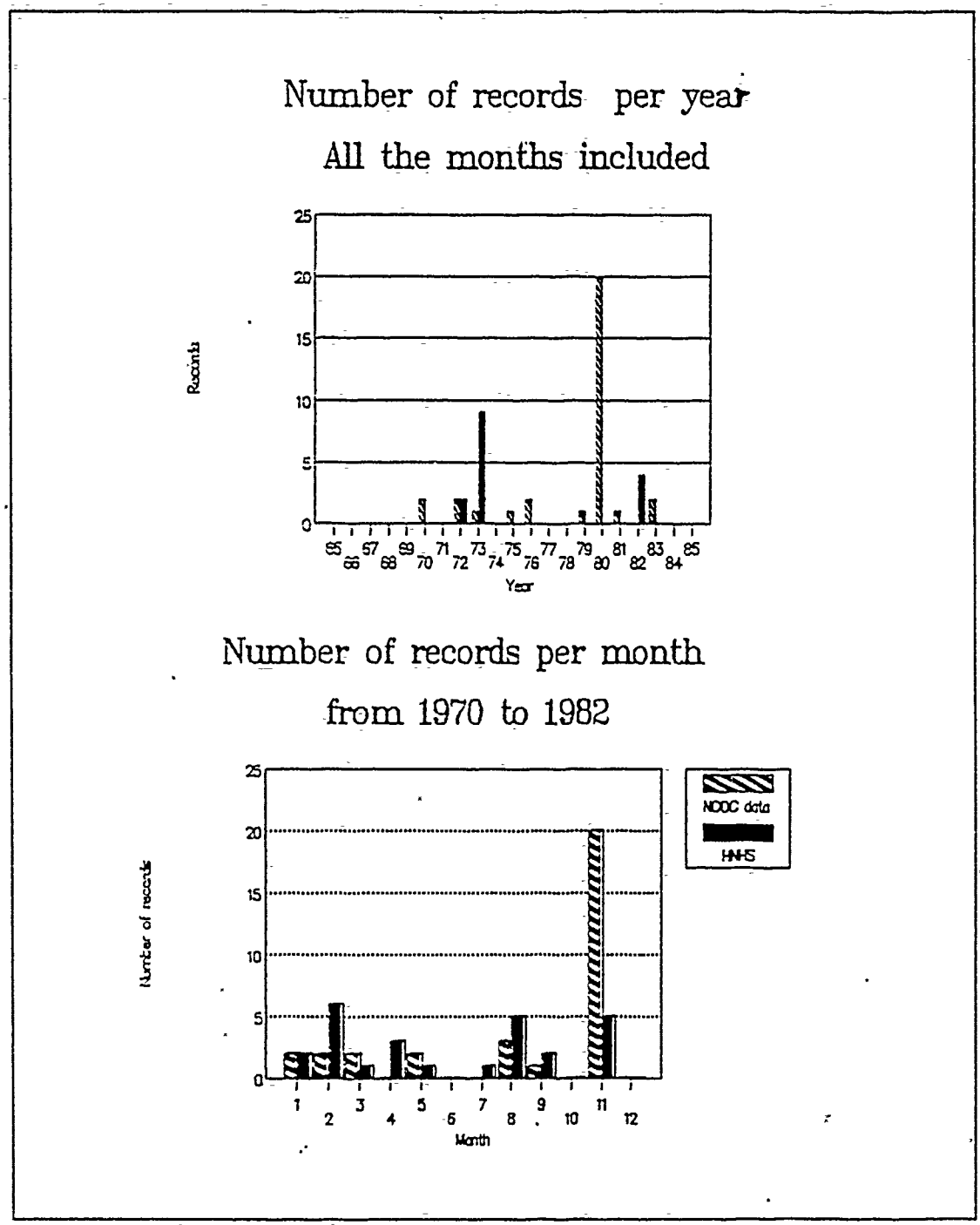

Figure 13. Annual and monthly distribution of used records: Only non-synoptic records are shown for each year and each month from all the years summed.

(Fig. 14). The continental shelf is present from the mainland to the Ionian Islands; then the bottom precipitately descends to the Ionian Basin. The selected study areas are distributed such that area Alpha lies above the continental shelf while areas Bravo and Golf lie over the continental slope and the Ionian Basin. Based upon data from the HSHN (1988b and 1989) the sea bed is observed to be mostly mud with a small percentage of silt (less than 4.5%). This percentage increases shoreward from 12.8% to 29.4% depending on the bottom slope.

Data for acoustical modeling of the sea bed were taken from the data bases associated with the bottom loss model BLUG and NAVOCEANO charts (H.O, 1972).

Two HSHN small scale charts, No 22 (HSHN, 1982) and No 65 (HSHN, 1983) were used to extract the bathymetry along each selected transmission path for later insertion into the PE transmission model (Fig. 14 and 15).

B. SEASONAL VARIABILITY

1. Winter

In the winter season (January through March) a total of 15 records were examined from observations taken within the study area. These observations were taken over a time span of nine years. As expected, wind and convective mixing produce a well mixed isothermal layer below the surface. This layer in shallow areas, like Alpha, extends throughout the entire water column. In area Alpha the winter is characterized by an isothermal profile of 14.5°C (Fig. 16). The mean values from these 15 records result in temperature, salinity and sound speed profiles as shown in Figure 17, where a low surface salinity (S = 38.0) is observed followed by a positive salinity gradient. The same characteristics can be seen in the deep areas, Bravo and Golf, where the surface temperature is 15.0°C and decreases slowly with depth (Fig. 18). At 300 m the temperature is about 14.0°C; at 1500 m it is 13.5°C. The salinity gradient is also positive with surface values of 38.44 in the deeper offshore areas. Salinity increases with depth until at 300 m it is about 38.75. This is true for both deep and shallow areas. AW is hence observed to occupy the upper 300 m, LIW the deeper waters (Fig 19).

2. Summer

In summer a total 5 of records from the HSHN data base were examined. The principal features of the temperature profile are its hot surface layer followed by a sharp decrease in temperature. The profiles for area Alpha (Figures 20 and 21) show the pres-

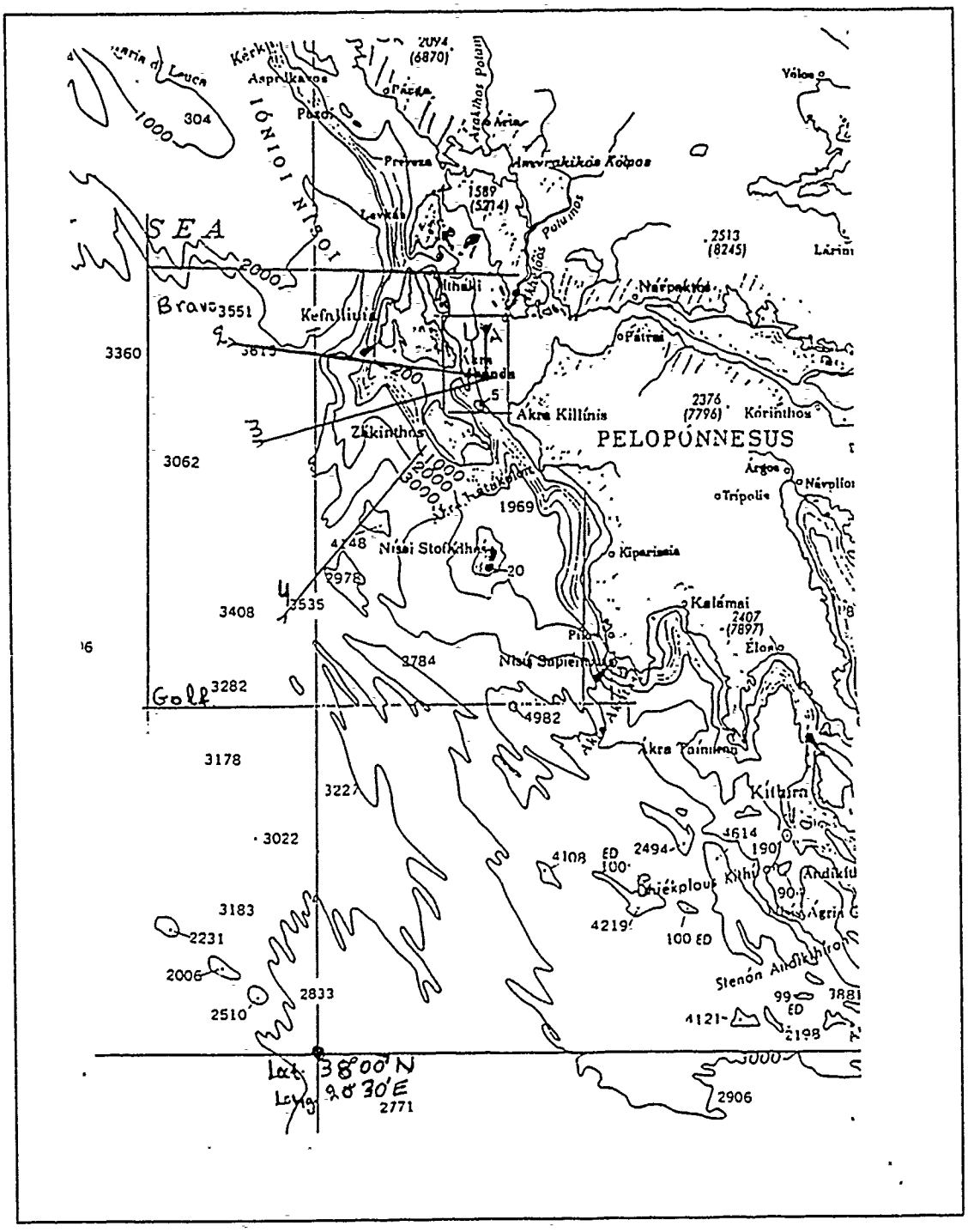

Figure 14. Bathymetry of the Ionian Sea (from HSHN, 1988a): The location of the four transects used is also shown (depths in meters).

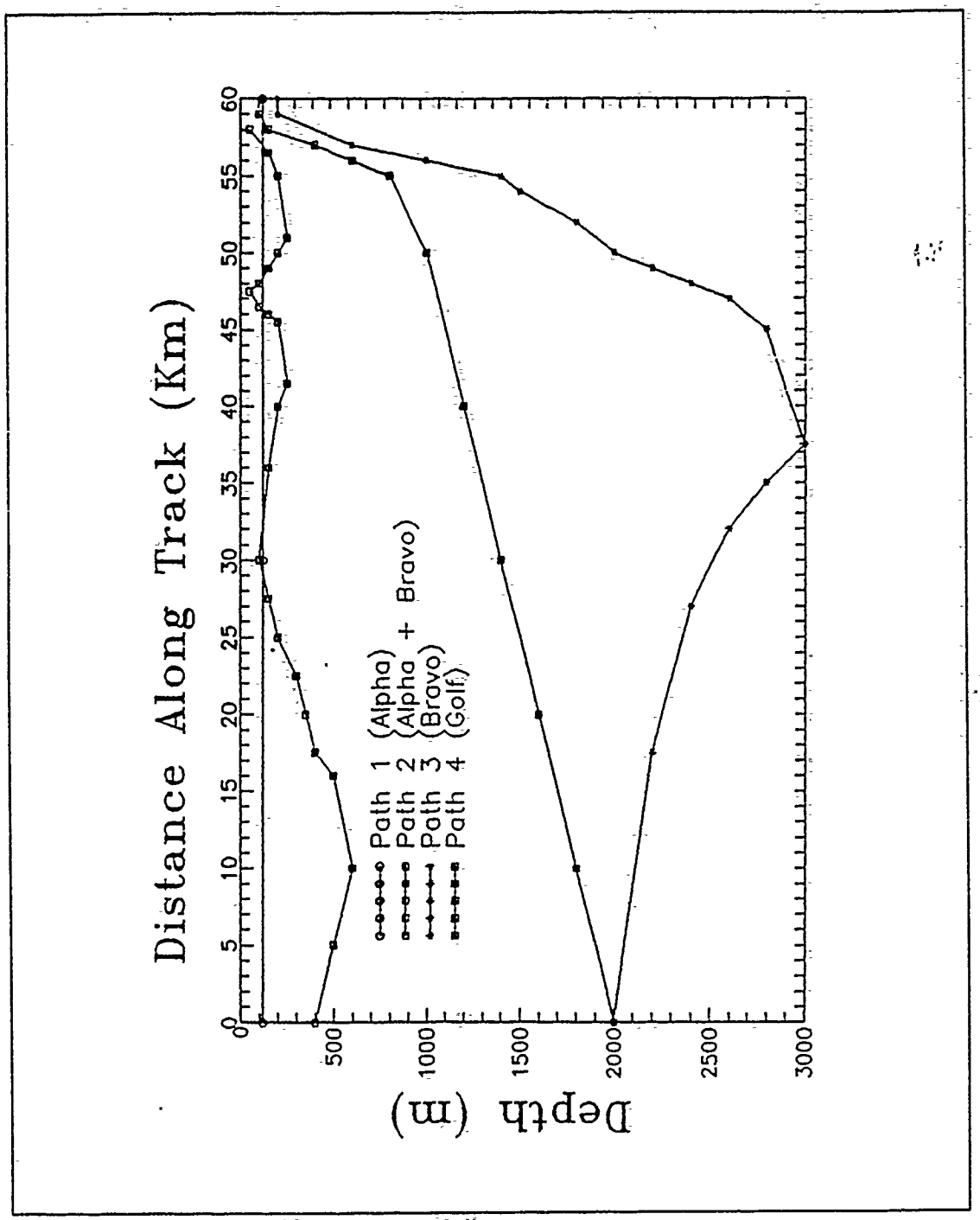

Figure 15. Bathymetry along the selected paths: The discrete values shown here were used in the PE model to simulate the actual bathymetry found in areas Bravo and Golf.

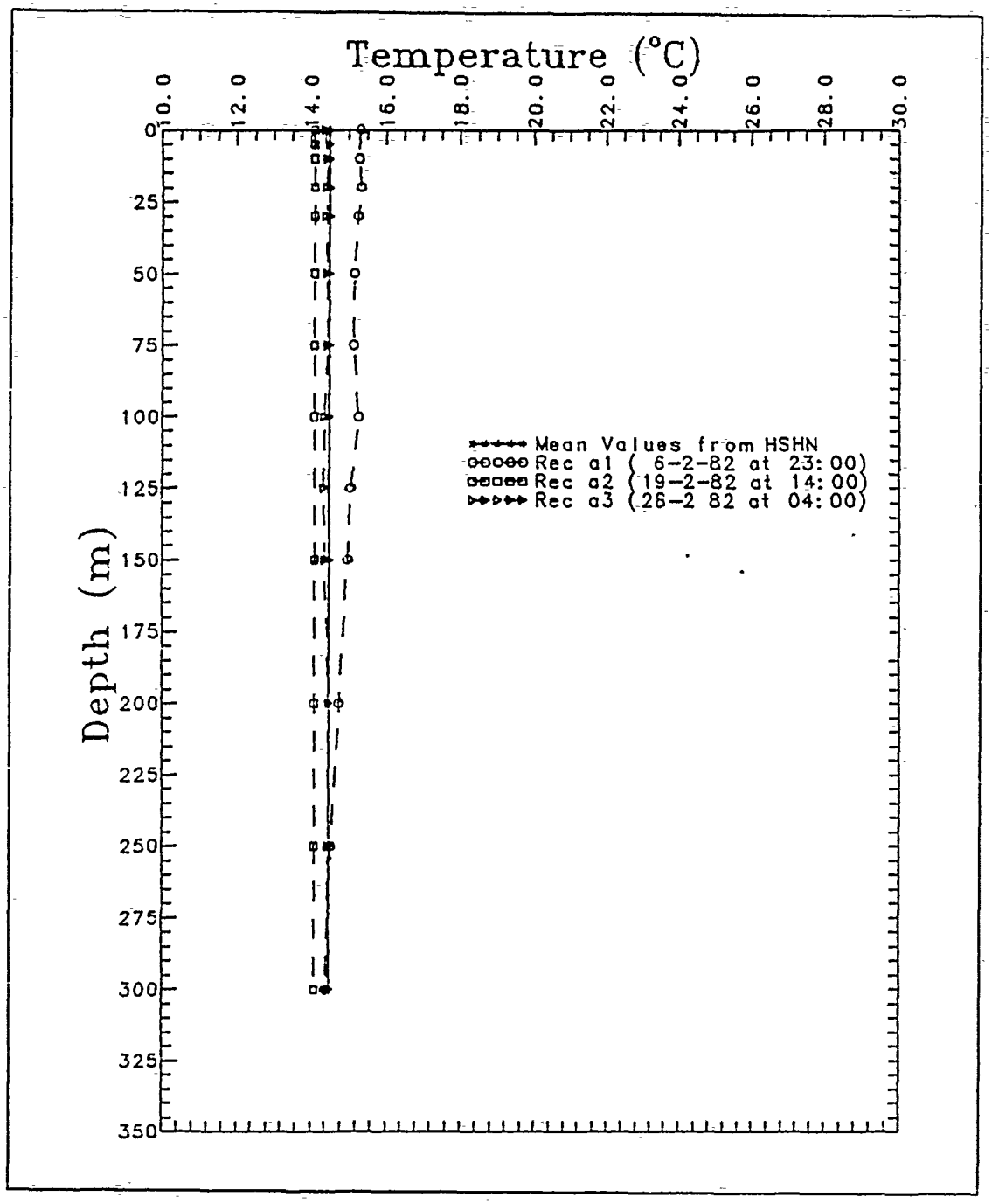

Figure 16. Temperature profiles in area Alpha winter 1982: These records show the existance of isothermal conditions with small variations from day to day.

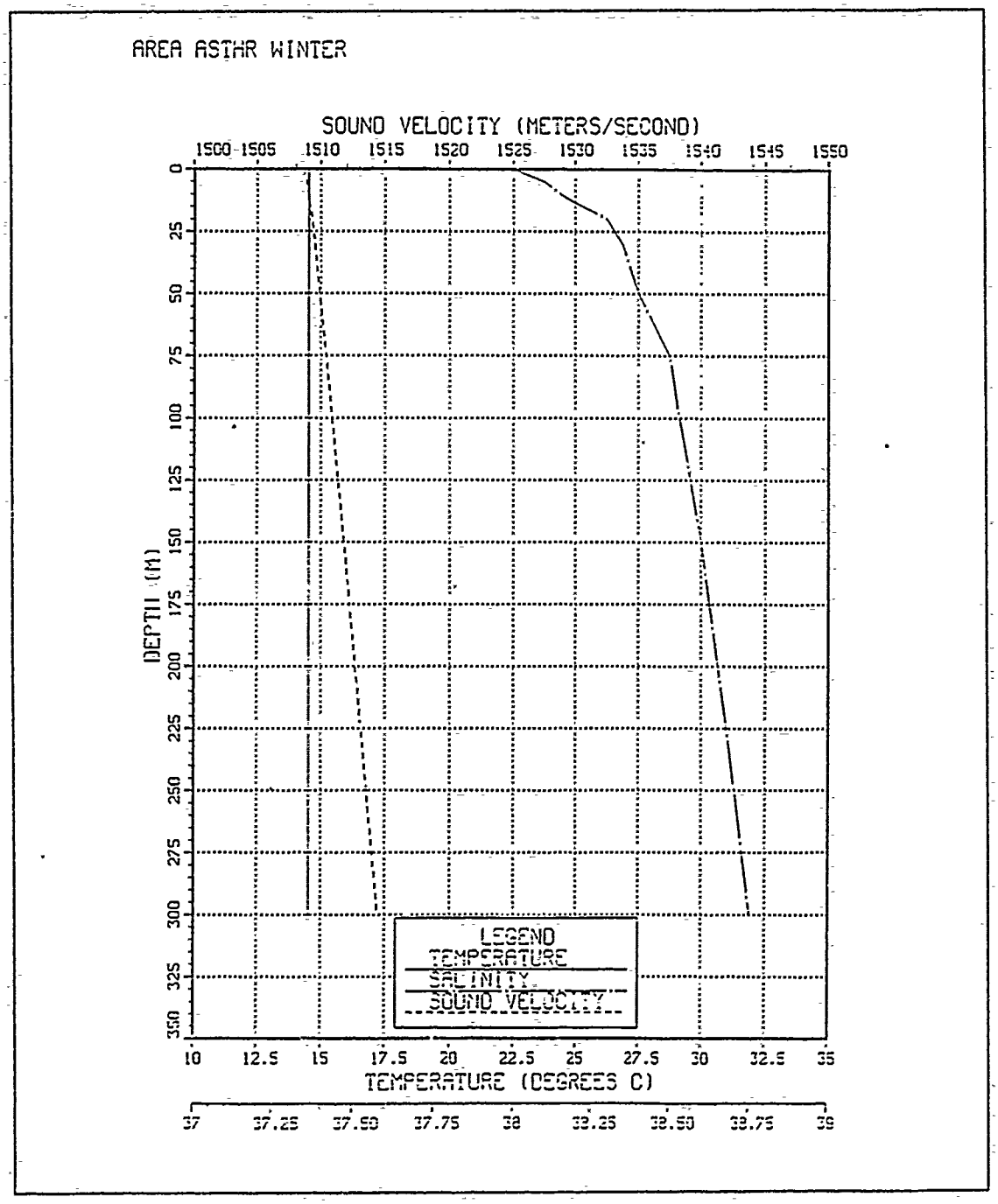

Figure 17. Mean profiles of temperature, salinity and sound speed profiles in area Alpha, winter : The SSP produces a half channel propagation path.

ence of a mixed layer to 20 m. The mixed layer is better developed in the synoptic profiles acquired between 9 and 19 September 1973 (mean values only). Farther seaward in

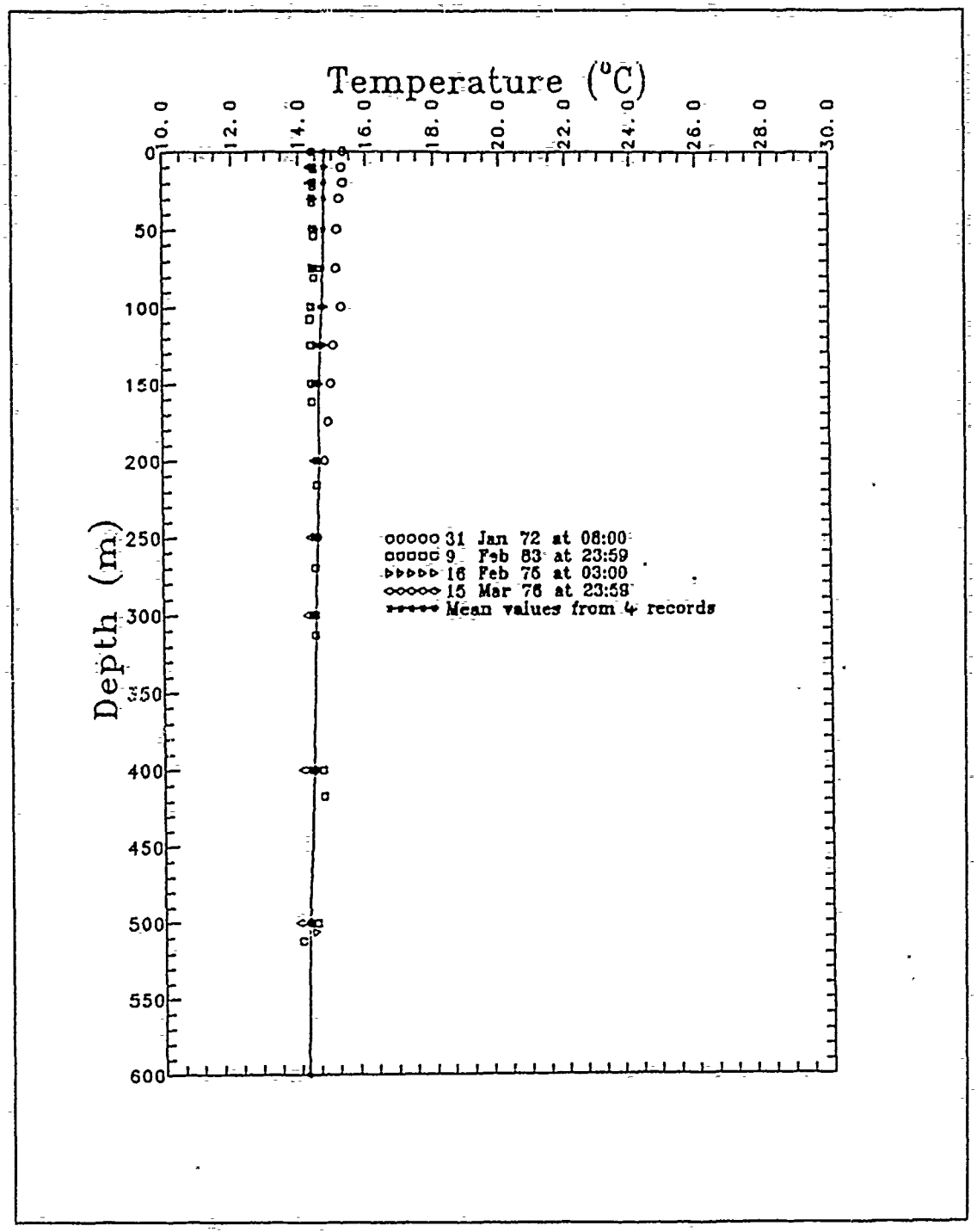

Figure 18. Winter temperature profiles in area Golf: The variation between these records taken over an interval of nine years is minimal.

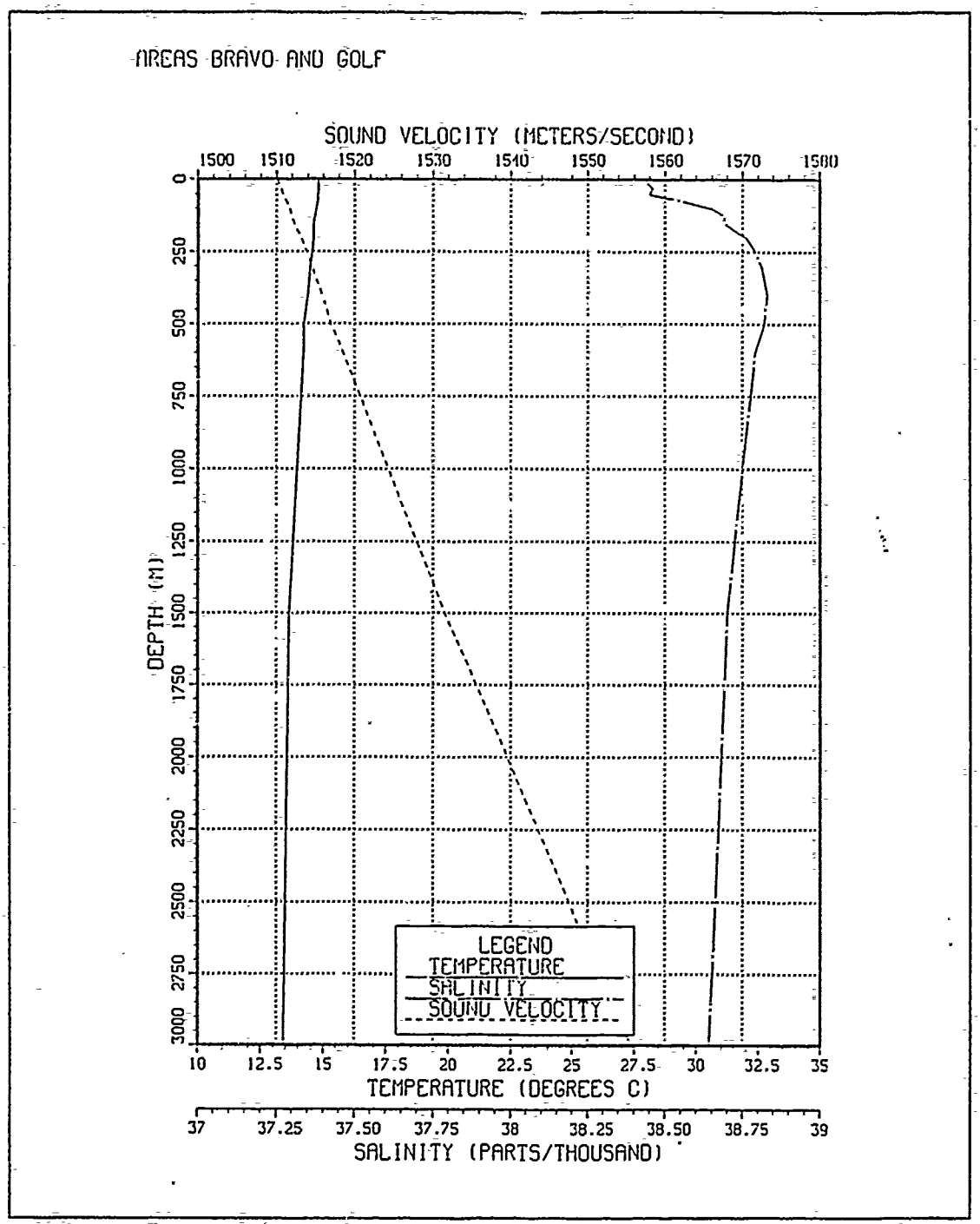

Figure 19. Temperature, salinity and sound speed profiles in areas Bravo and Golf, winter : The presence of Atlantic, Levantine and Deep (Adriatic) Water can be seen by the salinity minima and maxima.

areas Bravo and Golf the existence of limited mixing is evident as the temperature at first decreases slowly to 15 m, followed by a sharper gradient beneath. The salinity profile in shallow waters (Alpha) shows a nearly isohaline condition with a sharp increase close to the bottom, evidence of the presence of LIW flowing on to the shelf (Fig. 21). In the deep water areas, the salinity exhibits a minimum at 30-40 m (AW) and then increases to 38.75 between 300 and 500 m (LIW). Below the LIW it slowly decreases to values below 38.7 (Deep Waters) (Fig. 22).

C. SPATIAL VARIABILITY OF DATA

To investigate evidence of spatial variations in the study areas all the available synoptic data were used. For area Alpha these synoptic records covered all the seasons of the year; for areas Bravo and Golf the only available data were limited between 2 and 28 November 1980.

The compilation of synoptic records from area Alpha shows that the maximum deviation of each group does not exceed 0.5°C from the mean values (Figures 16 and 20) for both seasons, winter and summer. Hence, in area Alpha, bathythermographic conditions have negligible spatial variation for each of the seasons examined in this study.

For deeper areas Bravo and Golf, as noted before, the spatial investigation was done using groups of records taken between 2 to 28 November 1980. Again the differences between the records do not exceed 0.5°C in temperature or 10 m in MLD.

The comparison between selected groups of records taken in area Bravo on 19 November 1989 and in area Golf on 11 and 26 November 1989 verify that area Golf is usually 0.5 to 1°C warmer than Bravo. The differences are in the mixed layer where (Figures 23, 24 and 25) records from Golf have a MLD of 30 m and a surface temperature 21.3°C on 11 November. Four days later Bravo has a MLD of 30 m and a surface temperature 20.0°C and then Golf on 26 November has a MLD of 35 m and surface temperature 19.4°C.

The above selected records indicate a negligible spatial variation across the study areas. In addition the examination of single records taken in winter and summer shows small differences between them. Records taken in these areas from the same seasons with a five to nine year time span seem very similar and close to those compiled by Podeszwa (1980). Hence, the assumption that the spatial variations of temperature and salinity in these areas are negligible is valid. Accordingly the SSPs in the study area do not have horizontal variations, at least for the time period for which an ASW prediction is required.

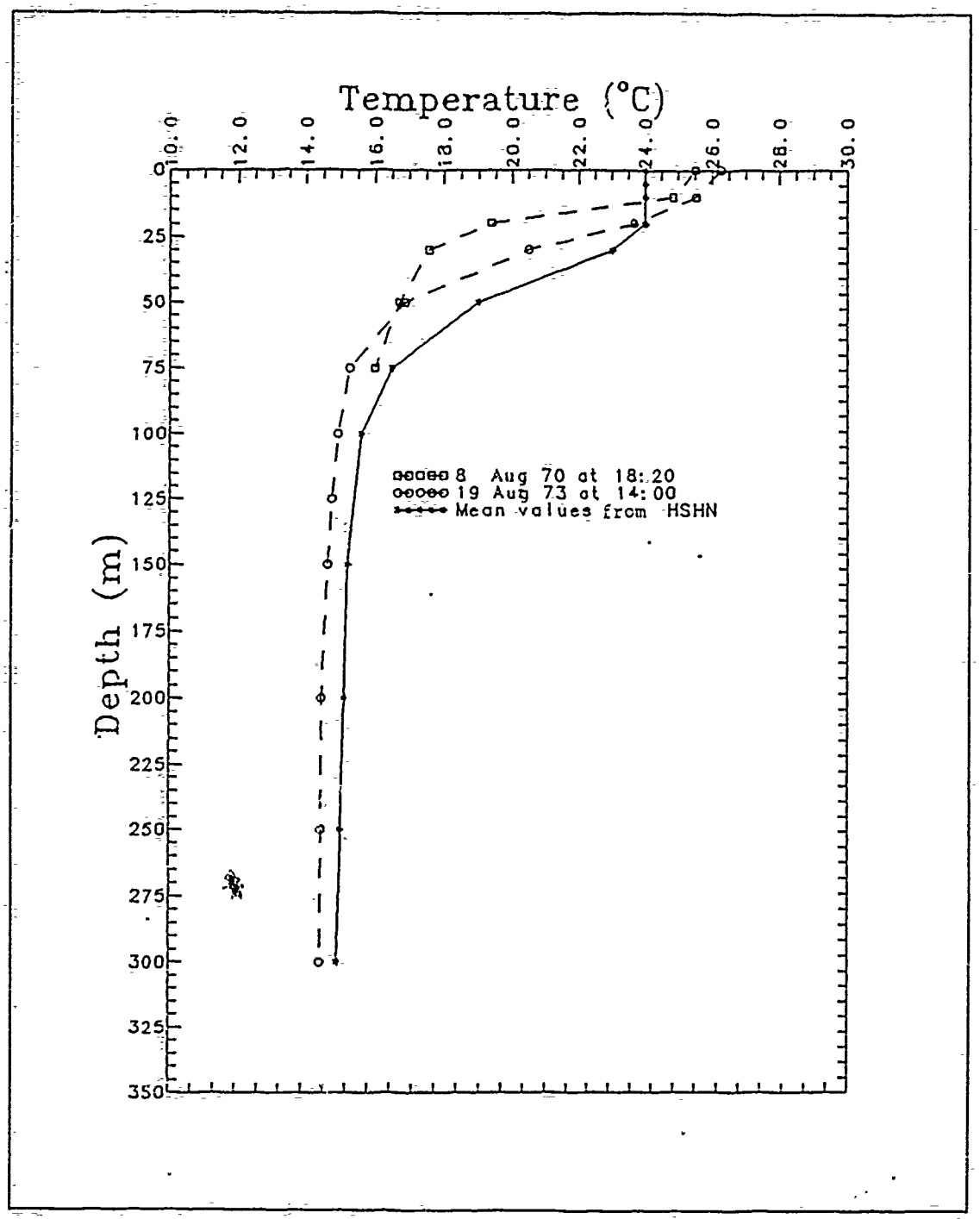

Figure 20. Temperature profiles in area Alpha, summer: The existence of a mixed layer can be verified by the data collected during September 1973 (HSHN, 1988b).

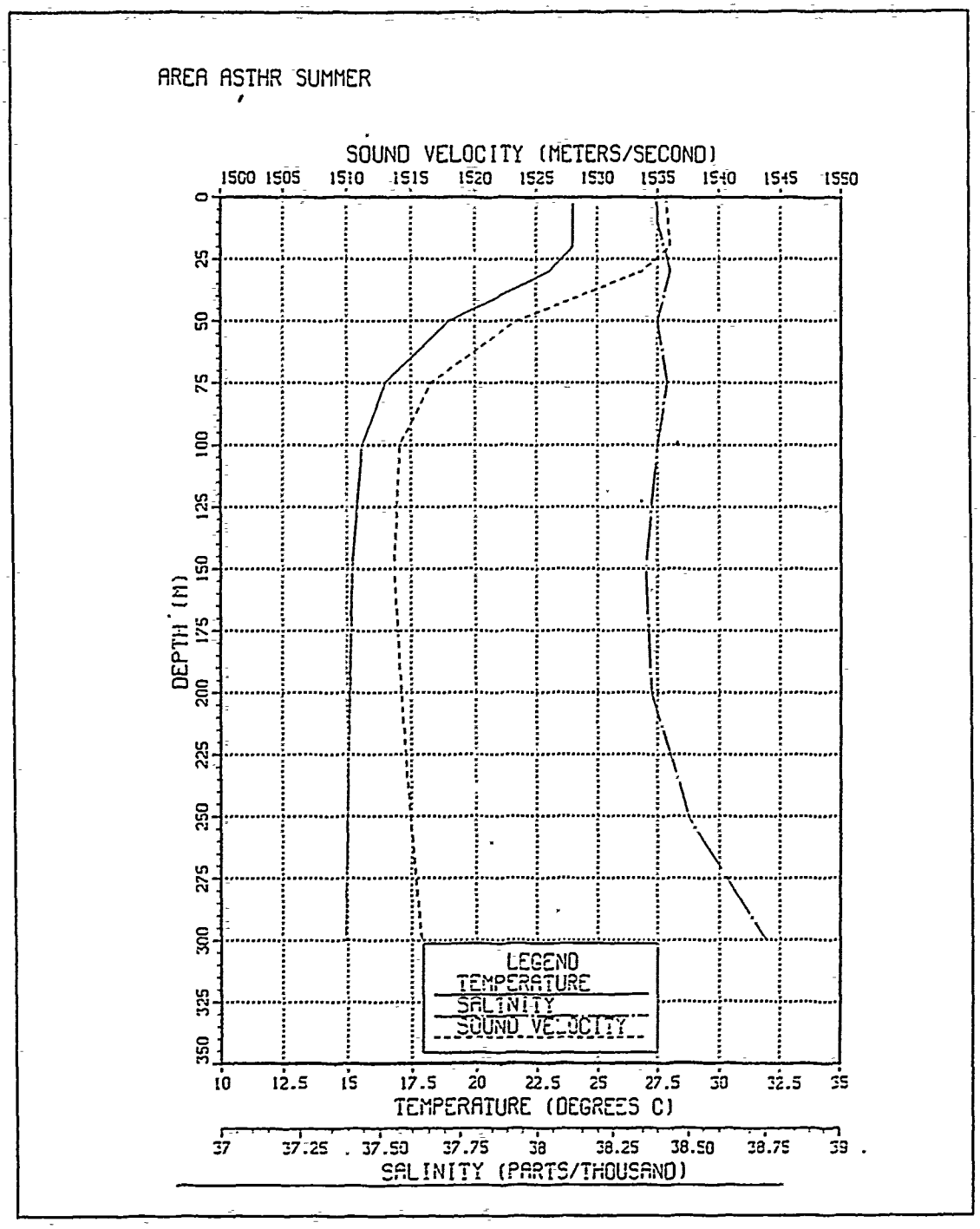

Figure 21. Temperature, salinity and sound speed profiles in area Alpha, summer : In this season the formation of a mixed layer of 25-40 m is more likely depending on weather effects.

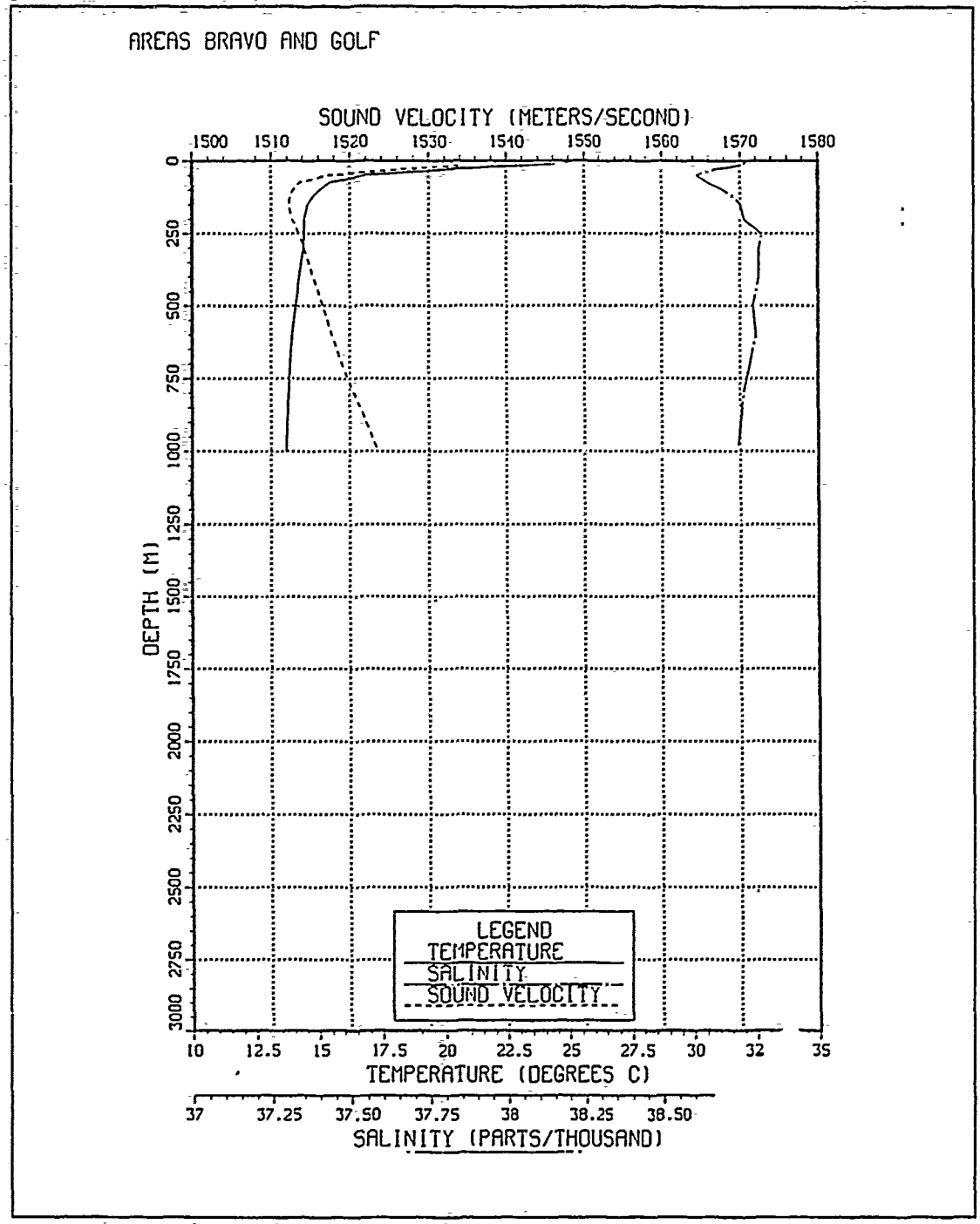

Figure 22. Temperature, salinity and sound speed profiles in areas Bravo and Golf, summer : The very hot surface preserves the AW being detected easily by its salinity minimum at 20-50 m. .

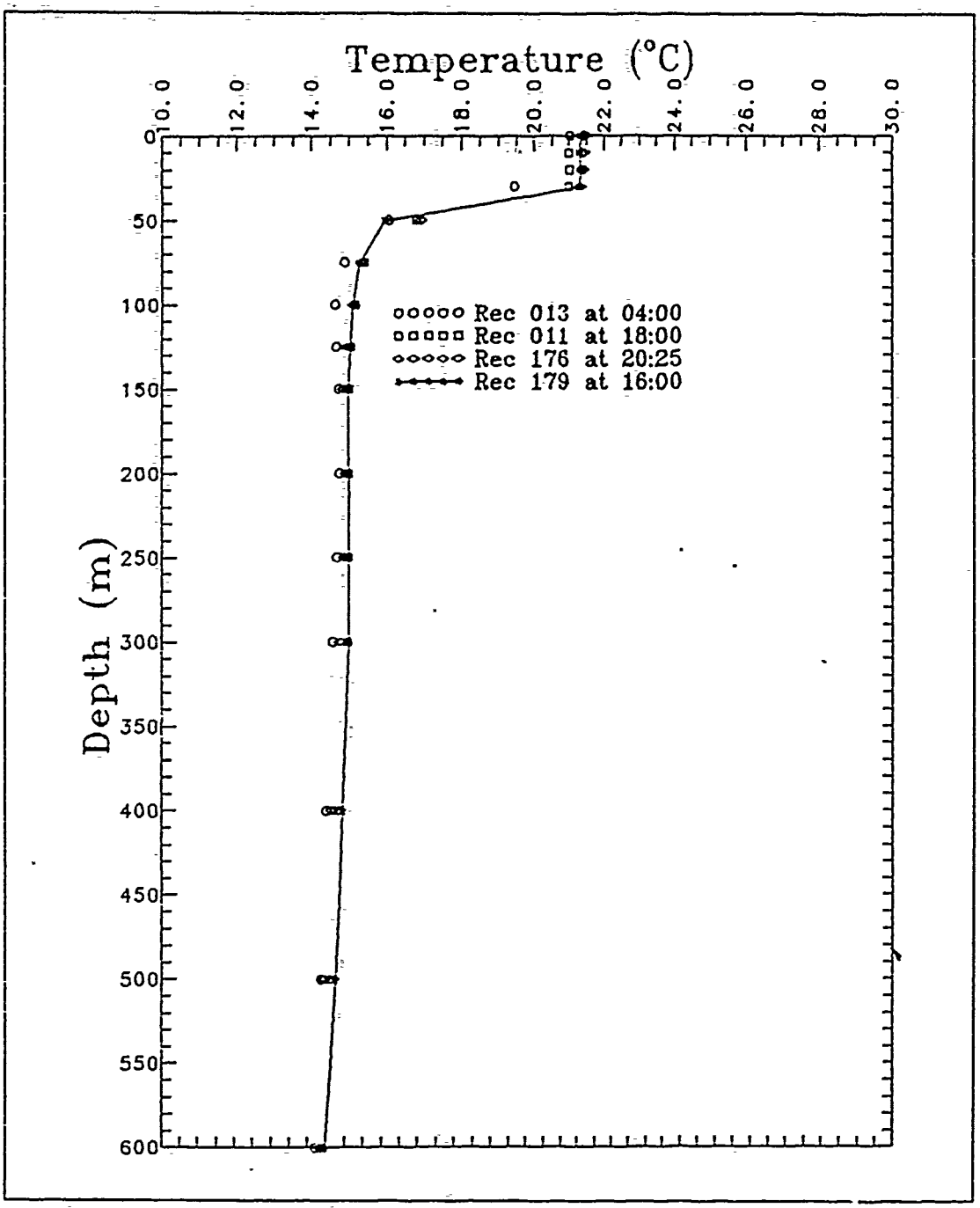

Figure 23. Synoptic temperature profiles in area Golf: The differences between four observations taken on 11 November 1980 are less than 0.5°C. The MLD is at 30 m.

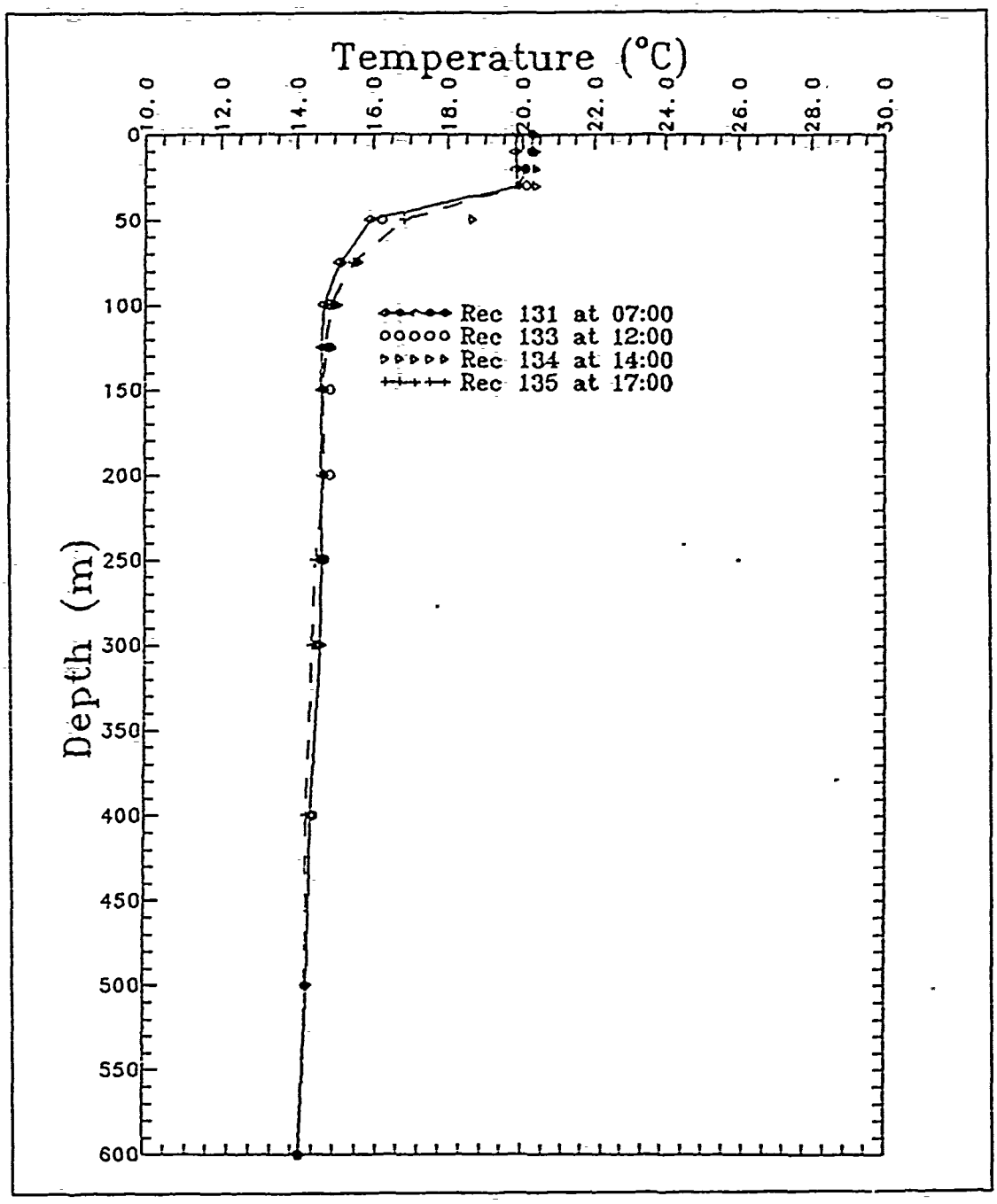

Figure 24. Synoptic temperature profiles in area Bravo: The distance between each of these observations, taken 19 November 1980, is 30 to 50 km. The differences are negligible.

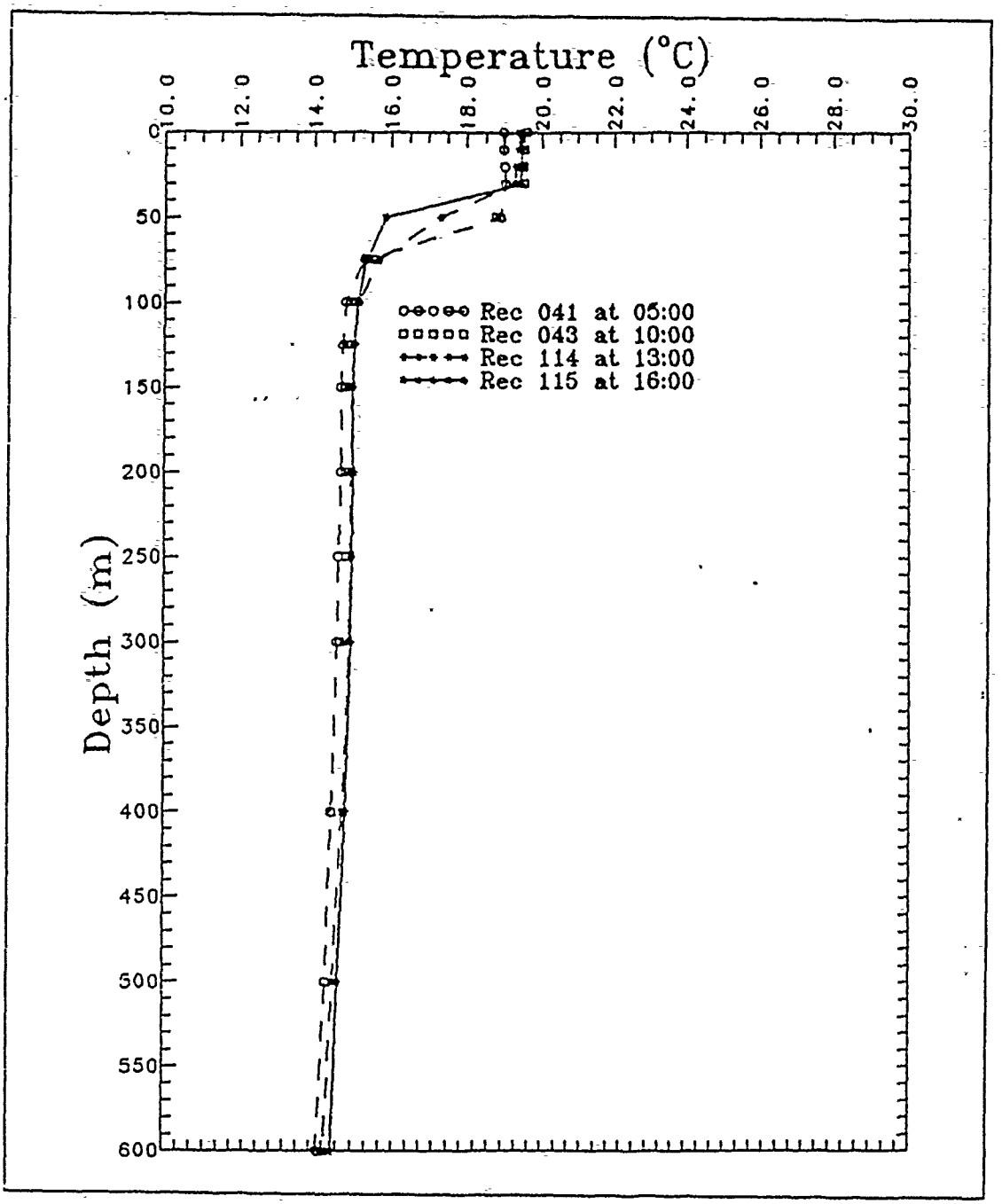

Figure 25. Synoptic temperature profiles in area Golf: Records taken at 05:00 (rec 041) and 16:00 (rec 115) on 26 November 1980 show a daily variation of 20 m in MLD and 0.5°C in temperature.

IV. ACOUSTIC ANALYSIS

A. ACOUSTIC MODELS

In this study the examination of sound propagation was performed by using two acoustic models available at the Naval Postgraduate School, the PE Model and the RAYMODE model. These two models represent two different techniques to calculate the propagation loss in a given oceanographic environment. A number of runs were compiled using both models and relative comparison performed.

Brief qualitative descriptions of the two models are given below and the implementations of bottom interactions into each model is discussed.

1. GENERAL

The purpose of these models is to provide attenuation for sound propagation into the sea. Specifically they are designed to calculate or estimate a number of propagation factors, the major ones being geometric losses (spreading and convergence), diffraction, absorption, scattering, leakage and boundary effects (surface and bottom). A number of methods, mostly empirical, for estimating the effects of some of the above factors in underwater sound propagation have appeared in numerous tactical publications in the years following the close of the second world war. Such methods were used by surface ships and submarines to estimate, for example, detection ranges of the day or best depth to avoid detection.

One of the next progressive steps was the implementation of ray theory. An immediate result of Snell's law, raytracing is a simple and fast method for determining sound paths either graphically or with the assistance of a computational machine.

Sound propagation in the sea can be expressed by the linearized, lossless and source free wave equation (Kinsler et al., 1984),

$$\nabla^2 p = \frac{1}{c^2}\frac{\partial^2 p}{\partial t^2} \tag{4.1}$$

Ray theory assumes that a solution to the wave equation (Kinsler et al., 1984) takes the form,

$$p(r,z) = A(r,z)e^{jw[t-\frac{\Gamma(r,z)}{c_o}]}$$

where A(r,z) is the spatially dependent pressure amplitude and Γ is a propagation vector locally normal to the isophase pressure surface; hence $\nabla\Gamma$ is the local direction of propagation,

$$\nabla\Gamma = \eta(\cos\phi\hat{r} + \sin\phi\hat{z}).$$

where ϕ is the local elevation angle of the ray path.

This solution, when applied to the wave equation (4.1), will result in:

$$\frac{\nabla^2 A}{A} - \frac{\omega}{c_o}^2 \nabla\Gamma \cdot \nabla\Gamma + \frac{\omega}{c}^2 - j\frac{\omega}{c_o}\left(\frac{2}{A}\nabla A \cdot \nabla\Gamma + \nabla^2\Gamma\right) = 0.$$

The above equation can be simplified by a number of approximations to provide a form known as the Eikonal equation,

$$\nabla\Gamma \cdot \nabla\Gamma = \eta^2,$$

where η is the refractive index,

$$\eta(x,y,z) = \frac{c_o}{c(x,y,z)}.$$

The assumptions and restrictions used in the derivation are that the pressure amplitude A is significant within a finite aperture beam and that the speed of sound varies little over distances compared to a wavelength, so

$$\frac{\nabla^2 A}{A} \ll \frac{\omega}{c}^2, \nabla^2\Gamma \ll \frac{\omega}{c},$$

and

$$\frac{\nabla A}{A} \cdot \nabla\Gamma \ll \frac{\omega}{c}.$$

The applied assumptions will make this method fail in cases where the pressure coefficient A has to decay rapidly from the center of the ray to the edges or the SSP has sharp changes. Such conditions are expected in caustics, shadow zones and the boundary between the ocean and some type of sediments. In this theory no diffraction of the sound at the edges is permitted as the acoustic energy trapped within a beam may not leak out of it. In contrast to normal mode theory, ray theory easily accepts different

densities in the sediment so reflection of the incident rays can be calculated. In general, ray theory is valid and useful when the frequency is high (short wavelength) and the SSP changes slowly.

The continued improvements of passive detection in frequencies below 1 kHz resulted in new theories and techniques, followed by a number of complicated acoustic models as electronic computing power became more available. Normal mode theory provides a solution to the wave equation using the summation of an orthogonal set of functions, each one being a solution to the wave equation. Each of these characteristic functions, called normal modes, has its own attenuation factor for the given boundaries. The final pressure field can be calculated after these modes have been combined additively. This solution is formally complete but it is difficult to calculate and interpret.

A simple approach (Kinsler et al., 1984) to normal mode theory can be performed by inserting a source term in the wave equation

$$\nabla^2 p - \frac{1}{c^2}\frac{\partial^2 p}{\partial t^2} = \frac{1}{2\pi r}\,\delta(r)\delta(z - z_0). \tag{4.3}$$

The solution for a sinusoidal wave propagating into a sound channel can be written as the summation:

$$p(r,z,t) = e^{j\omega t}\sum_n R_n(r)Z_n(z)$$

where :

$$\frac{d^2 Z_n}{dz^2} + \left(\frac{\omega^2}{c^2(z)} - k_n^2\right)Z_n = 0$$

and

$$R_n(r) = -j\pi e^{j\omega t} Z_n(z_0) H_o^{(2)}(k_n r).$$

For r > > 1 the solution will be :

$$p(r,z,t) = -j\sum_n \sqrt{\frac{2\pi}{K_n r}}\, Z_n(z_0)Z_n(z)e^{j(\omega t - K_n r + \frac{\pi}{4})} \tag{4.4}$$

where the Hankel function has been replaced by its asymptotic form, with the use of the far field approximation. The value of K_n and the depth dependence of $Z_n(z)$ can be evaluated from the appropriate boundary conditions and the given c(z).

The above values must be calculated for the whole propagation space which, due to the mathematical complexity, makes the use of a computer necessary except the most easy cases.

An alternative method to the above solutions is an approximation using a parabolic approximation to the wave equation. The wave equation can be expressed also as:

$$\nabla^2 p + k^2 p = 0,$$

where

$$k = \frac{\omega}{c}, \; k = k_0 \eta, \; \eta = \frac{c_0}{c}.$$

In cylindrical coordinates and with an omnidirectional source the wave equation is

$$p_{rr} + (\frac{1}{r}) p_r + p_{zz} + k_o^2 n^2 p = 0.$$

Then the acoustic pressure, p, can be expressed as

$$p = u(r,z) H_o^{(2)}(k_o r)$$

and use of the far field approximation yields

$$u_{rr} + u_{zz} + 2ik_o u_r + k_o^2 (n^2 - 1) = 0.$$

Finally, the assumption that $u_{rr} \ll 2k_o u_r$ gives the form

$$u_r = a(k_o,r,z)u + b(k_o,r,z)u_{zz}$$

which is amenable to numerical solution.

This method was introduced by Tappert and Hardin in 1973 who used in their work a computational technique called the Split Step Fast Fourier Transform (SS-FFT). The advantages of this method are that we do not need to solve for the entire field si-

multaneously as in the normal mode case but given initial conditions at some range r_o (close to the source) the solutions for larger r's can be obtained by increasing r incrementally. This is equivalent to neglecting back scattering as the solution for any range r has no effect on any previous range.

The disadvantages of this technique are errors introduced, if the initialization of the problem is not correctly selected, and if the requirement of SS-FFT for continuous functions of depth '-' are not met. The PE is inherently restricted to narrow spectral angles. A number published techniques ease the initialization problem by using raytracing or a directional pseudosource (see, for example, a discussion from Coppens, 1982) and a number of "wide angle" PE Models have been published. (see, for example, Lee et al., 1982).

2. RAYMODE

The passive RAYMODE model, U.S.Navy's standard acoustic model, uses an integration method developed in 1968 (Medeiros, 1985). A number of modifications and improvements have been added, such as mode summation and low frequency paths into the sediment. The model used in this study was the Passive RAYMODE, specifically the 1987 baseline edition. This model utilizes ray and normal mode theories in an attempt to minimize errors and computer run time. Up to four different paths of sound propagation can be formed and the total pressure field is defined by summing the contributions over all paths. Boundary interactions are calculated by invoking a number of other models, like BLUG.

The inputs to the program are:

Sound speed profile,

Bottom depth and bottom type (BLUG or NAVOCEANO),

Wind speed,

Source depth,

Receiver depth,

Sonar D/E angle and vertical beamwidth,

Frequency,

Range span and range step.

The program will process these data to produce a piecewise SSP and then partition it into areas of different wave number (Medeiros, 1985). These wave number domains represent different paths such as the surface duct or the deep sonic layer or sediment paths (Fig. 26).

Based on the entered data for each path the model will calculate two parameters : the number of cycles that exist between source and receiver, and the number of modes existing in each wave number interval. From these parameters there are four different ways that the algorithm will proceed. If the number of modes is less than 10, the normal mode summation technique is used. If the propagation angle exceeds a computed limit, then a bottom bounce integration is used. For paths employing neither of the above cases the original method of RAYMODE integration is used (Raytracing). Finally, if the frequency is more that 3 kHz, a fast integration subroutine is used (High frequency RAYMODE).

For each path absorption is calculated as well as the relative phase of each ray. Bottom interactions are computed using models including the Naval Oceanographic Office MGS algorithm (NAVOCEANO charts), the BLUG (Bottom Loss Upgrade) and a low frequency bottom loss model developed by G.Gustave (NUSC, 1987). The surface loss is calculated according to a Surface Reflection Coefficient Model. For the present time no range dependency is assumed, neither for the SSP nor bottom depth. RAYMODE at the present time uses only a flat bottom and a single SSP.

3. PE Model

This is a relative new model based on the parabolic equation approximation. It is designed to operate at relatively low frequencies as computer run time for higher frequencies, more than 1000 Hz, increases significantly. The PE Model is not restricted by depth dependency along the axis of propagation (range r) nor by horizontally changing sound speed profiles. It is best used whenever a duct-like transmission occurs, for example, in the Arctic, shallow channels, etc., or where non-homogenities in the water mass exist. The entered parameters in this model are:

Sound speed profiles,

Bottom depth (discrete depths),

SSP and attenuation profile in the sediment or bottom loss vs grazing angle (BLUG output),

Source depth,

Receiver depth,

Source vertical beamwidth,

Range step (increment).

The surface is assumed to be a pressure release boundary with reflection coefficient -1, the bottom is assumed to be a continuation of the water mass. After the initial boundary conditions have been specified the program will march the solution forward

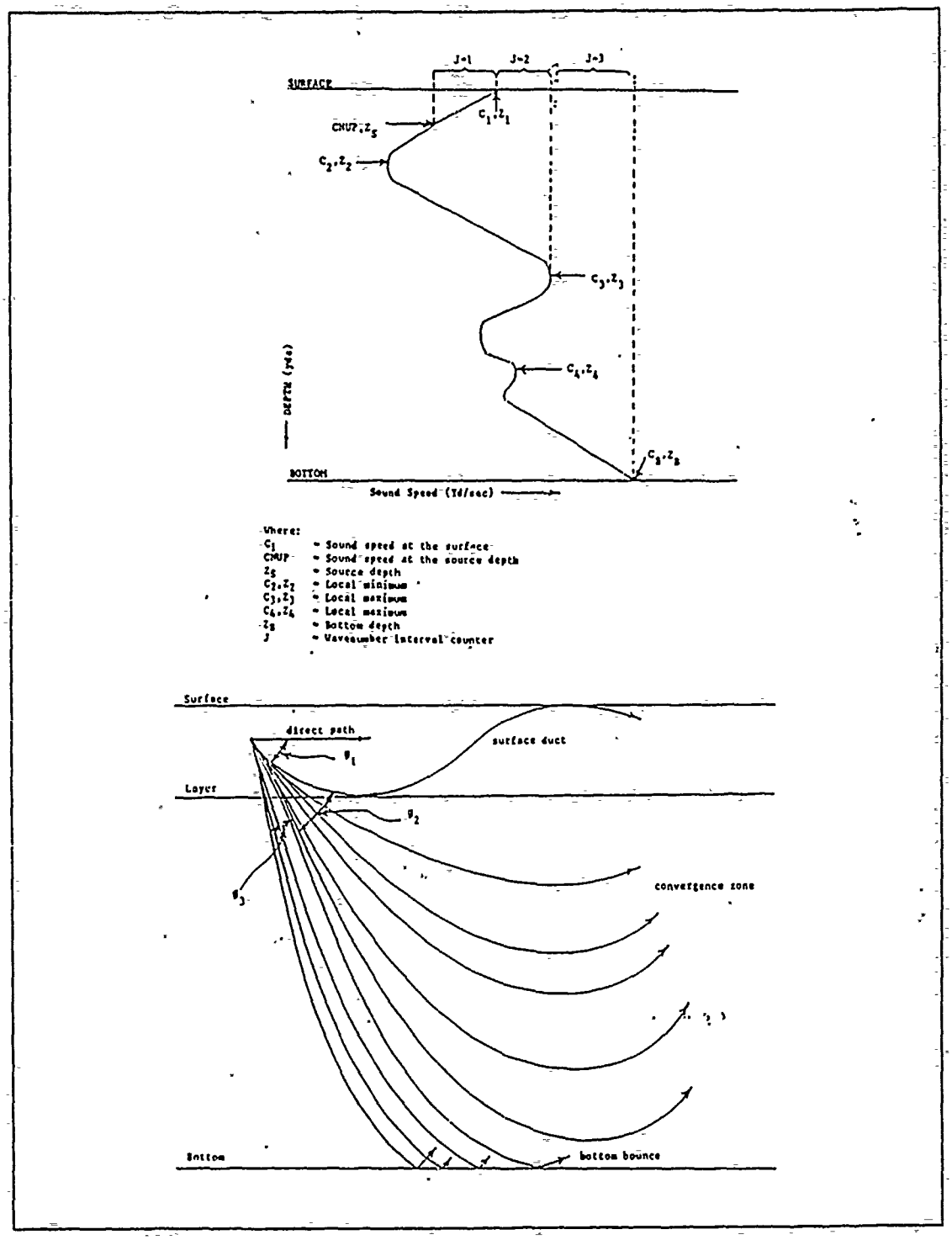

Figure 26. Partition to wavenumber domains (RAYMODE): The equivalence between duct-like paths and rays (from Medeiros, 1985).

in range using a split - step fast Fourier transform algorithm (SS-FFT) until the entire field has been calculated (Tappert and Hardin, 1973).

4. Bottom Loss Models

The influence of the sea bottom in sound propagation is modeled using two different approaches. The earlier encompares the geo-acoustic models where the sea bottom is assigned a number which represents the observed acoustic behavior of the sediment. Such a representation are NAVOCEANO curves, used by the U.S.Navy for high frequency operation (> 1000 Hz). Nine different loss curves are used to characterize the types of existing sediment. These curves represent loss per bounce (dB/bounce) for only reflected rays. Type 1 is the most reflective and Type 9 the most absorbing.

For low frequencies, where both reflection and refraction into the sediment have to be calculated, the Bottom Loss Upgrade (BLUG) model is used by most of the Navy's models. In the BLUG model a partition of the oceans is done similar to the NAVOCEANO model, but instead of loss curves a total of nine geo-acoustic parameters has been assigned to each area. These parameters are used by the BLUG program to produce a compressional sound speed profile into the sediment as well as an attenuation profile (Fig. 27). This will permit the acoustical model to incorporate the bottom loss and refraction by using a continuous profile into the water and sediment.

The BLUG output is given in loss per bounce vs grazing angle for each frequency and it is used, in this format, in the PE Model. RAYMODE uses an internal subroutine for the same task. The attenuation into the sediment is calculated from the formula (Medeiros, 1982):

$$a(z,f) = a_0(z,f) \times f_k.$$

This first power relationship between attenuation and frequency was made after the work of Hamilton in his numerous reports. Hamilton (1971 and 1974) derived this relationship in an empirical way from the collected data over a wide but relative high frequency spectrum, without any theoretical basis.

The density of the sediment is constant because any changes do not effect the propagation significantly. Finally a theoretical thin layer at the surface (Fig.27) is used to remove any discontinuities in the boundary between the water and the bottom.

The second and later approach is the geo-physical model where reflection, refraction and attenuation into the sediment must be calculated by physical parameters for each area. Recently a number of authors (e.g., Kibblewhite, 1989) reported a number

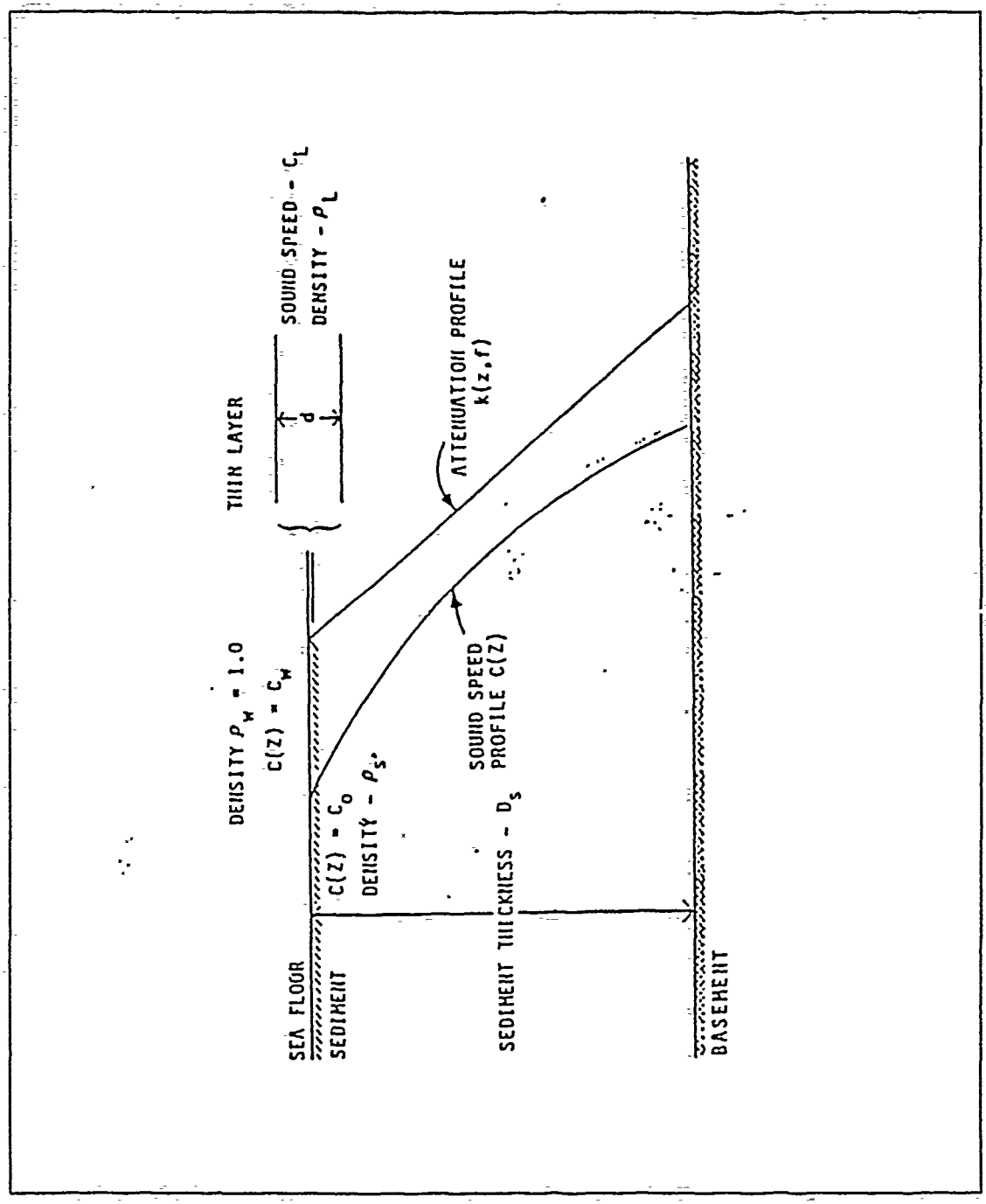

Figure 27. Simplified geo-acoustic model: The bottom SSP and attenuation profiles are calculated by the given parameters for each area using internal (RAYMODE, ASTRAL) or external (PE Model) subprograms (from Medeiros, 1982).

of experiments where the more fundamental analysis from Stoll (1980), using Biot (1962) theory, seems to be more adequate. Stoll (1980) cites a relation of the attenuation coefficient with the square of the frequency for fully saturated sediments.

The BLUG model is undergoing reconstruction whereby the attenuation will be related to frequency between the first and second power, depending on the bottom quality (type and depth).

B. APPLICATION OF DATA

1. Sound Speed Profiles

Two different sound profiles for both shallow and deep water columns were selected to represent the summer and winter seasons. Area Alpha is represented with the profiles representing the averaging of the winter or summer records, respectively. The main characteristic in the winter is a smooth positive sound speed gradient resulting in a half channel propagation (Fig. 28). Hence only reflected surface reflected (RSR) and reflected bottom refracted (RBR) rays will propagate. Higher frequencies will attenuate more rapidly due to enhanced scattering from surface reflections (Urick, 1983). In the summer a mixed layer exists to a depth of 20 m resulting in a slight positive sound speed gradient, followed by a sharp decrease (Fig. 28). A weak sound channel exists with an axis at 150 m but is bottom limited so that this will not be a viable propagation path. Using the formula,

$$f = \frac{2 \times 10^5}{D^{\frac{3}{2}}}$$

to determine the low-frequency cut off in the mixed layer (Kinsler et al., 1984) we find a cut off frequency of 2.2 kHz, a transition range of less than 200 m, and a skip distance of about 3.6 km. For both deep areas, Bravo and Golf, the representative profiles for each season were selected from among the existing records in order to examine the most significant cases (Fig. 29). The selected SSPs are common for both areas as no noticeable spatial differences occur and are shown in Figures 29 and 30. In the winter isothermal conditions will create a half channel. The presence of LIW will create a small "knee" along the SSP between 200 and 500 m as the high salinity of LIW will increase the sound speed in a small amount. In contrast, summer heating changes the upper 200 m, as noted before (Fig. 22), and increases the sound speed. Hence in the surface the sound speed is about 1540 m/s and a deep sound channel is formed with a height of 2000 m and an axis at 150 m (Fig.29). In this channel the transition range is about 8 km and the skip dis-

tance 30 km. For paths with more than 2200 m depth CZ propagation is expected at a skip distance of 29.5 km with a transition range of 8 km. The SSP used for areas Bravo and Golf for winter and summer can be seen in Figures 29 and 30 (upper 600 m).

2. Bottom Paths and Parameters

Using the appropriate data bases (BLUG and NAVOCEANO), all three areas in this study were found to be characterized by a fast bottom with a sound speed ratio along the boundary (water to sediment sound speed) of 1.091 for the continental self (Alpha) and 1.005 for the Eastern Ionian Basin. Area Alpha has a reflective bottom (Type 2 for NAVOCEANO charts) for frequencies over 1 kHz. Areas Bravo and Golf over the Ionian basin experience significant bottom reflection losses (Type 8, NAVOCEANO charts). The loss per bounce for each incident angle and frequency, as produced by the BLUG model, can be seen in Figure 31.

A number of paths were selected to simulate the most likely sea sediment morphology in the region (Figs. 2 and 14). The first path represents shallow area Alpha and is assumed to be a flat bottom with a depth of 120 m. The second path is a combined path which starts over the continental slope and continues onto the shelf in such way that one third is in area Bravo and the rest in Alpha. Path three is also a combined path which starts at a depth of 3000 m and extends from area Bravo towards the shelf with a sharp rise. It is the only path were the depth at the source position exceeds 2300 m and for which convergence zone propagation exists. Finally, path four is a sloping bottom case which starts at a depth of 2000 m and decreases smoothly towards shore (100 m) into area Golf.

3. Source, Receiver Data

Three depths were selected for the source according to the MLD and bottom depth along each path. For the shallow paths (No 1 and No 2) these depths are 10 and 60 m. For the remaining paths 10 and 150 m were selected. The source frequencies are defined to be 50, 250, 500 and 1000 Hz. The receiver depths were also set to 10 and 60 m. These definitions of source and receiver depth were made in order to consider all the available depth configurations with respect to MLD and DSC axis. A standard Figure of Merit (FOM) of 80 dB was selected to produce relative results between seasons.

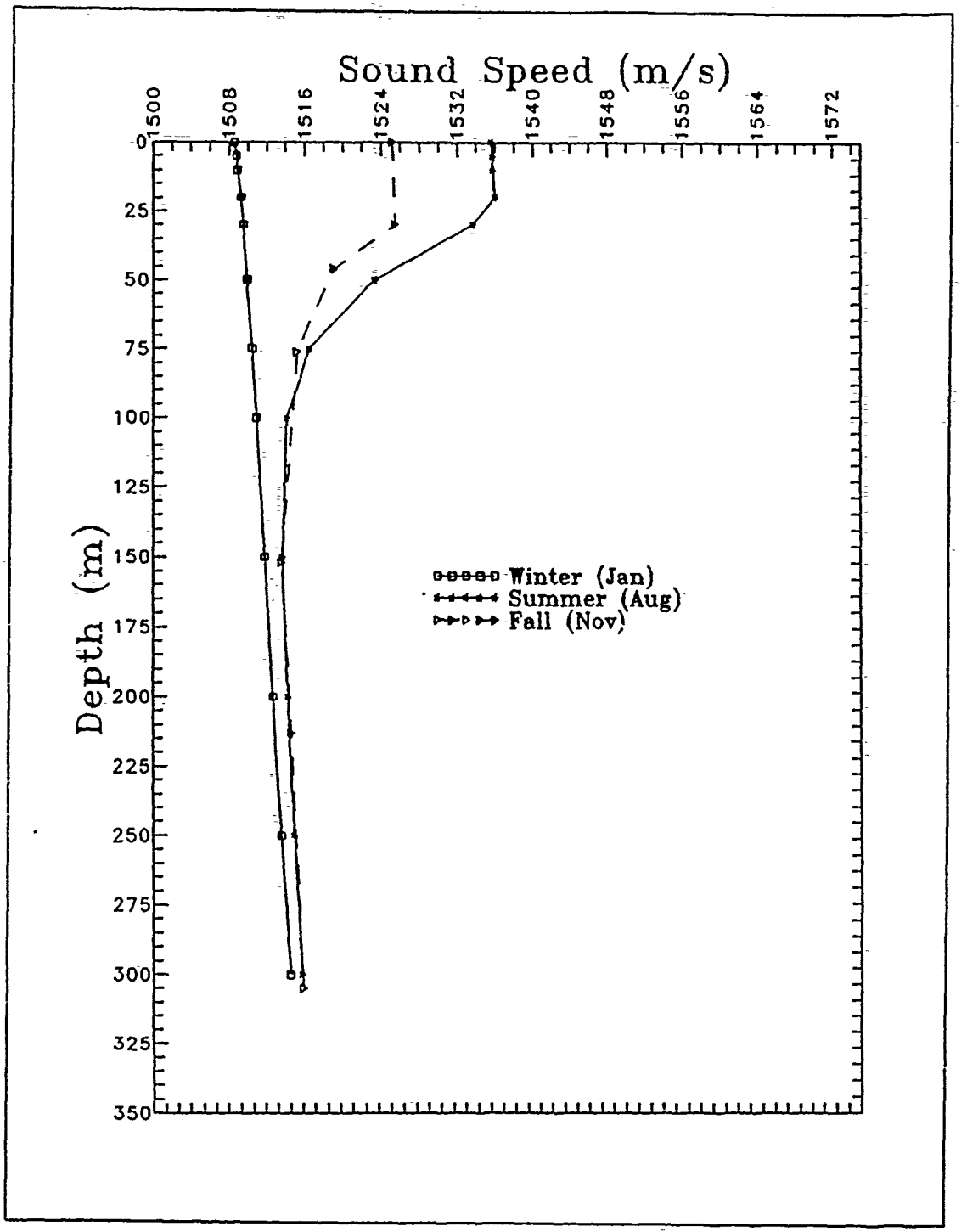

Figure 28. Sound Speed Profiles for area Alpha: Summer, fall and winter profiles are shown for comparison.

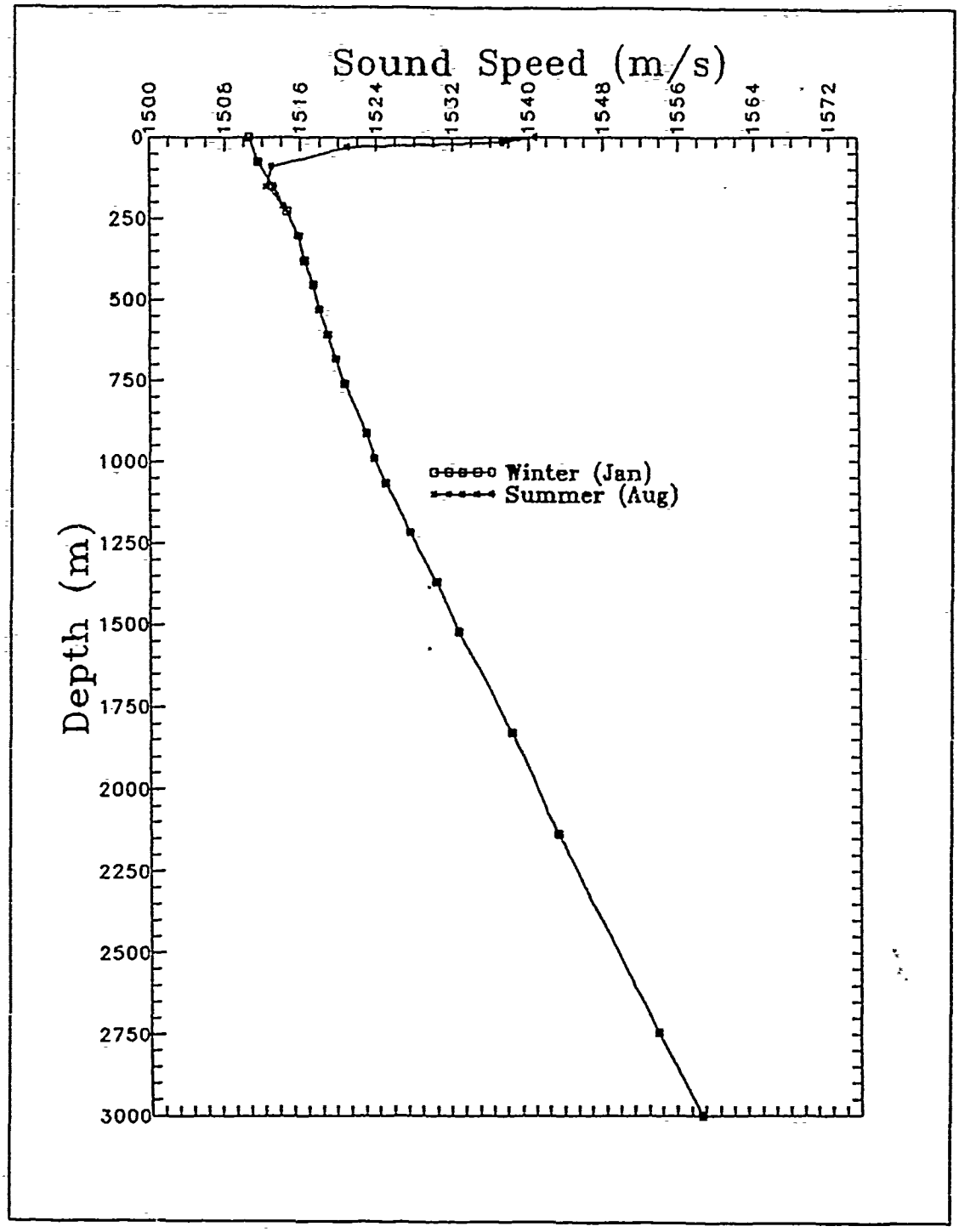

Figure 29. Sound Speed Profiles for areas Bravo and Golf: Both summer and winter profiles are shown for comparison.

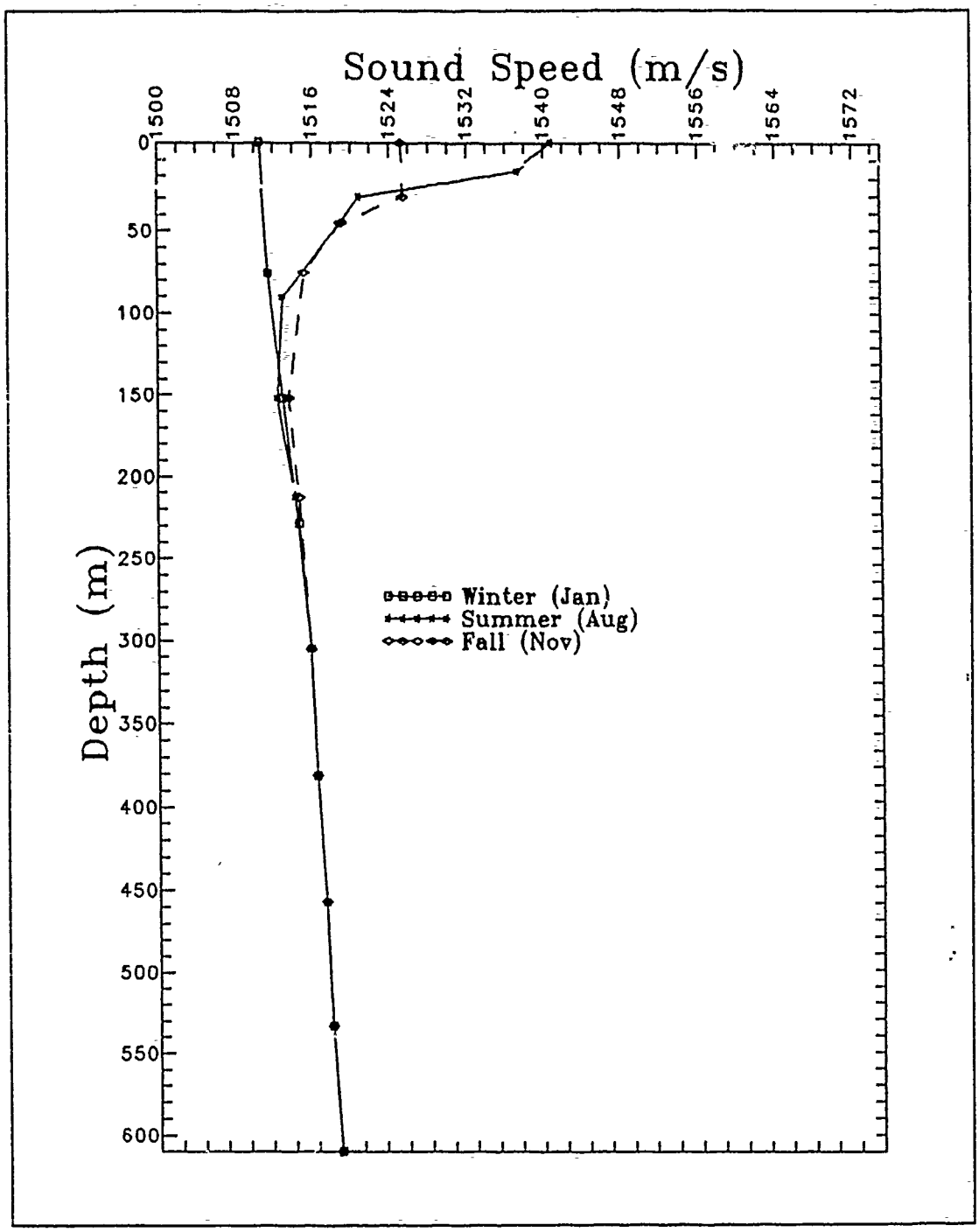

Figure 30. Sound Speed Profiles in areas Bravo and Golf (Detail): The differences between the two seasons (winter-summer) seems to occur in the upper 200 m.

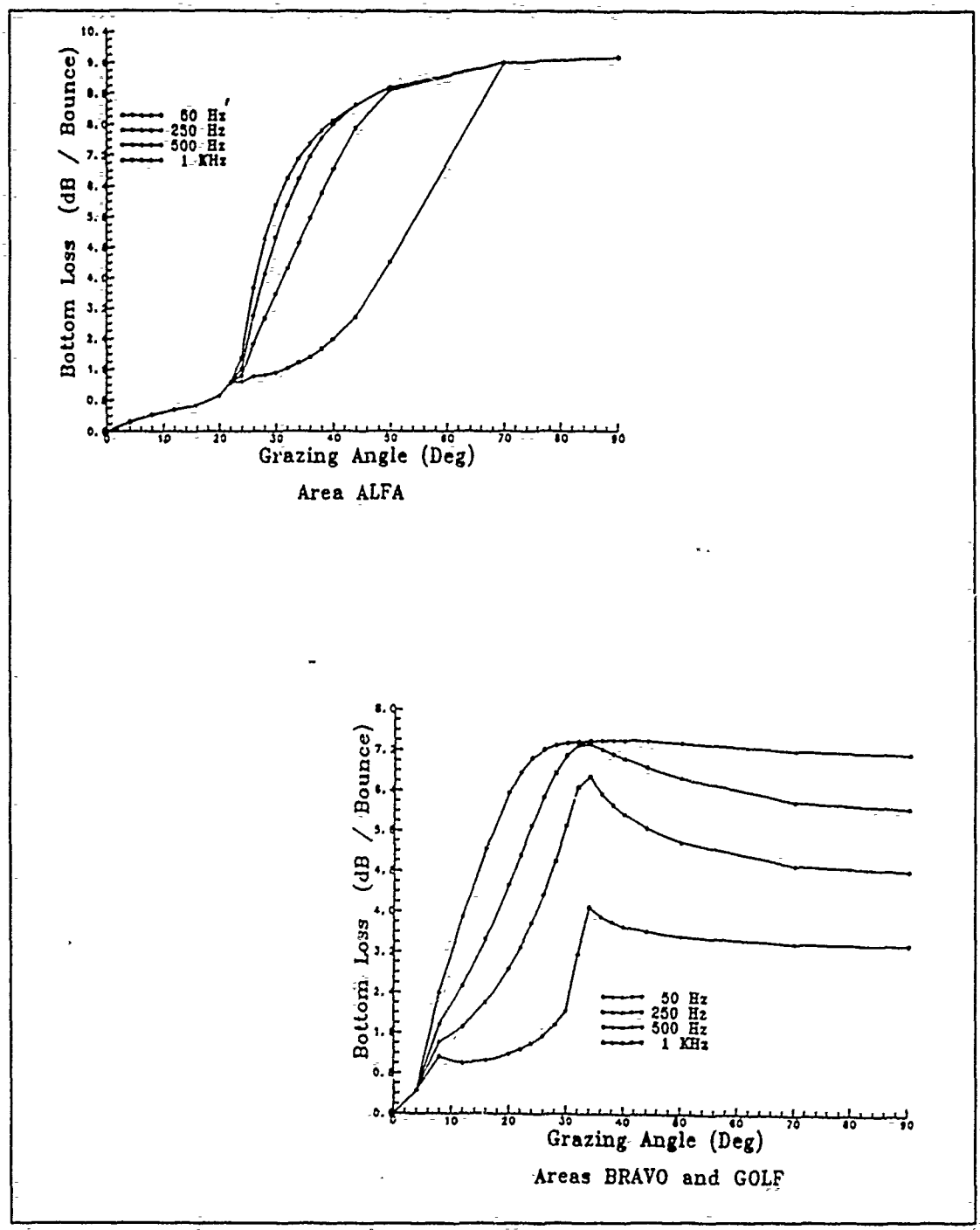

Figure 31. BLUG output for shallow and deep areas: Deep areas Bravo and Golf have significantly more absorbing sediment than shallow area Alpha for low to moderate grazing angles.

C. ANALYSIS OF RESULTS

1. BLUG Output

The calculated attenuation for each selected frequency and grazing angle shows a critical angle of about 24° for the continental shelf (Fig. 31). This is in accordance with the water sediment sound speed ratio in the boundary (1.091). Rays less than this critical angle suffer a loss less than 2 dB per bounce while those greater than this angle experience a loss exceeding 6 dB. Similarly for the deep area the critical angle is about 6° which is also consistent with the 1.005 speed ratio as above. Because no other sources are available to verify these sea sediment parameters, these data were used as input to the two models. The BLUG uses standard values for this ratio, c_w/c_s, with no seasonal variation. In shallow areas, where the seasonal variation can penetrate the whole water column, this ratio changes and some errors are expected as the sound speed in the sediment will be less affected. For the most cases in this study the seasonal changes in sound speeds in the water close to the bottom are small (Fig. 28) and errors due to the ratio c_w/c_s are negligible. This remark is only for the PE Model as the RAYMODE model calculates the ratio from the data given from the BLUG database directly (Medeiros, 1985).

2. Path No 1: PE Model and RAYMODE

This path, a flat shallow area, is used in order to examine both models simultaneously in a shallow waveguide case. (RAYMODE always uses a flat bottom). The results from both RAYMODE and PE Model (Figures 32 to 34) in the winter show the losses are in agreement within 3 dB for all the same combinations of receiver and source depths. The big difference occurs in summer where the PE Model shows a sharp loss of 10 dB/km and then a number of refracted / reflected rays decreasing along the path (less echo) (Figures 35 and 36). In contrast, RAYMODE shows a slowly increasing transmission loss of about 1 dB/km (Figures 37 and 38). Also for the cases where the source and receiver are at the same depth, the RAYMODE model predicts a decrease in the loss from 5 to 10 dB (stronger echo). The PE Model shows no difference for this case in the direct path but the group of RBR rays is more discrete. By neglecting the bottom interactions (fully absorbing), the PE Model calculated a loss similar to the previous runs for ranges close to source (< 5 km), which is the direct path source-receiver (Fig. 39). A number of selected runs is included in Appendix A.

3. Path No 2: PE Model

In this relative shallow channel with anomalous morphology the PE Model for both seasons shows a loss 80 dB in less than 5 km for the direct path at 50 Hz. A number

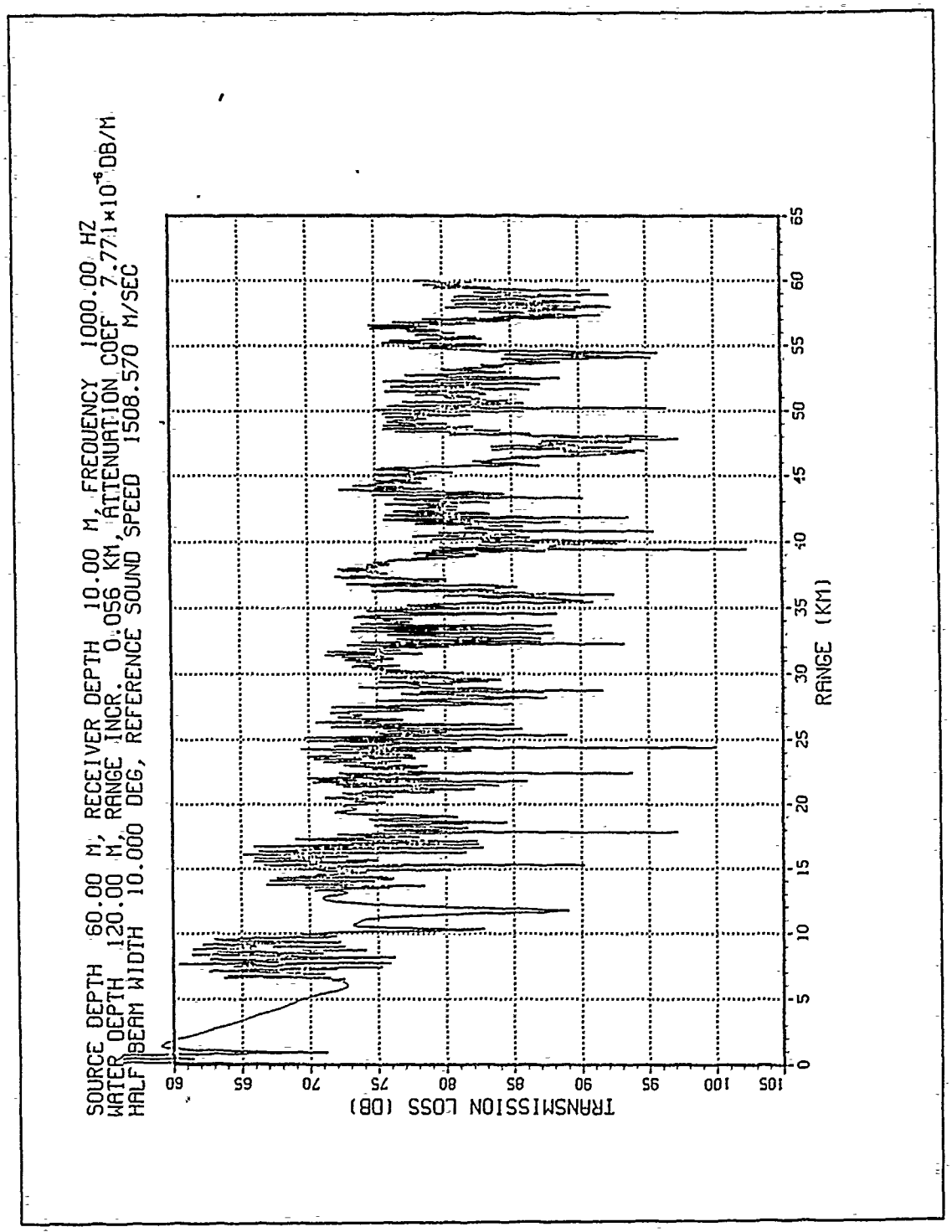

Figure 32. Path 1, PE Model at 1000 Hz winter.

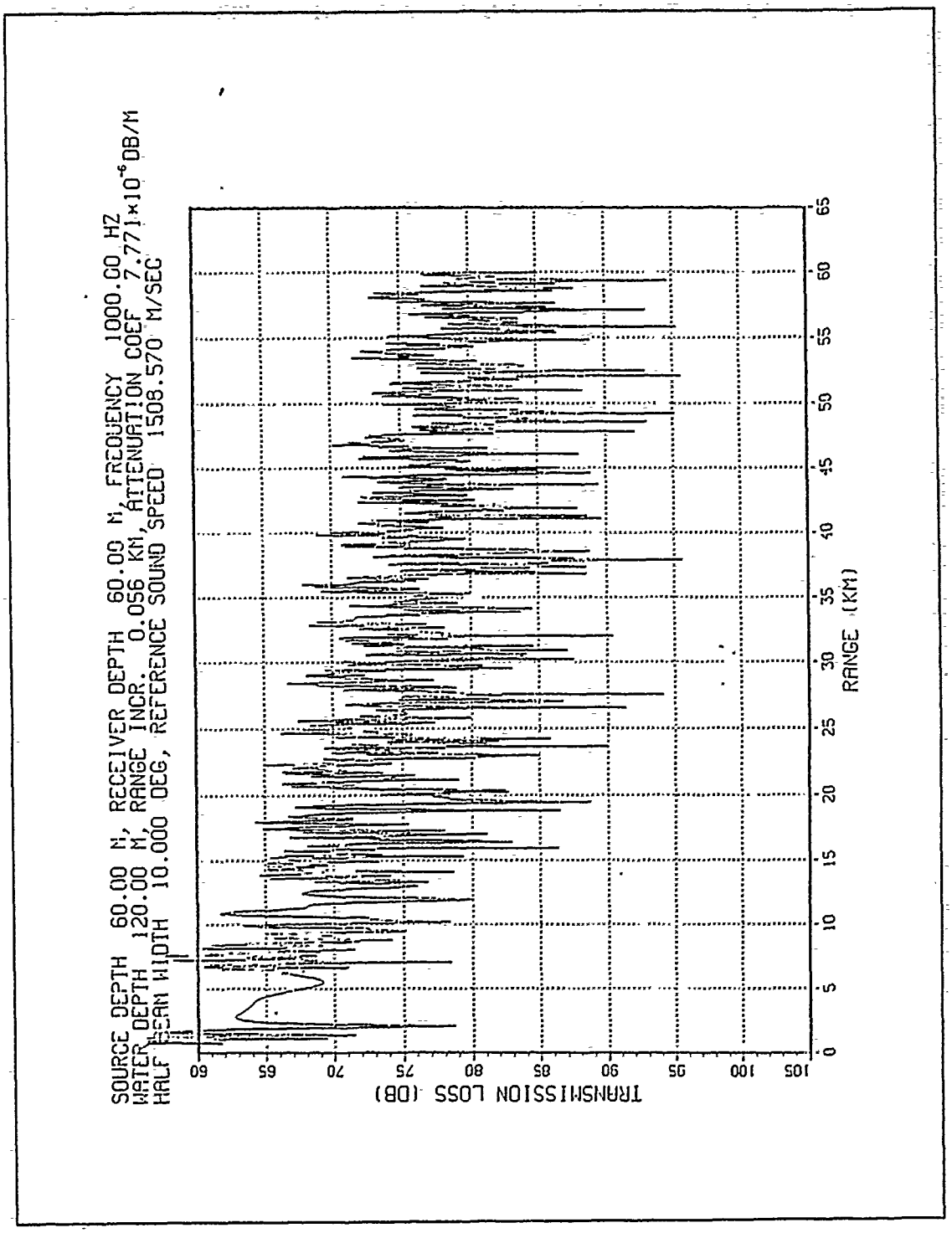

Figure 33. Path 1, PE Model at 1000 Hz winter same depth TX-RX.

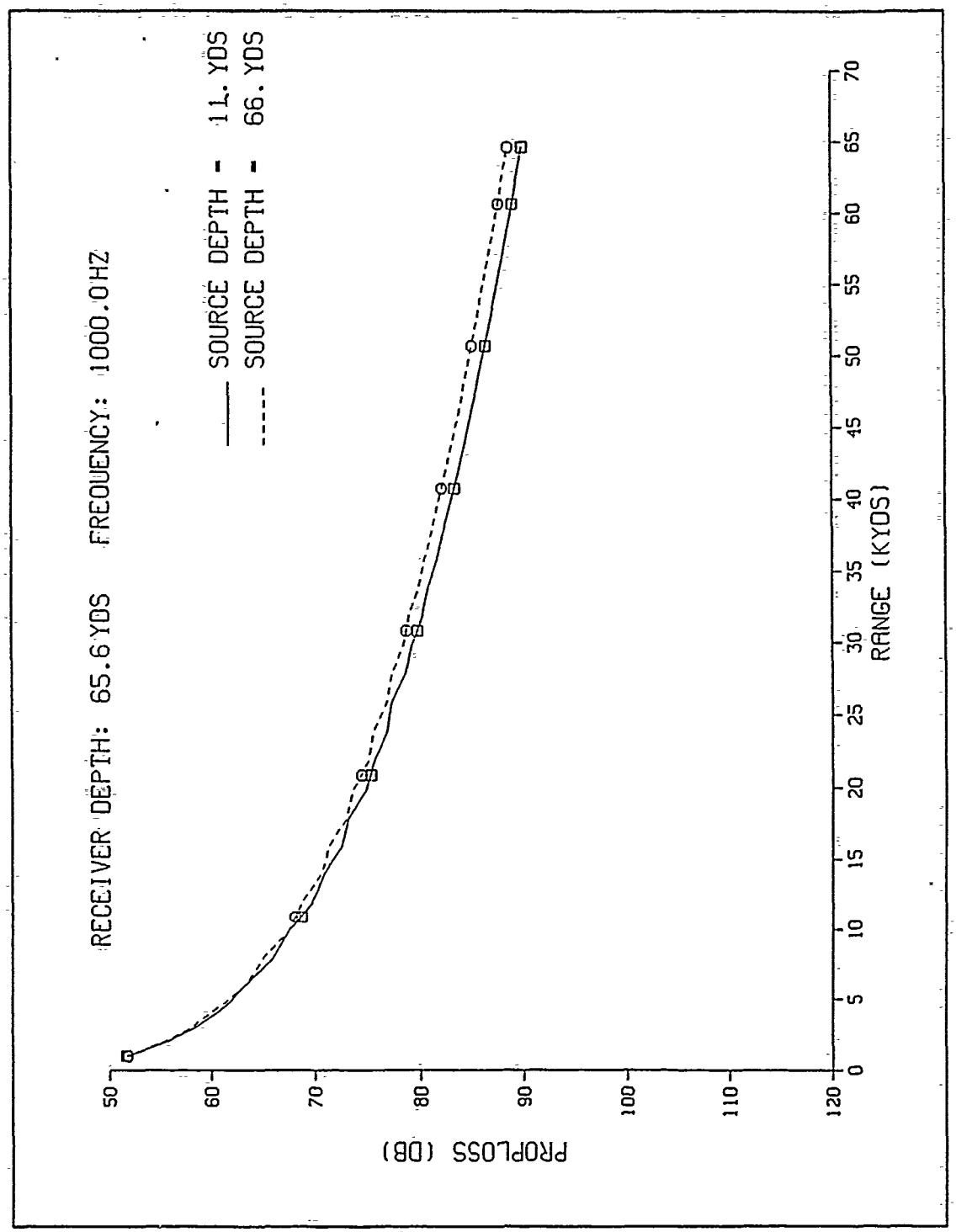

Figure 34. Path 1, RAYMODE at 1000 Hz winter.

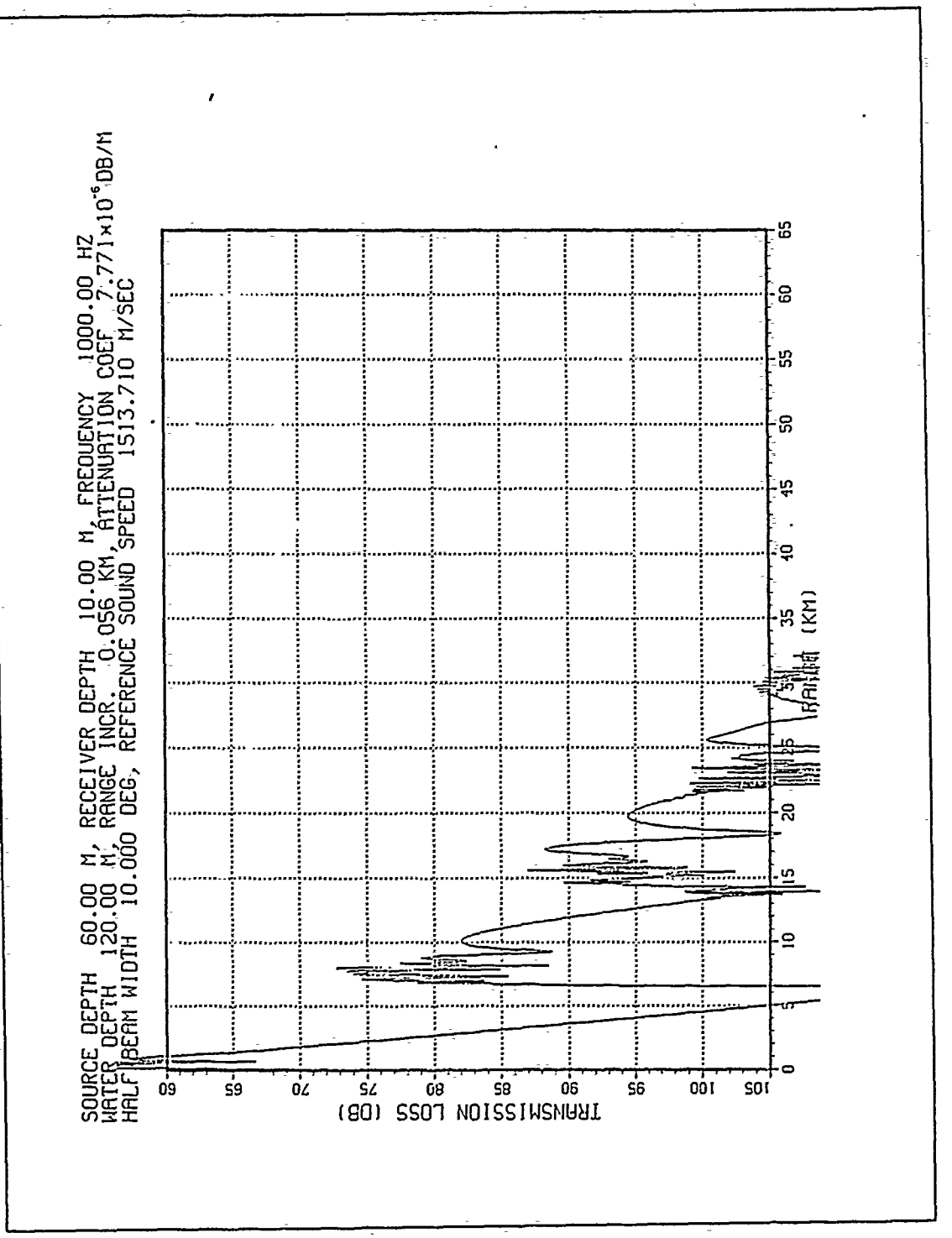

Figure 35. Path 1, PE Model at 1000 Hz summer.

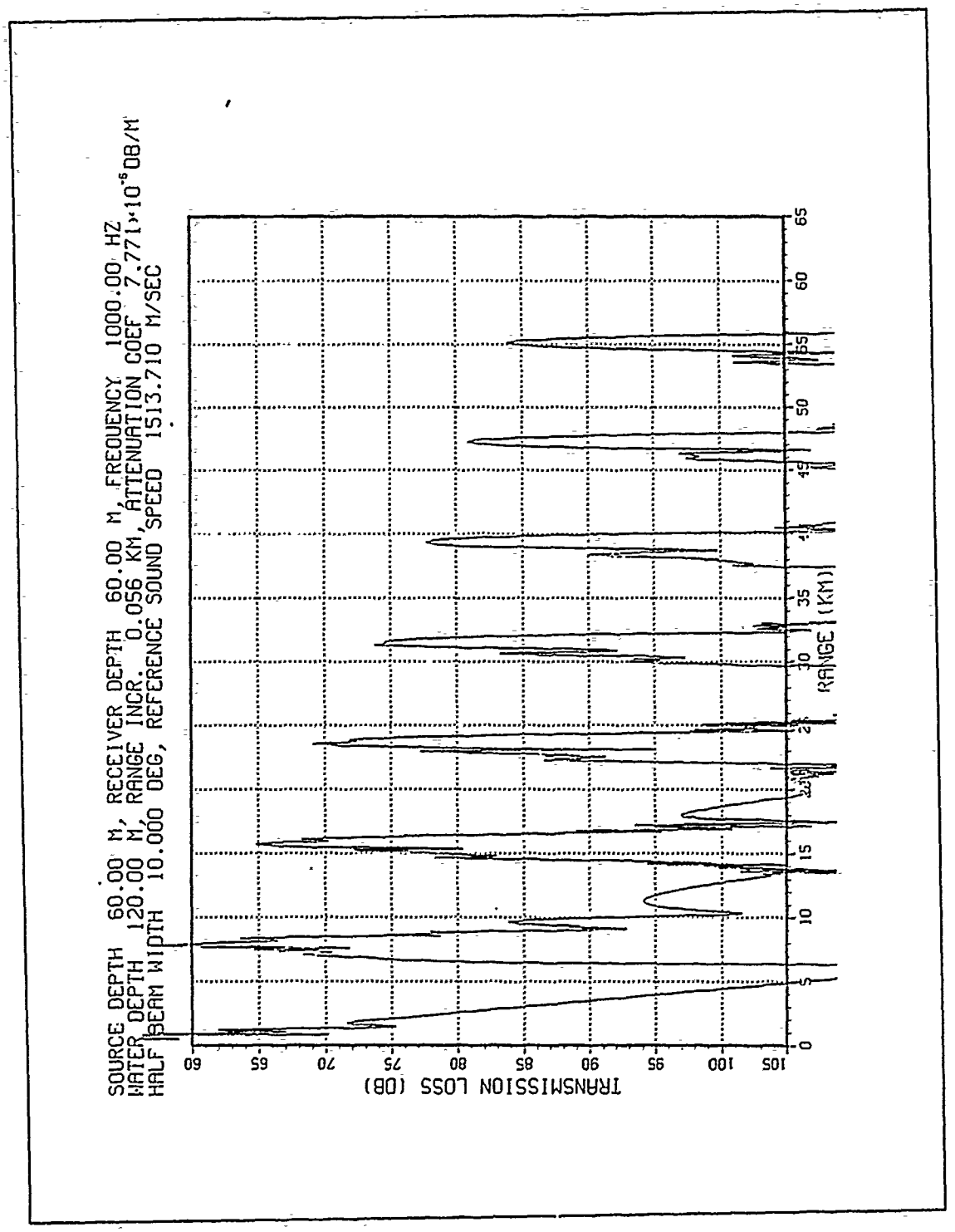

Figure 36. Path 1, PE Model at 1000 Hz summer same depth TX-RX.

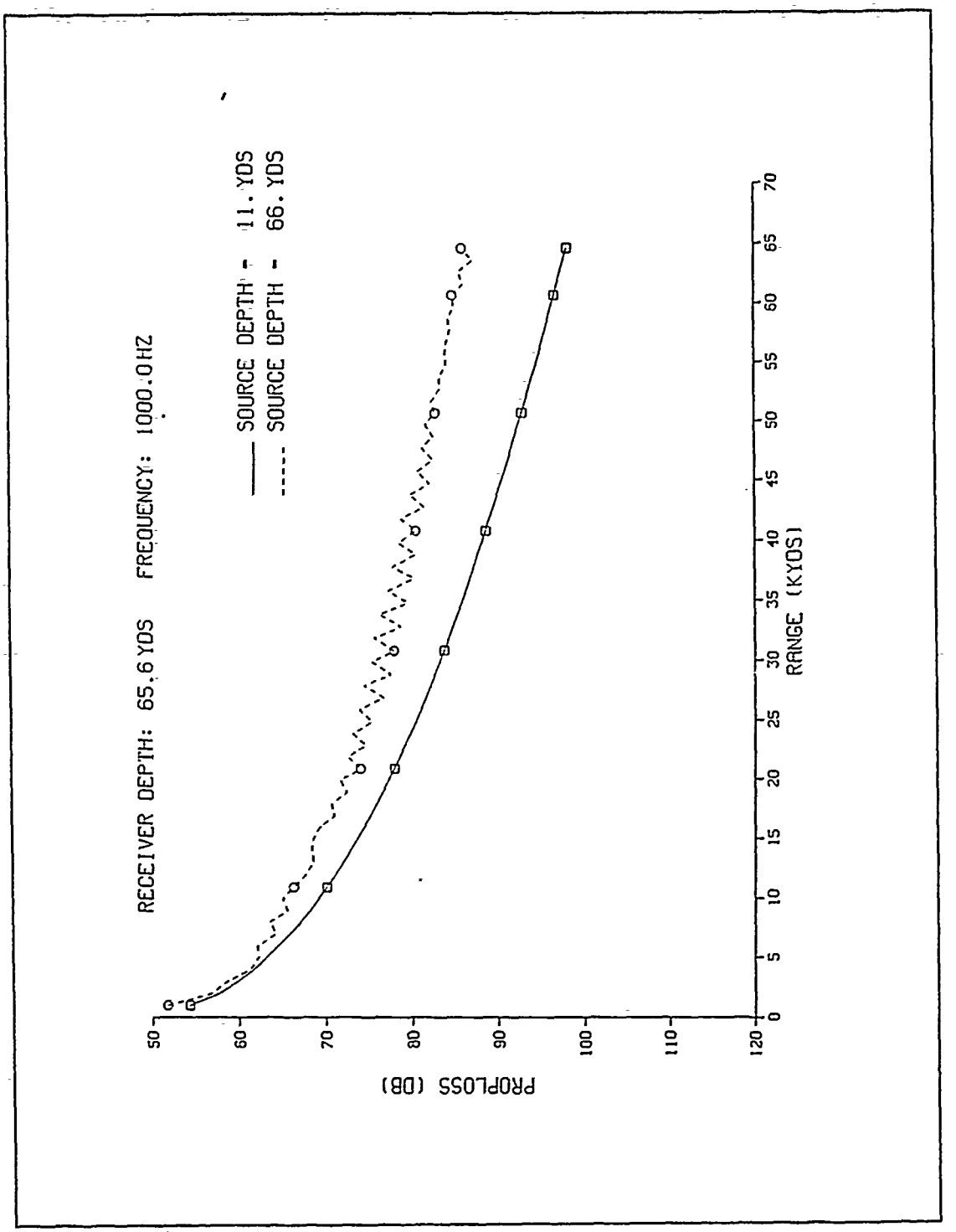

Figure 37. Path 1, RAYMODE at 1000 Hz, summer and receiver at 60 m.

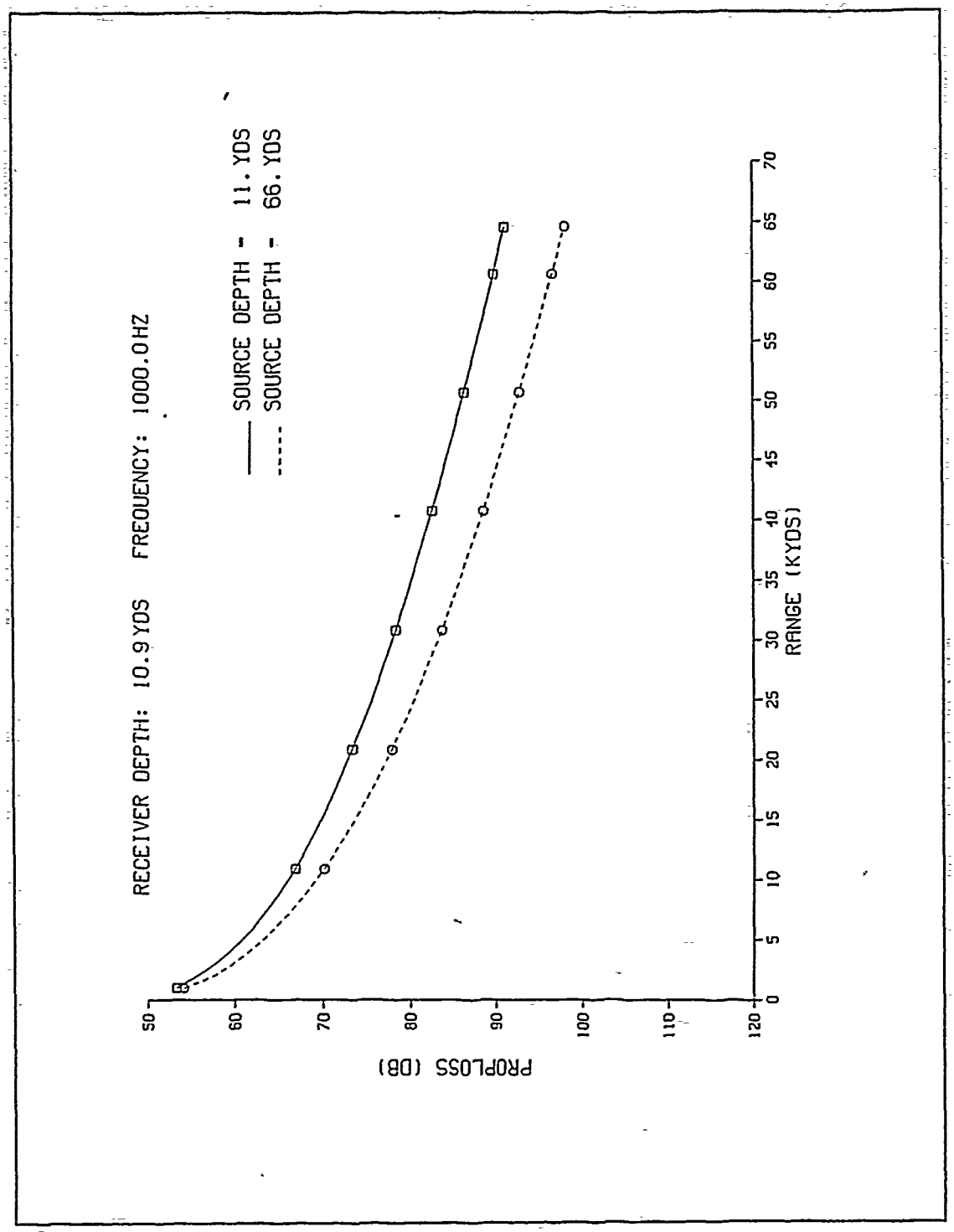

Figure 38. Path 1, RAYMODE at 1000 Hz, summer and receiver at 10 m.

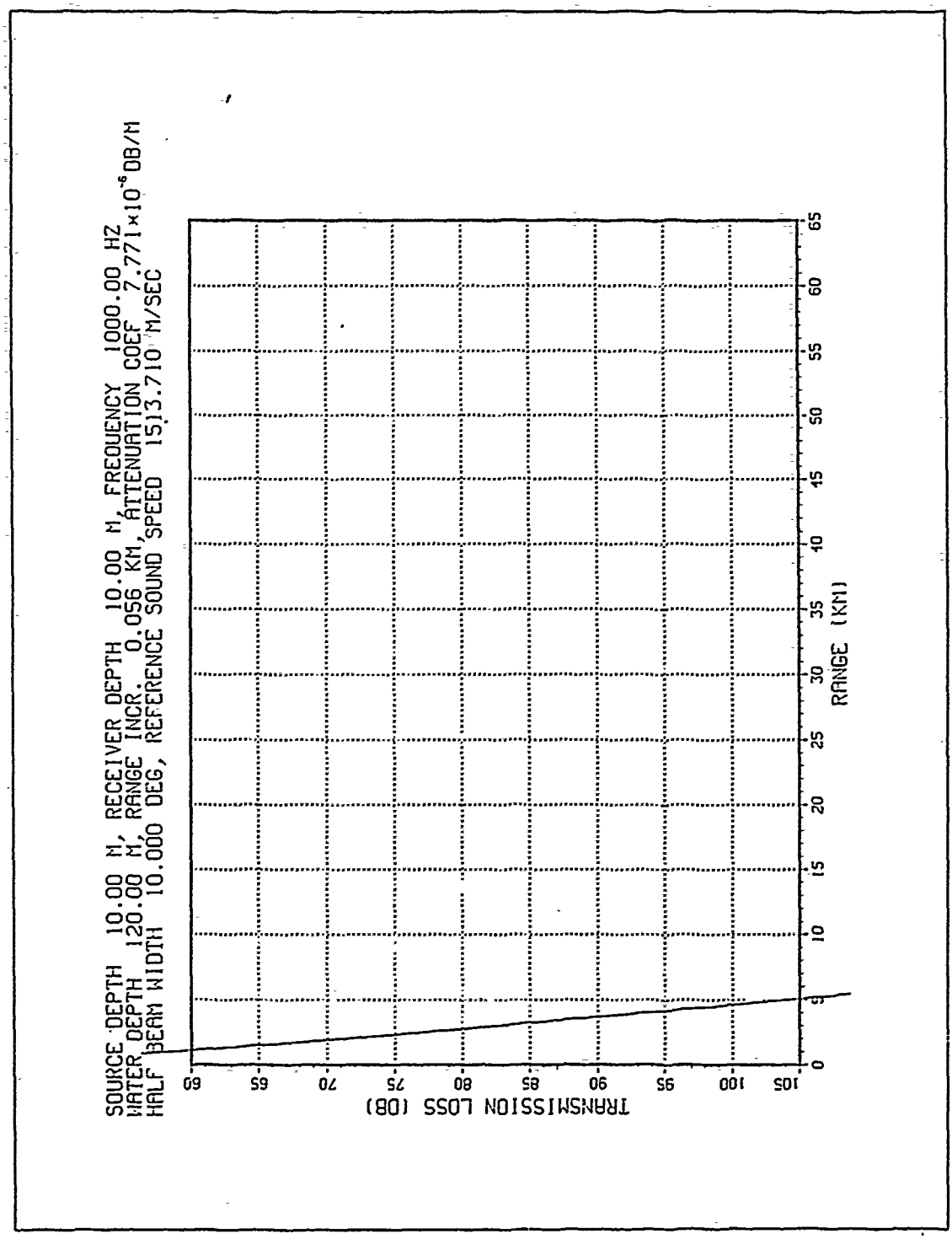

Figure 39. Path 1, PE Model with fully absorbing bottom.

of bottom refractions occur at intervals of about 10 km. Increasing (manually) the losses into the bottom, yields more attenuation of the bottom refracted energy and hence more loss in general. Also, higher frequency gives lower propagation losses in the winter for the direct path. In the summer the 1kHz frequency wave attenuates more than 105 dB at 2 km and then caustics occur from the bottom reflections which occur at intervals of 12 km. Selected runs for path 2 are also shown in Appendix A.

4. Path No 3. PE Model

Results for path 3 are similar to those experienced for path 2. Increasing the depth of both source and receiver increases the propagation loss. Bottom bounce rays can be detected converging every 30 km at 50 Hz for both seasons as well as refracted energy from the bottom. Increasing the frequency produces lower propagation losses in the winter. In the summer all frequencies attenuate rapidly and refraction occurs every 12 km. The higher the frequency the lower the refracted energy, due to the increased attenuation with increasing frequency (Appendix A).

5. Path No 4. PE Model and RAYMODE

The results for the PE Model are identical to path 3 for the direct path (Appendix A) as the SSP is the same and the depth below the source is the same. The first bottom return is now at 13 km (Fig. 40 to 42), about half of the path 3 range. The same SSP and a flat bottom at 3000 m used to run the RAYMODE model. The output (Fig. 43 and 44) shows a similar high loss for the direct path as PE but after that the loss is almost steady at 85 dB (bottom refracted) and at 38 km the convergence zone appears with an expected gain of 6 to 9 dB depending on the frequency used.

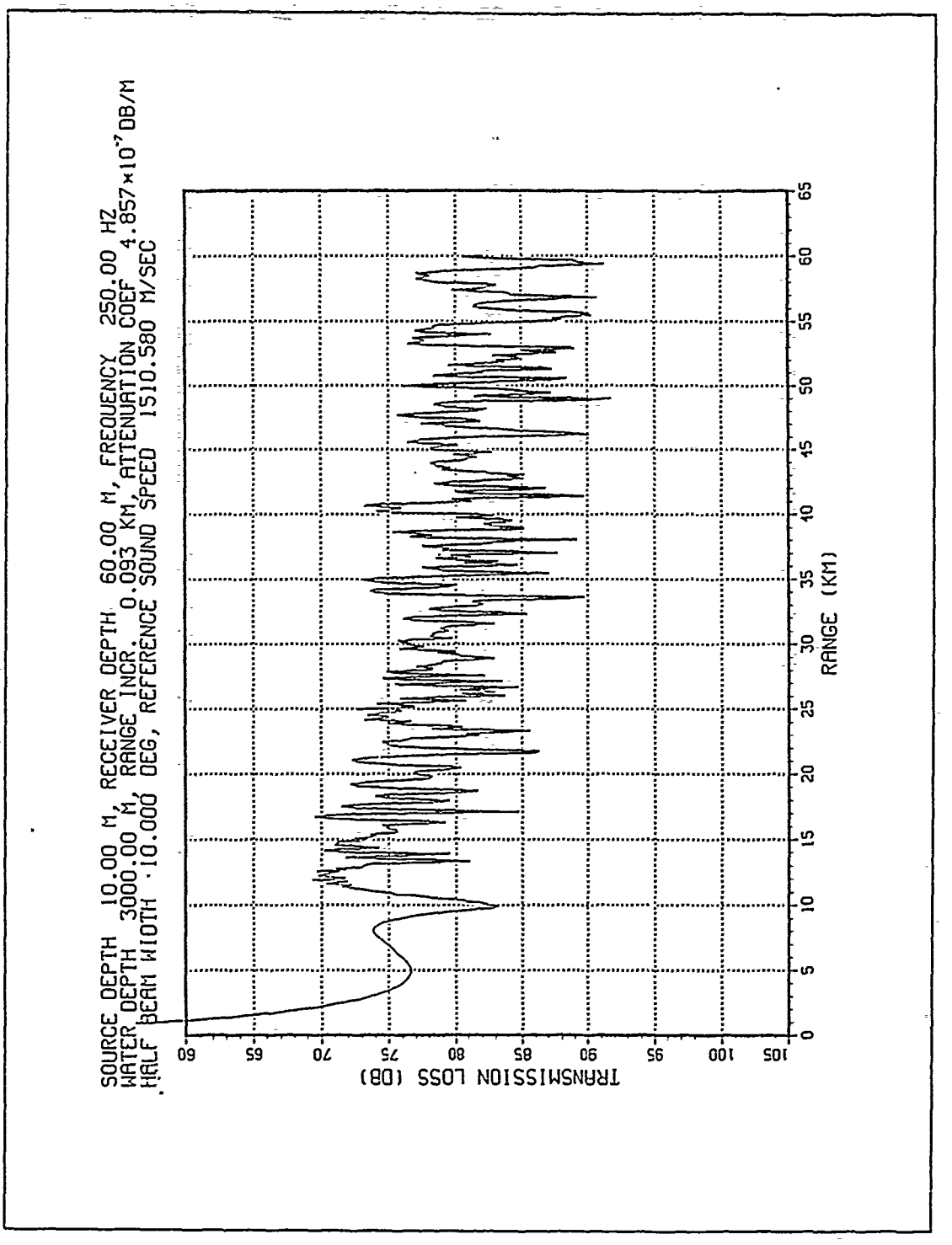

Figure 40. Path 4, PE Model at 250 Hz.

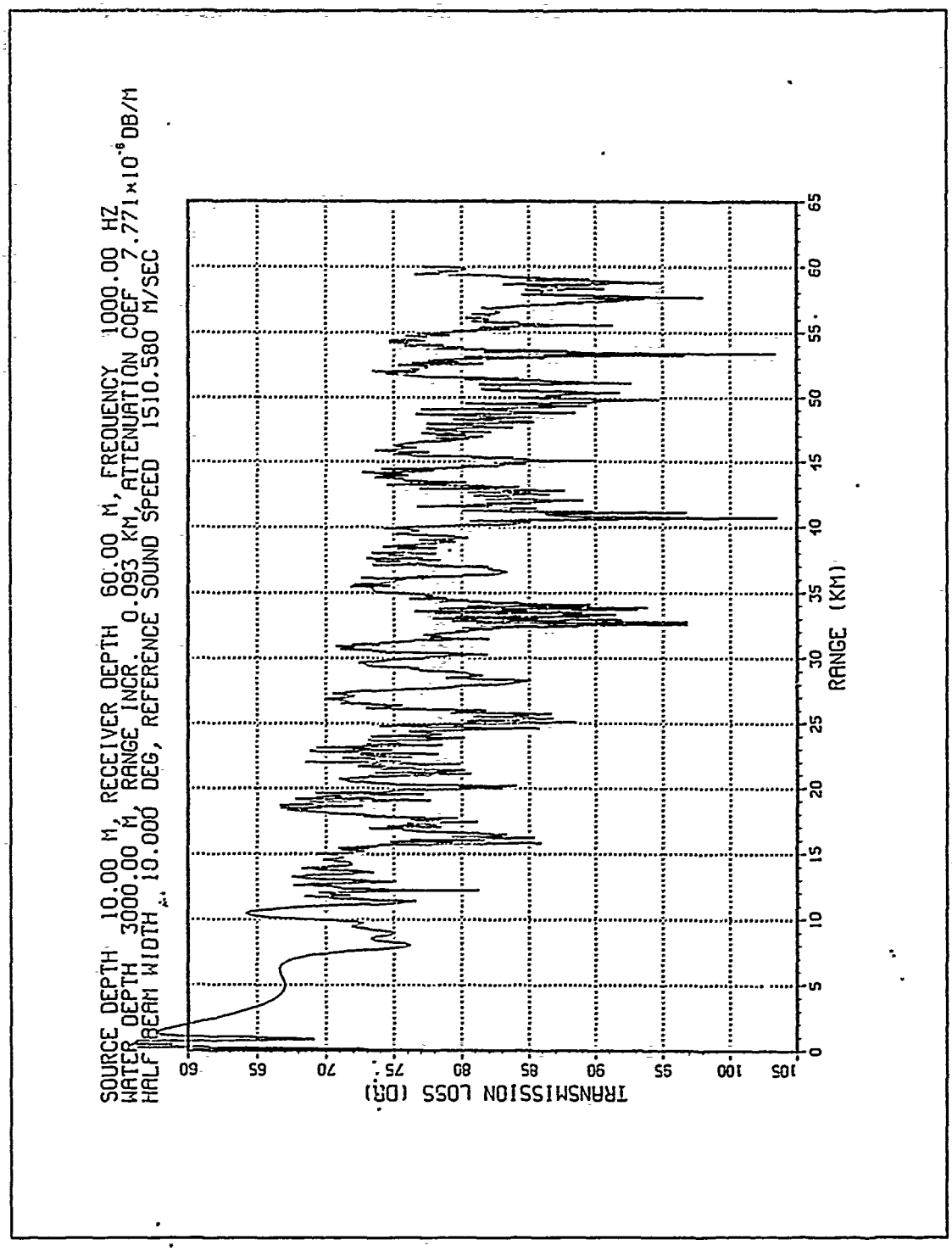

Figure 41. Path 4, PE Model at 1 kHz.

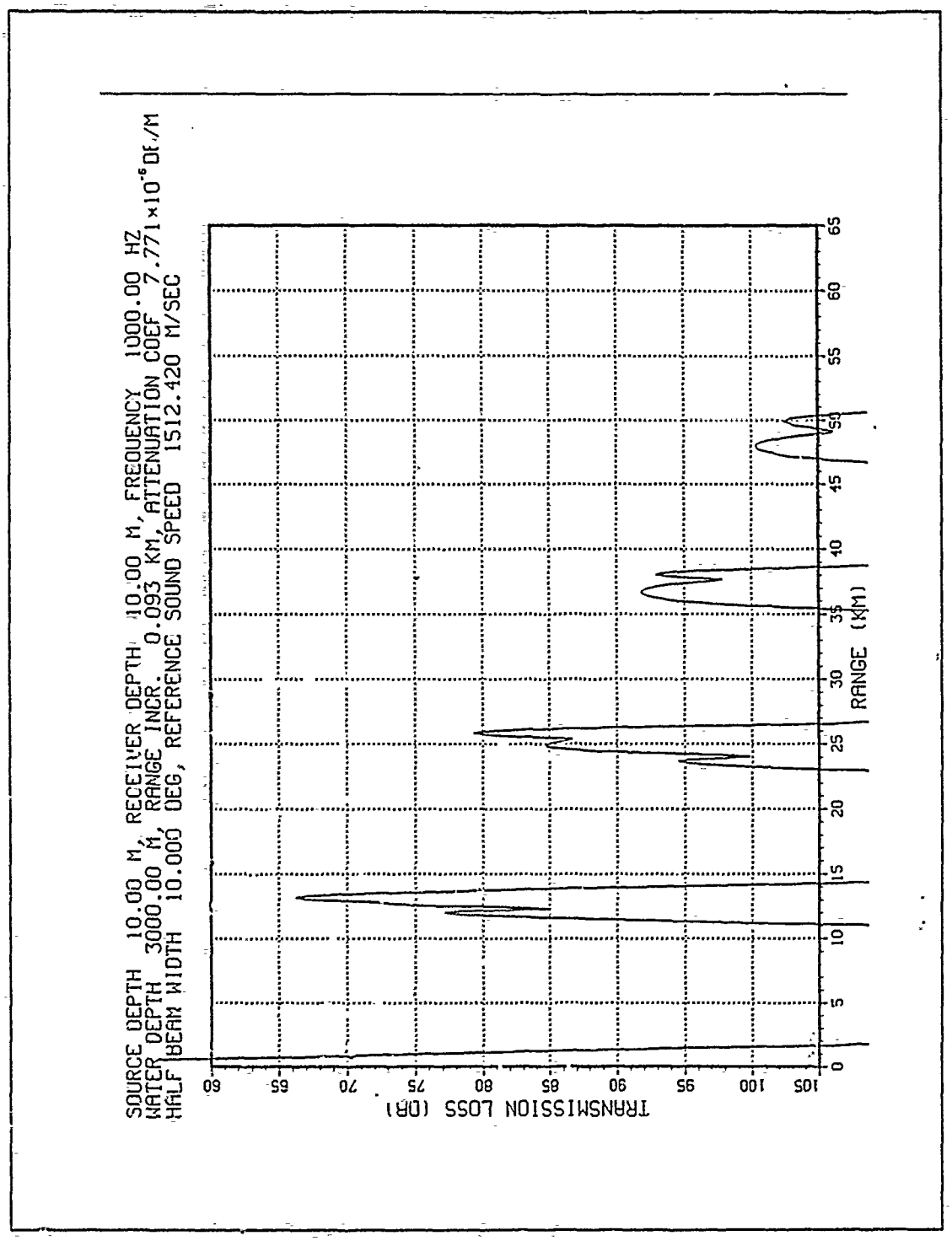

Figure 42. Path 4, PE Model at 1 kHz.

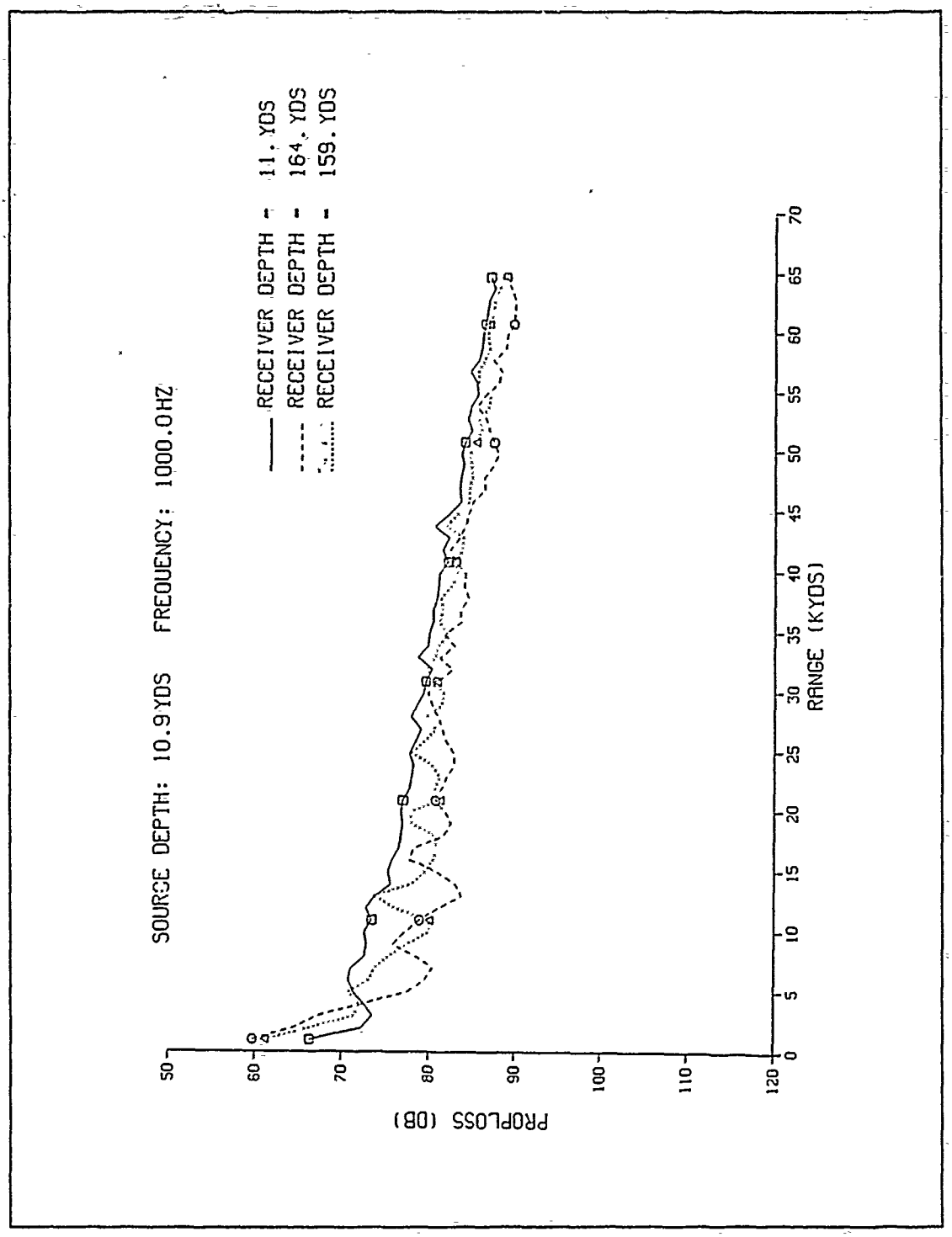

Figure 43. Path 4, RAYMODE at 1 kHz winter.

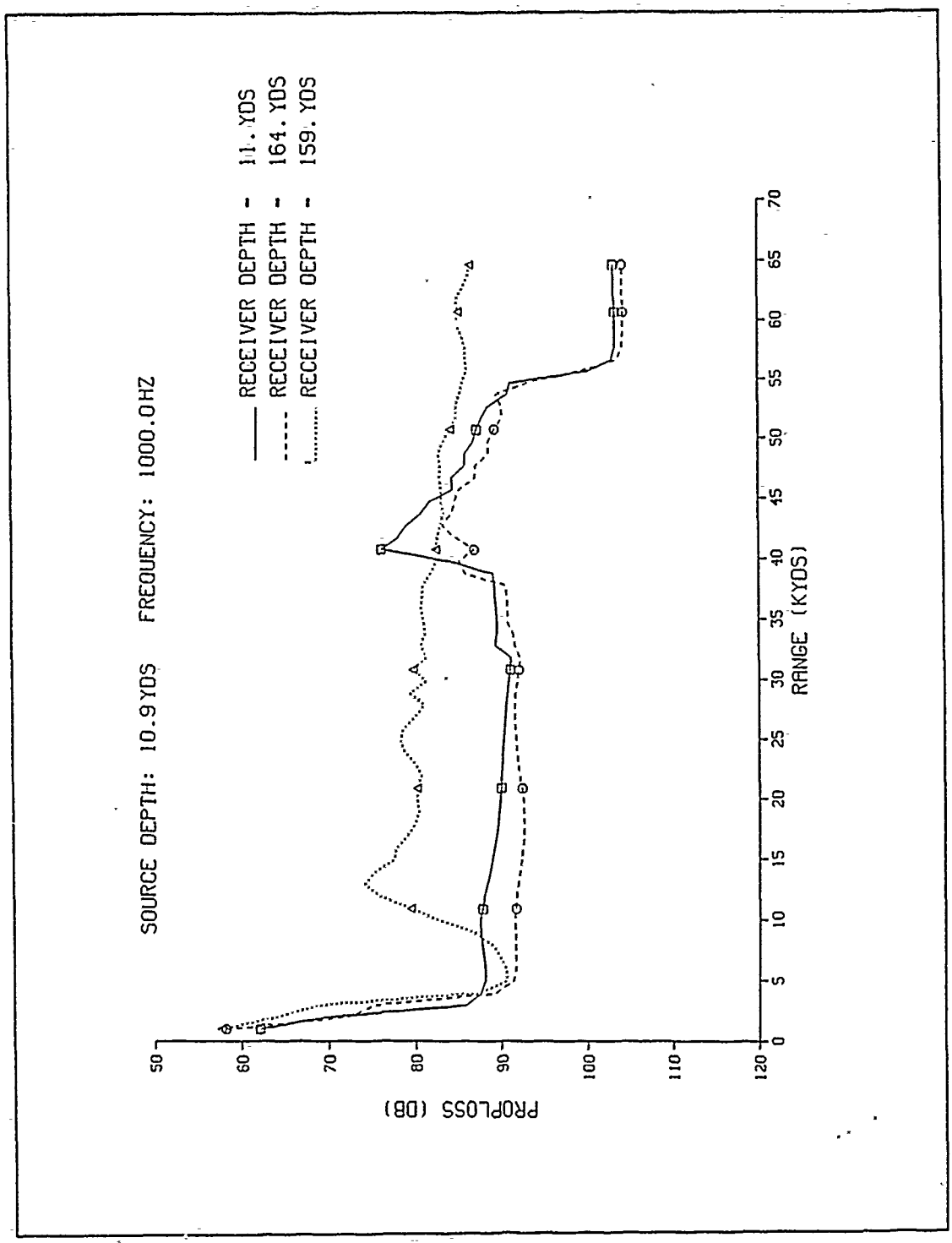

Figure 44. Path 4, RAYMODE at 1 kHz summer.

V. CONCLUSIONS

A. OCEANOGRAPHY

The oceanographic parameters in the Ionian Sea affecting sound propagation in the sea were examined. The results show that the study area is characterized by a seasonal thermocline of 300 m with small spatial and annual variations. In winter a half channel-type SSP exists. In summer high insolation prevents the creation of a mixed layer so a deep sound channel is created with an axial depth of 150 m. In areas where bottom depths permit, convergence zone propagation is possible and detection at long ranges can be achieved.

The sea sediment is highly reflective in the coastal regions and highly absorbing in the deeper regions. The bottom morphology and the presence of land masses prevent long range propagation at all the frequencies examined.

B. UNDERWATER SOUND

The modeling of acoustic propagation results in the general observations for the area studied. Between the two models examined, RAYMODE and PE, the former is adequate in presenting the loss for areas where the bottom is smooth, flat and deep with respect to the acoustic wavelength. It will fail in coastal areas with anomalous bathymetry, a situation common to the study area and to the Hellenic seas in general.

The PE model is better fitted for coastal areas because it can treat a variable depth morphology but the implementation by the Split Step Fourrier transform will create restrictions at sea sediment boundaries, especially in areas with sharp changes in sound speed in the sediment.

Both the models calculate propagation loss in a vertical only plane. In coastal areas like the Ionian Sea this will not permit interactions from nearby land masses. This can be solved by three dimensional programs and by the implementation of better algorithms.

The sea sediment models need improvement and a theoretical basis but the difficulties in collecting data from the bottom on a global basis will postpone the appearance of such a model in the immediate future.

In the study area propagation at frequ ·s between 50 and 1000 Hz is dominated by bottom reflection and refraction. Bo· seasons show relatively short direct path ranges.

Due to the number of parameters that can not be defined or measured with accuracy as well as the techniques used by the models, the results of such acoustic models must be treated qualitatively only.

APPENDIX A

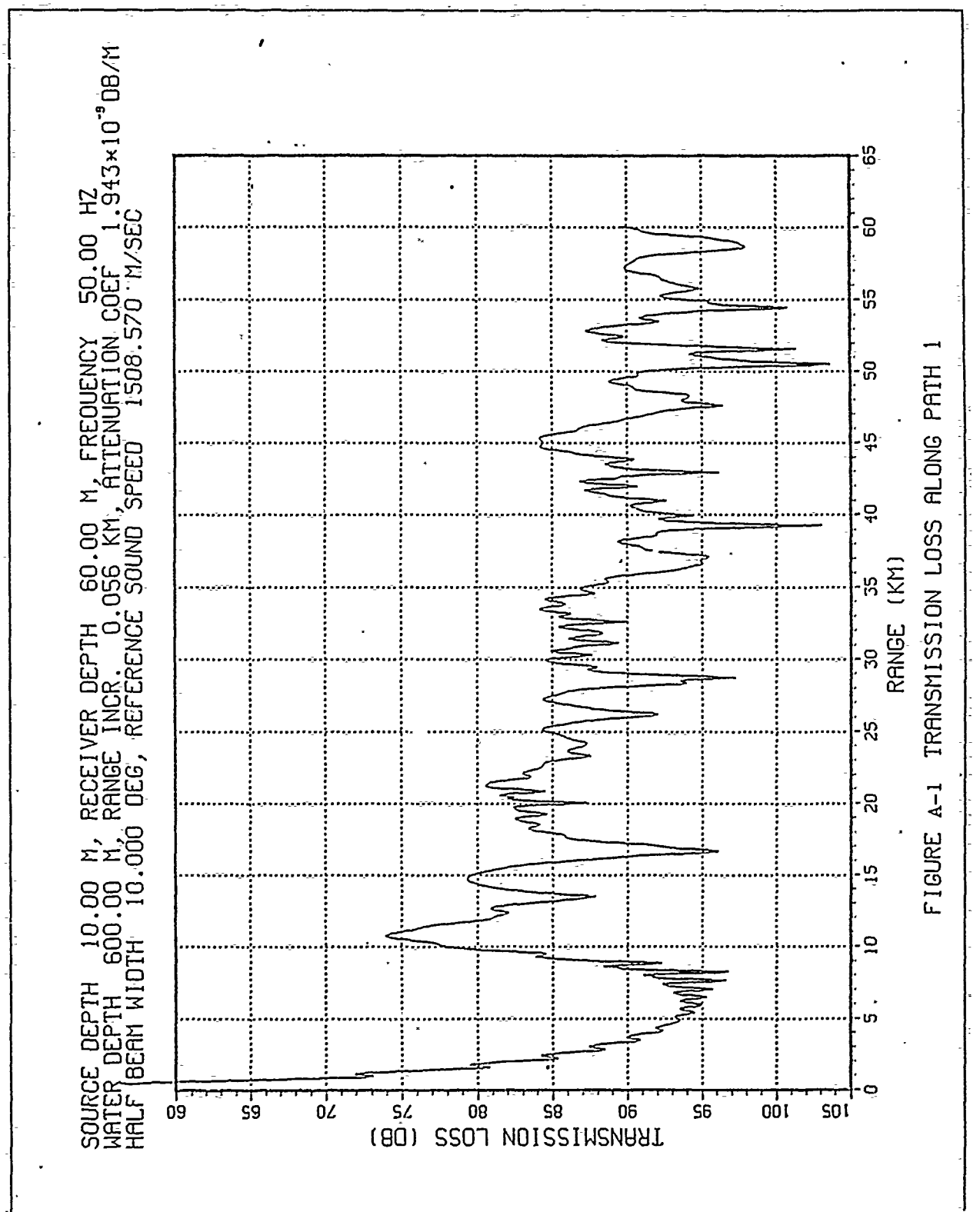

FIGURE A-1 TRANSMISSION LOSS ALONG PATH 1

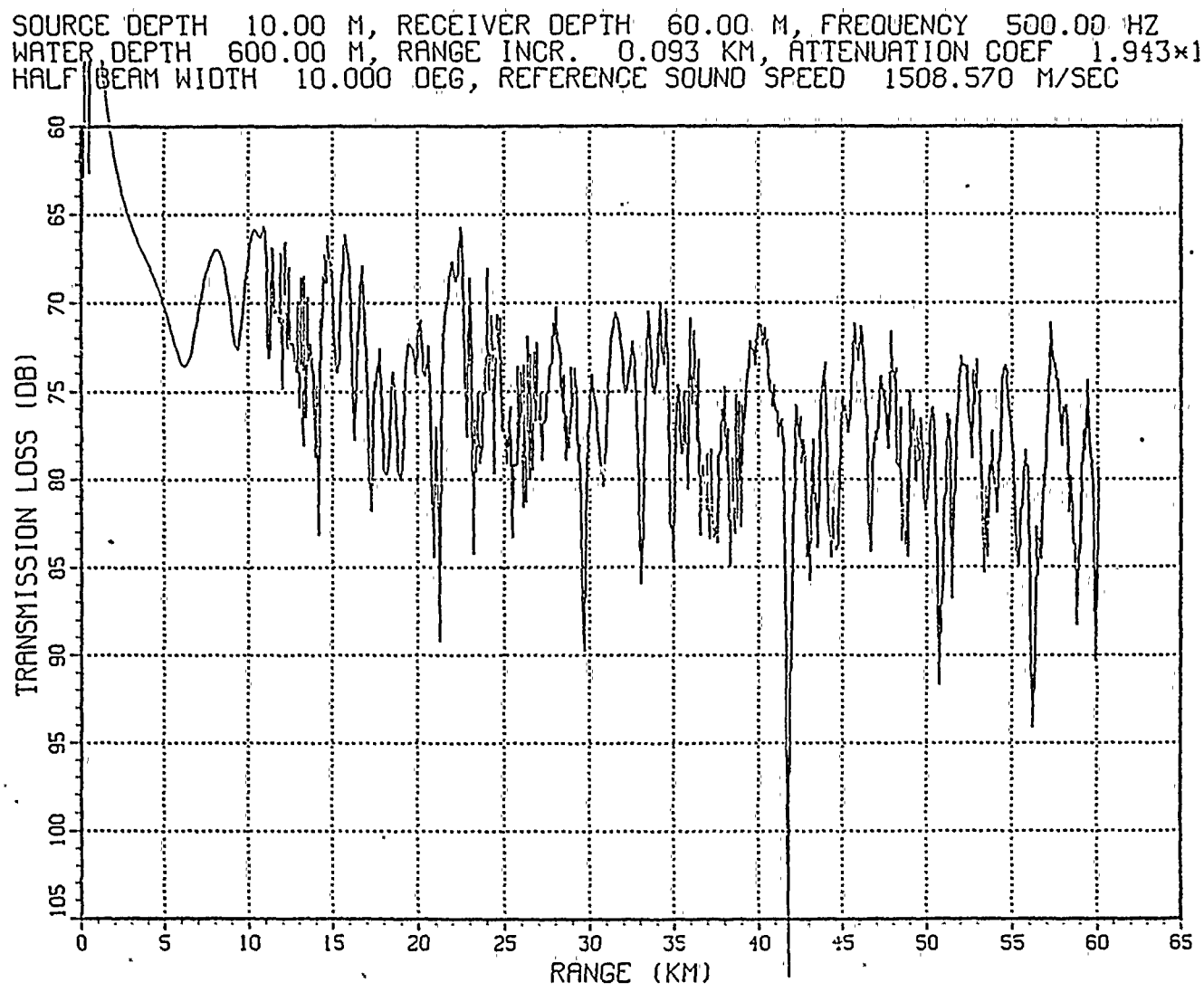

FIGURE A-2 TRANSMISSION LOSS ALONG PATH 1 IN WINTER

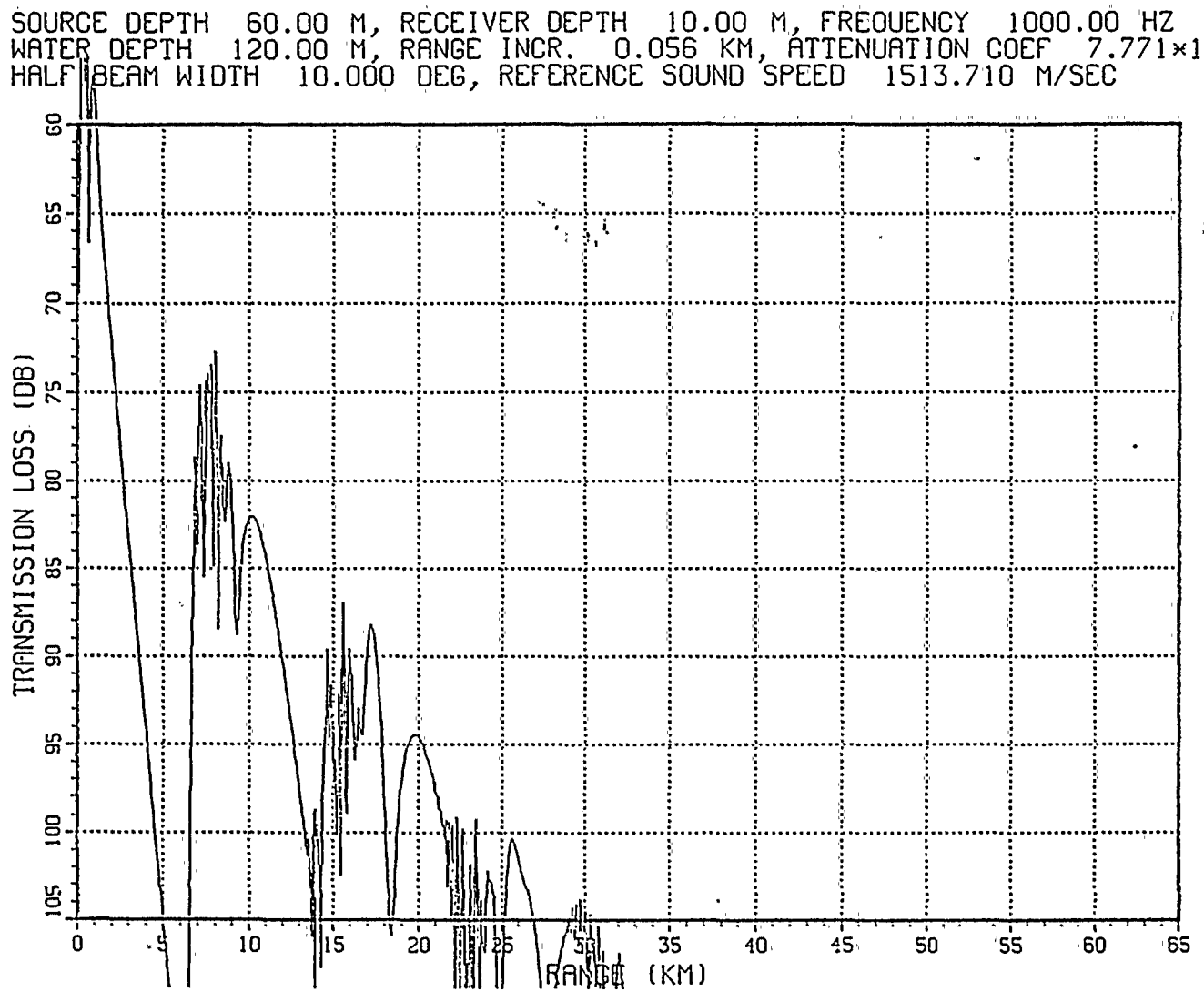

FIGURE A-3 TRANSMISSION LOSS ALONG PATH 1 IN SUMMER

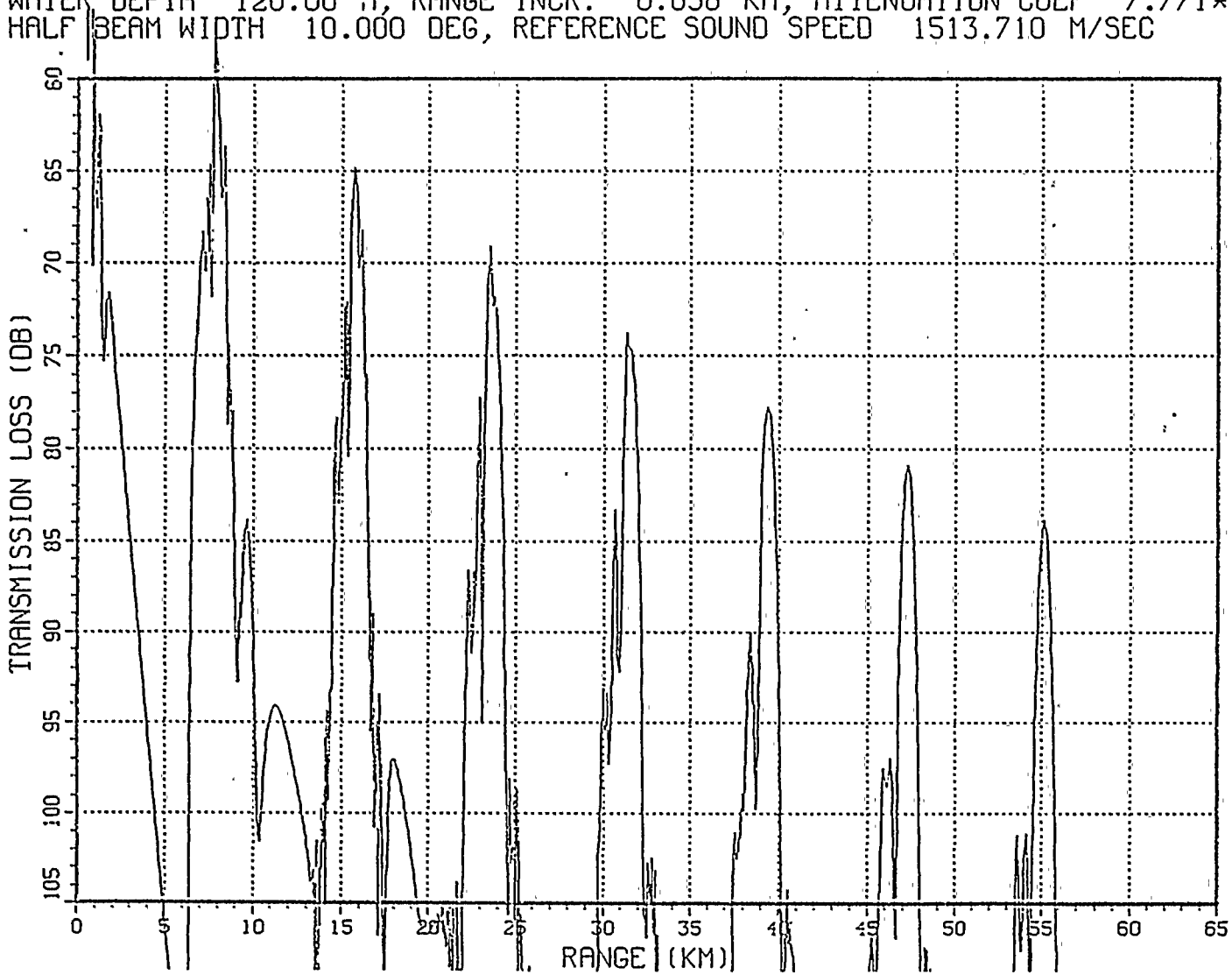

FIGURE A-4 TRANSMISSION LOSS ALONG PATH 1 IN SUMMER

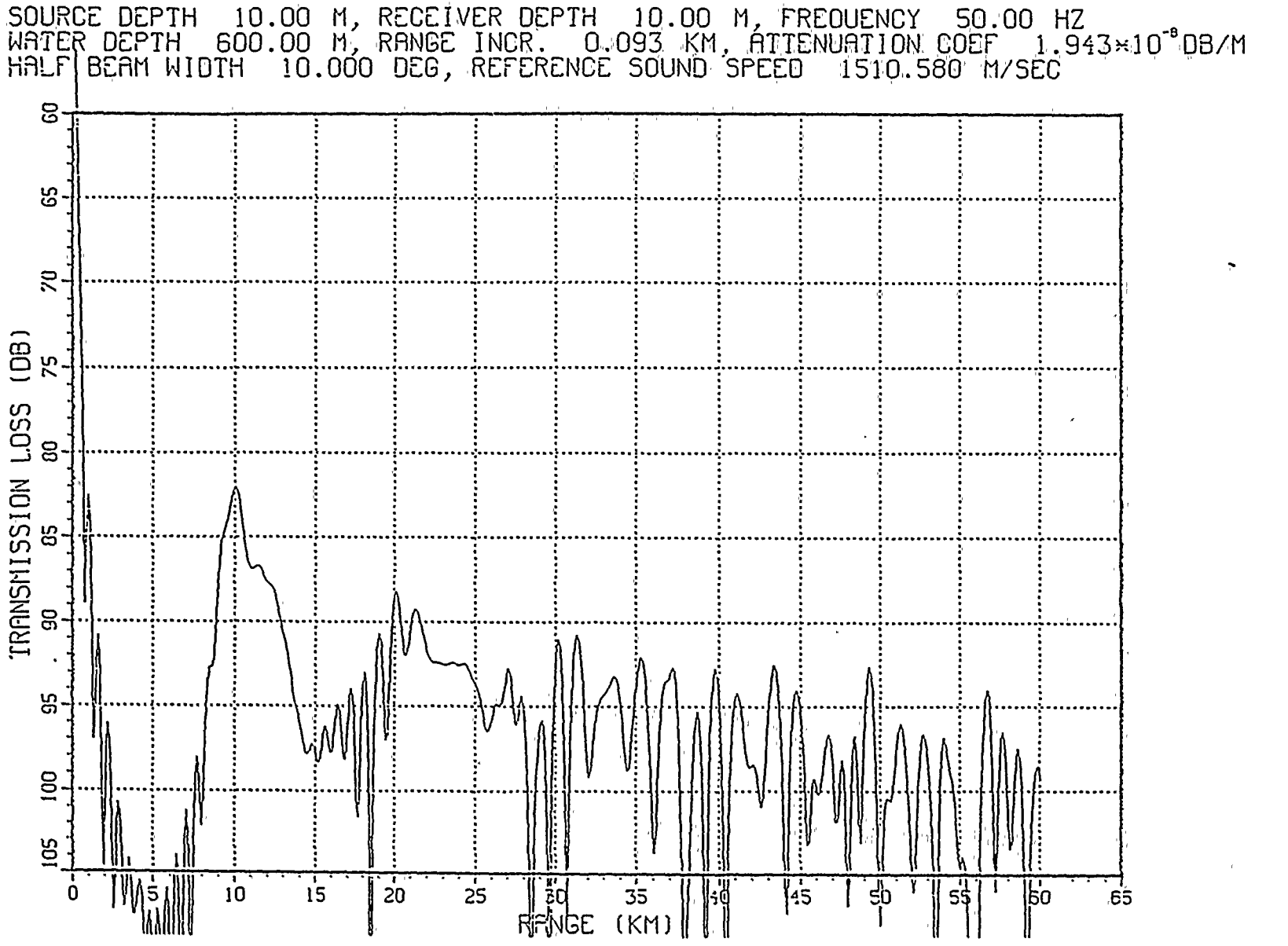

FIGURE A-5 TRANSMISSION LOSS ALONG PATH 2 IN WINTER

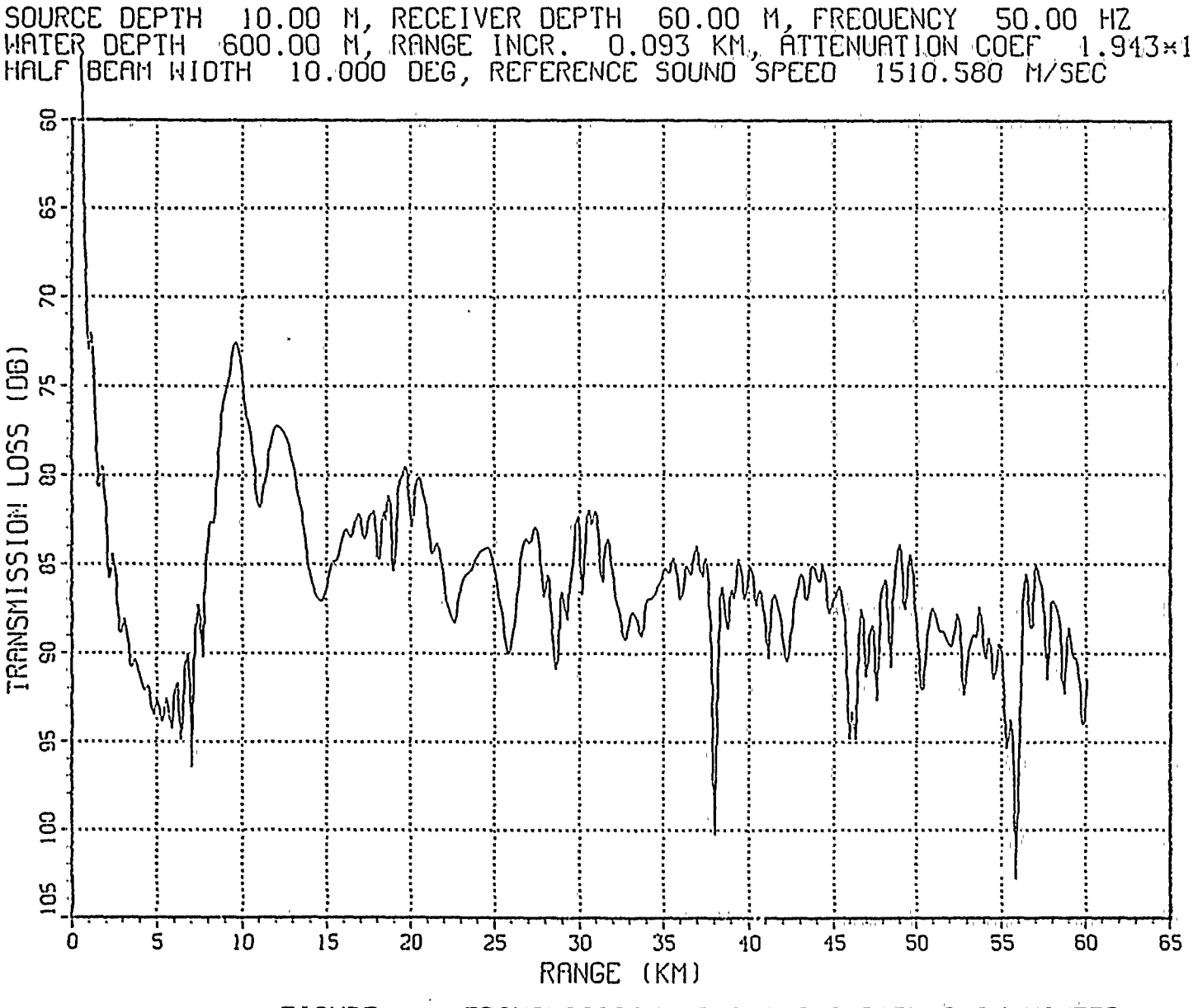

FIGURE A-6 TRANSMISSION LOSS ALONG PATH 2 IN WINTER

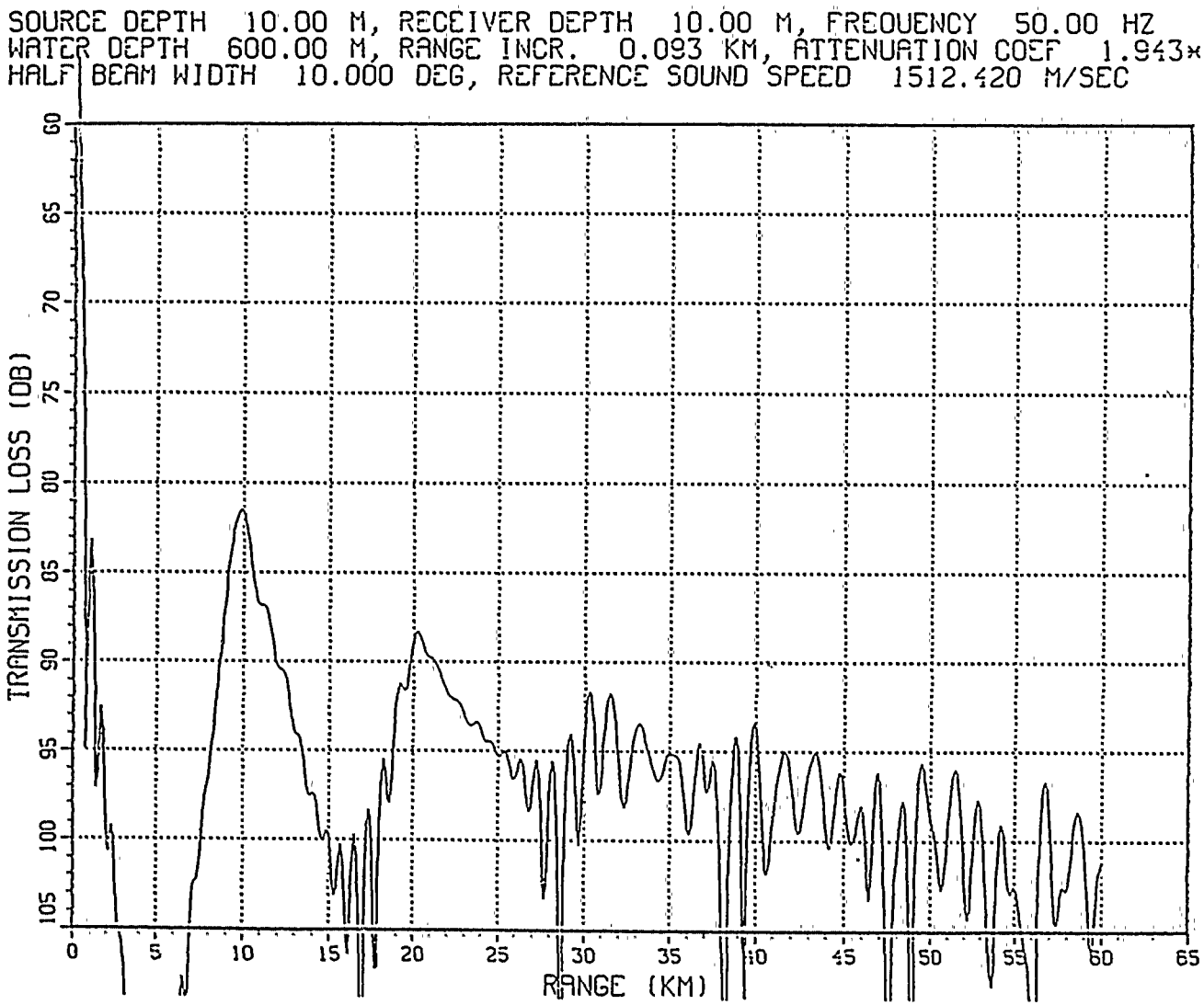

FIGURE A-7 TRANSMISSION LOSS ALONG PATH 2 IN SUMMER

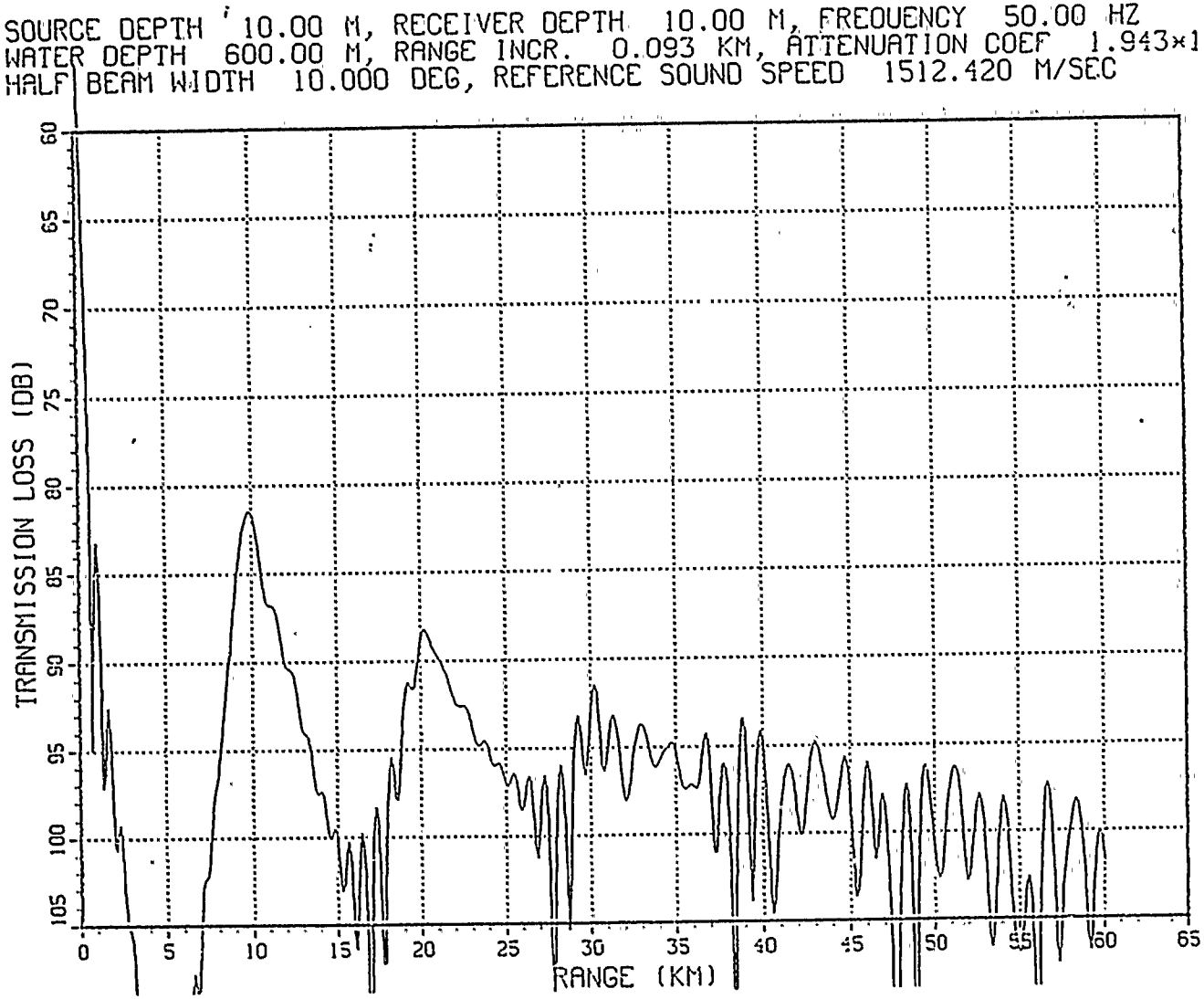

FIGURE A-8 TRANSMISSION LOSS ALONG PATH 2 IN SUMMER

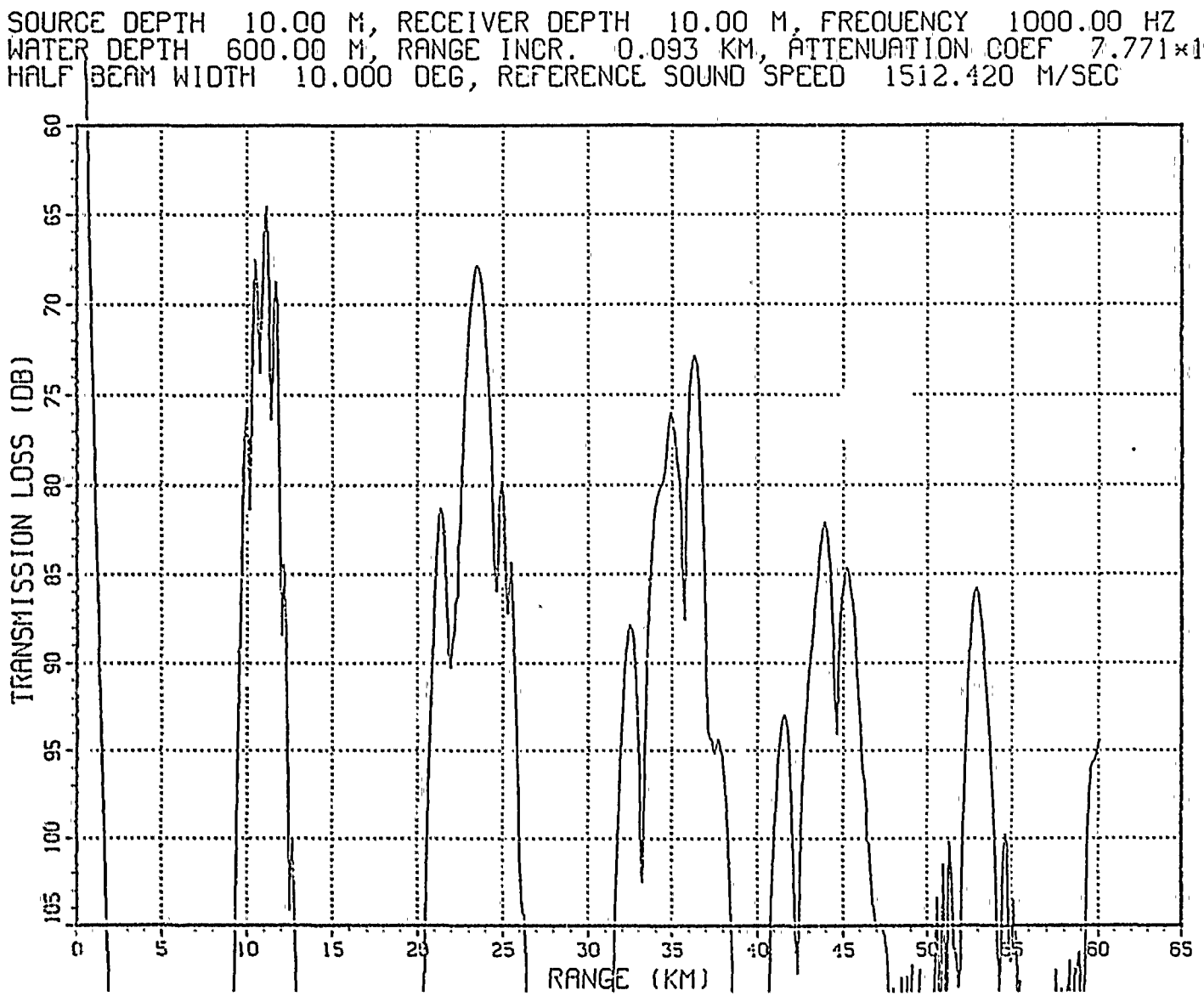

FIGURE A-9 TRANSMISSION LOSS ALONG PATH 2 IN SUMMER

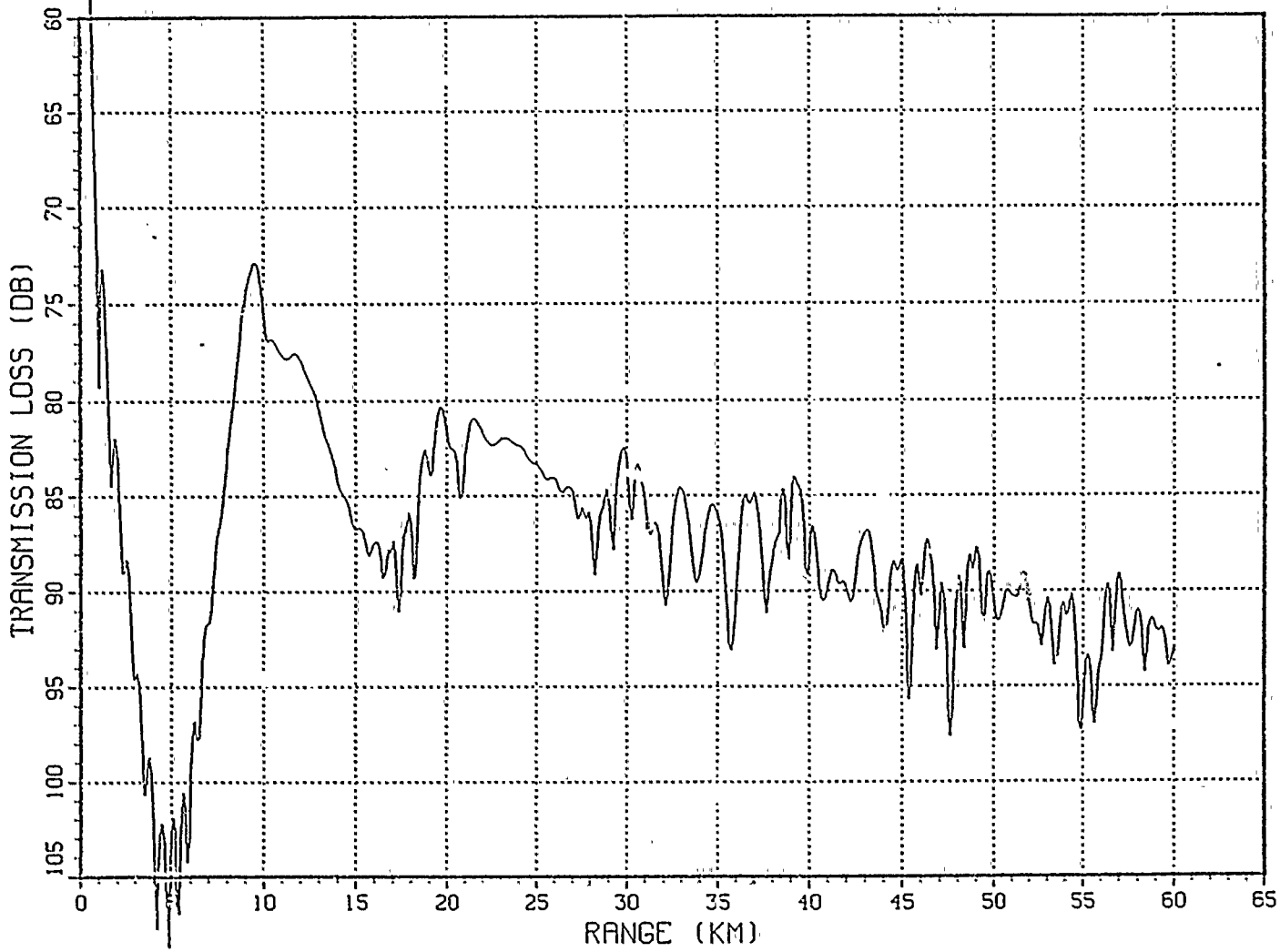

FIGURE A-10 TRANSMISSION LOSS ALONG PATH 2 IN SUMMER

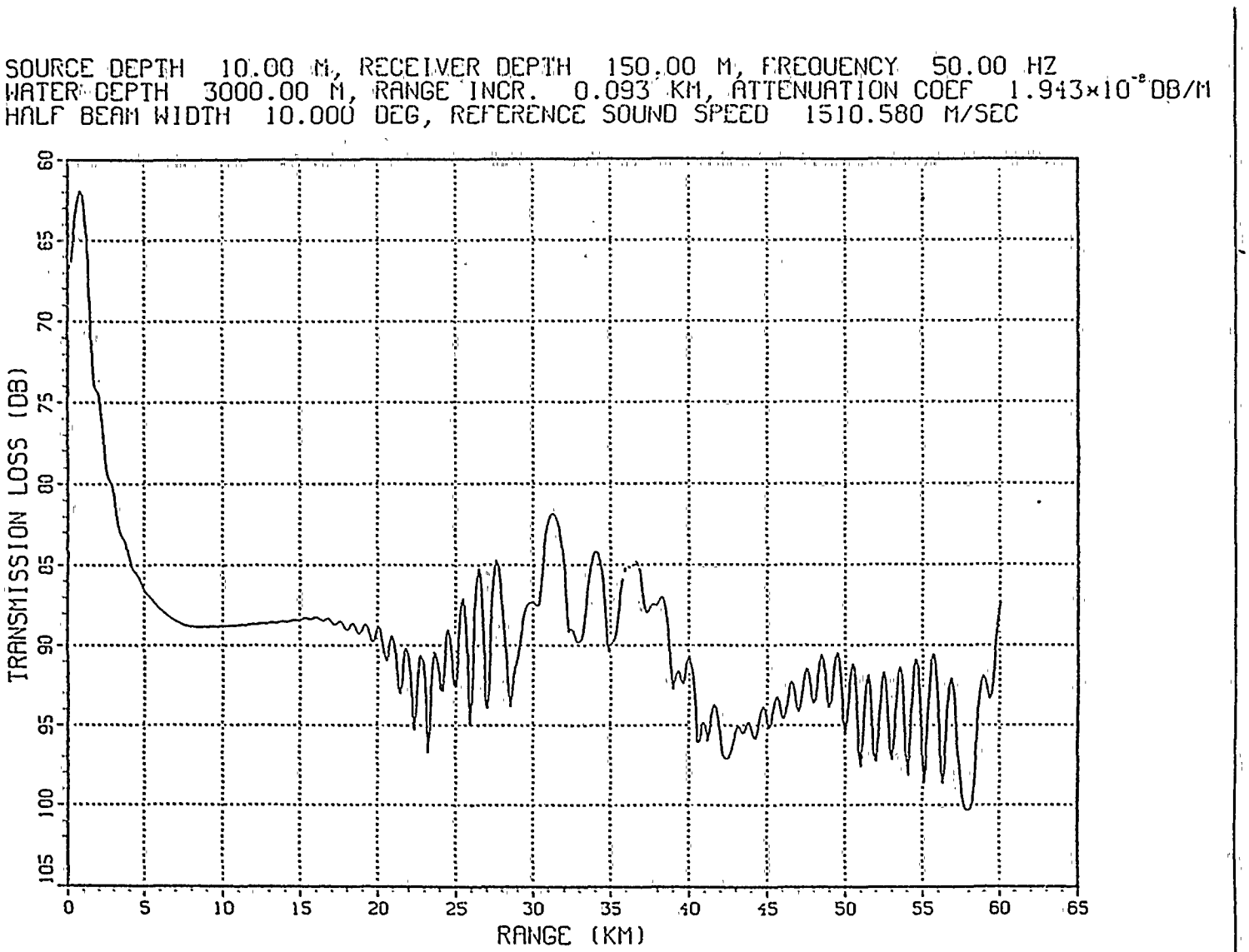

FIGURE A-11 TRANSMISSION LOSS ALONG PATH 3 IN WINTER

SOURCE DEPTH 10.00 M, RECEIVER DEPTH 150.00 M, FREQUENCY 50.00 HZ
WATER DEPTH 3000.00 M, RANGE INCR. 0.093 KM, ATTENUATION COEF 1.943×10^{-6} DB/M
HALF BEAM WIDTH 10.000 DEG, REFERENCE SOUND SPEED 1512.420 M/SEC

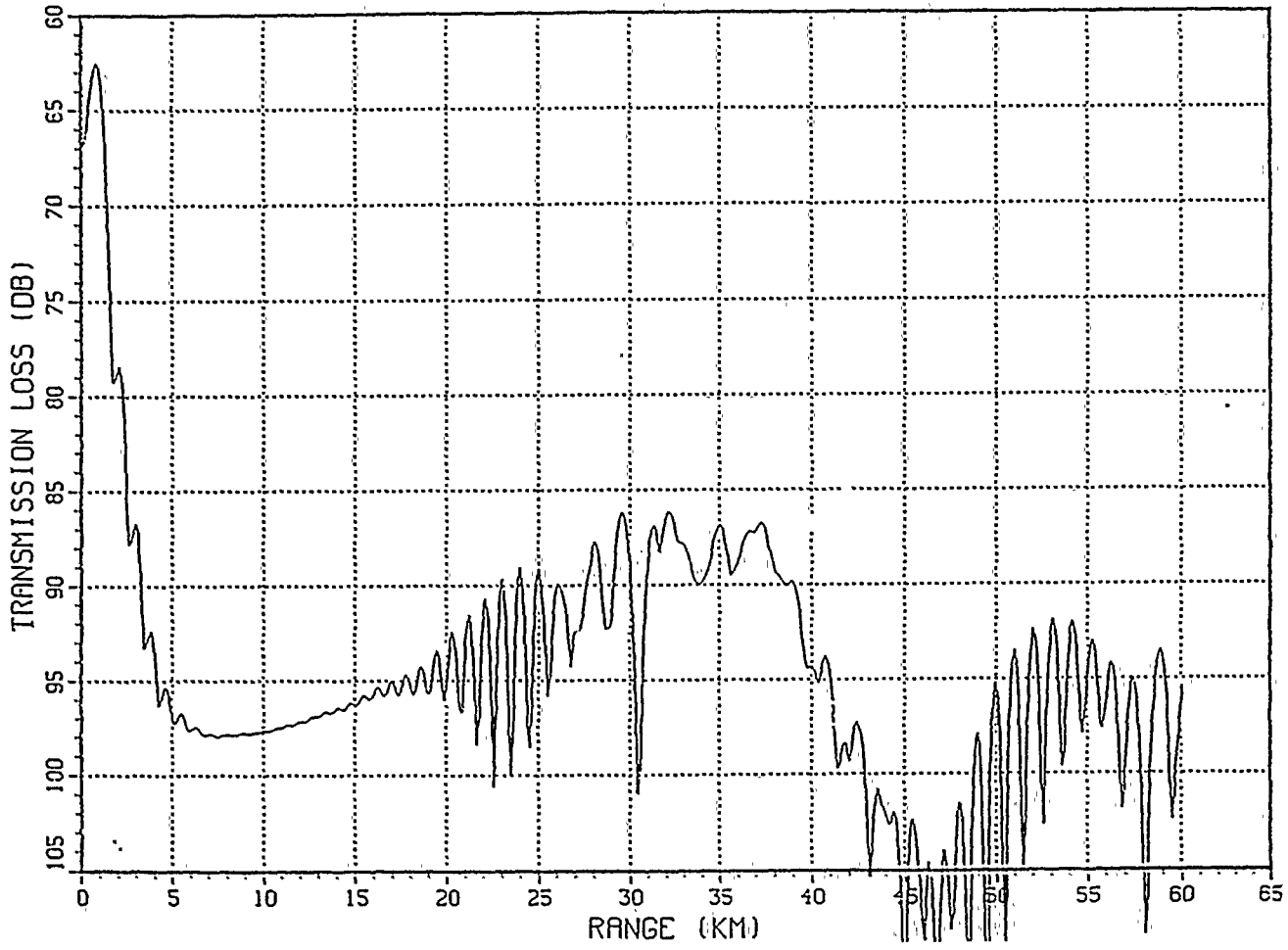

FIGURE A-12 TRANSMISSION LOSS ALONG PATH 3 IN SUMMER

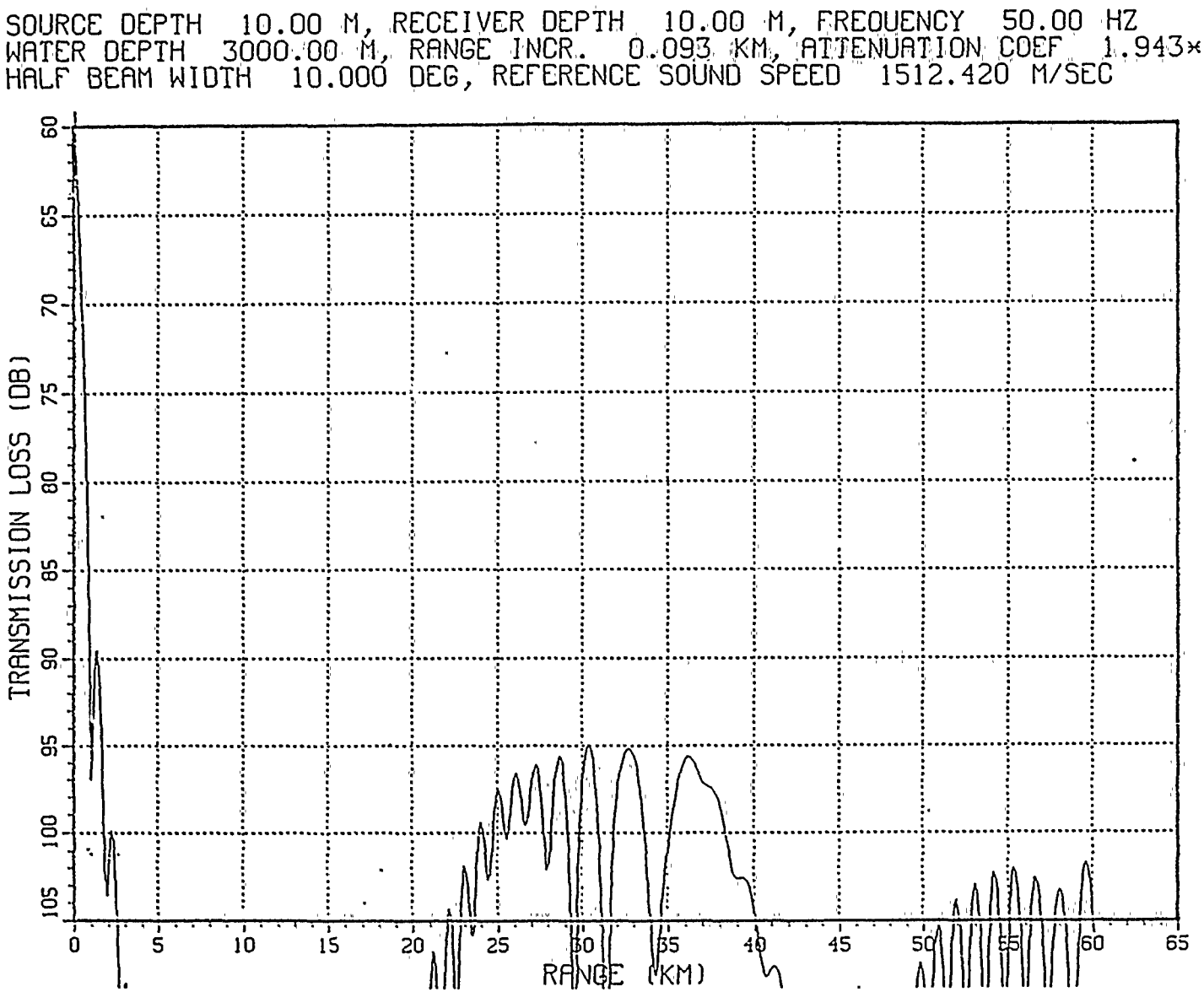

FIGURE A-13 TRANSMISSION LOSS ALONG PATH 3 IN SUMMER

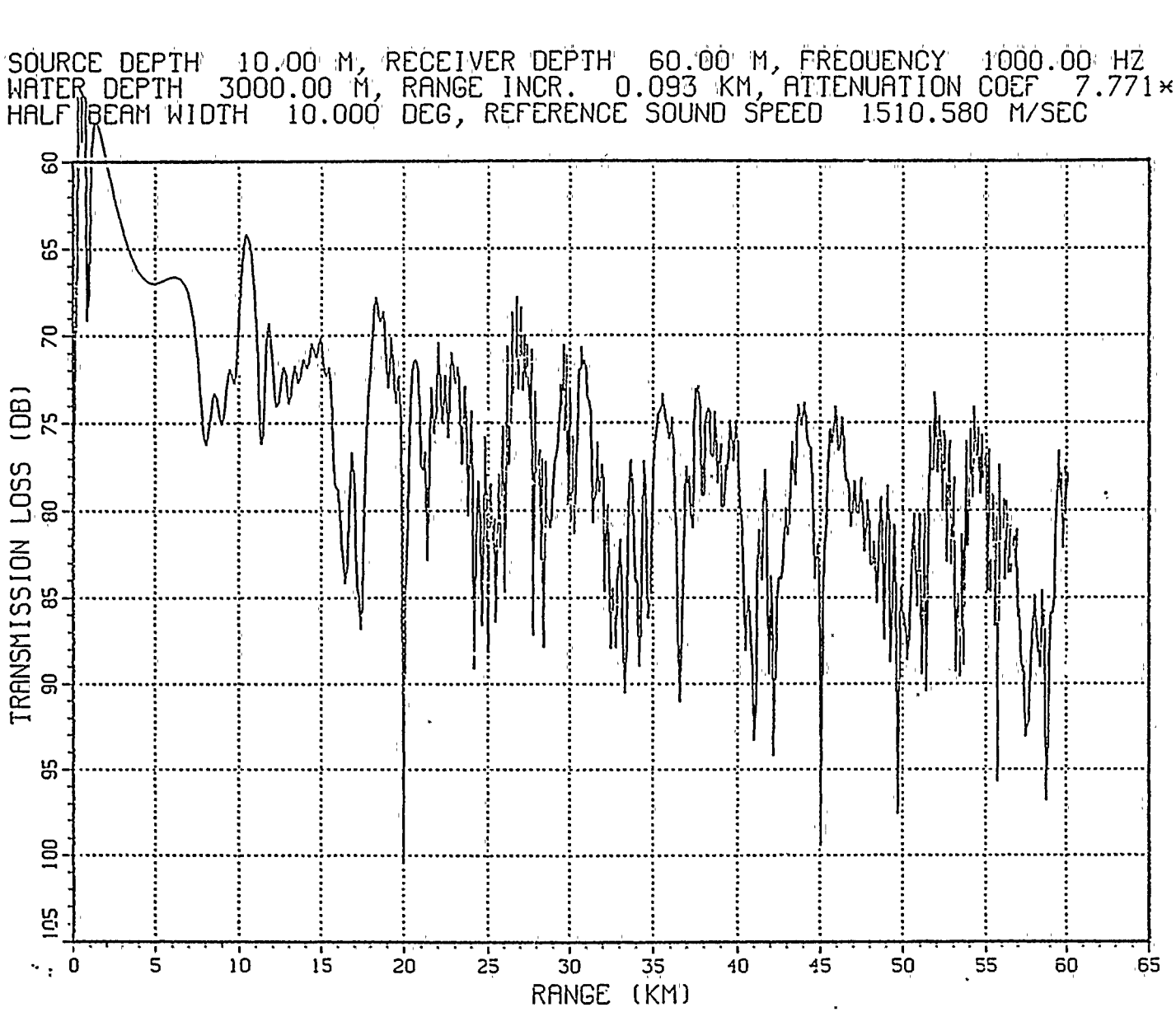

FIGURE A-14 TRANSMISSION LOSS ALONG PATH 3 IN WINTER

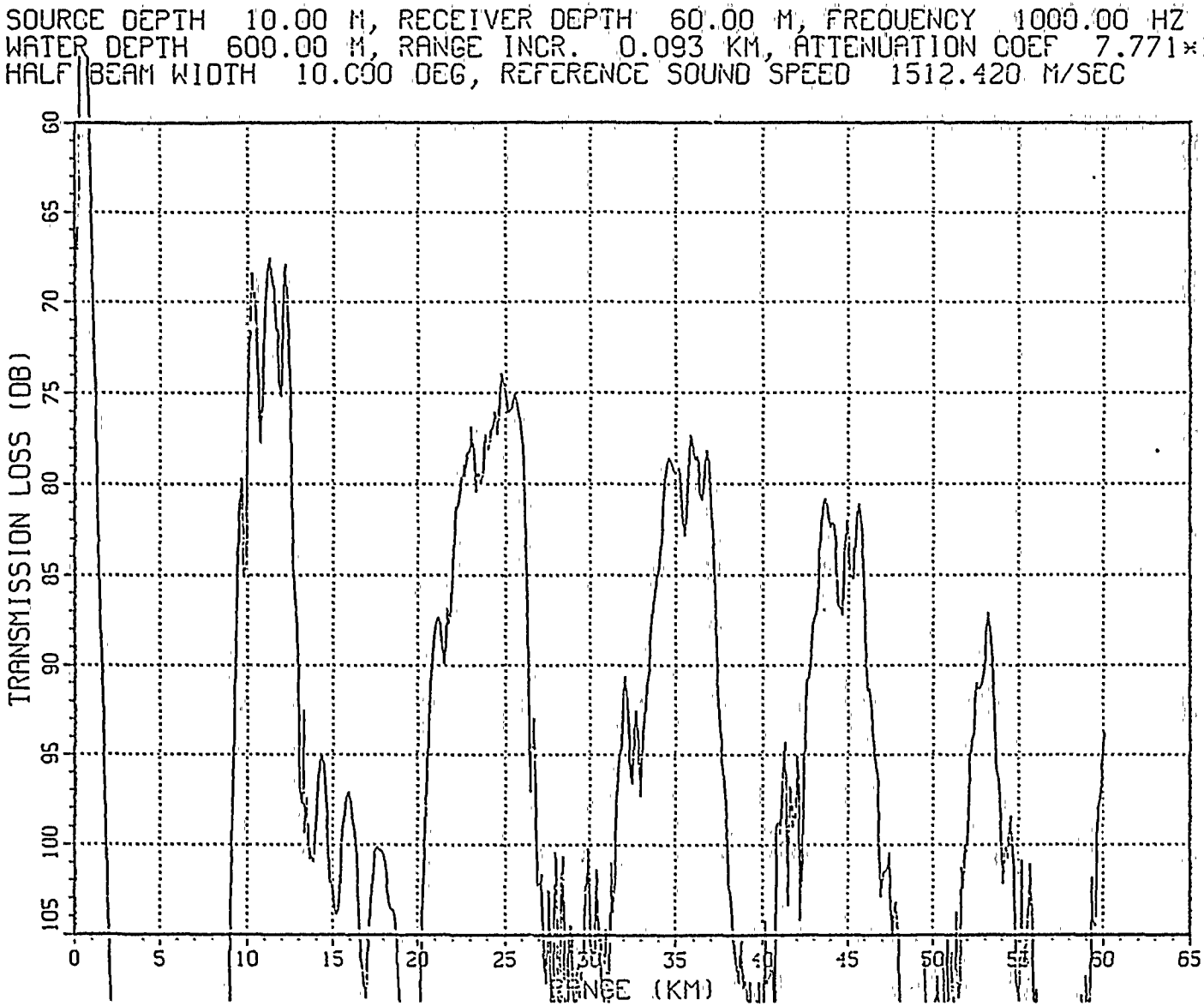

FIGURE A-15 TRANSMISSION LOSS ALONG PATH 3 IN SUMMER

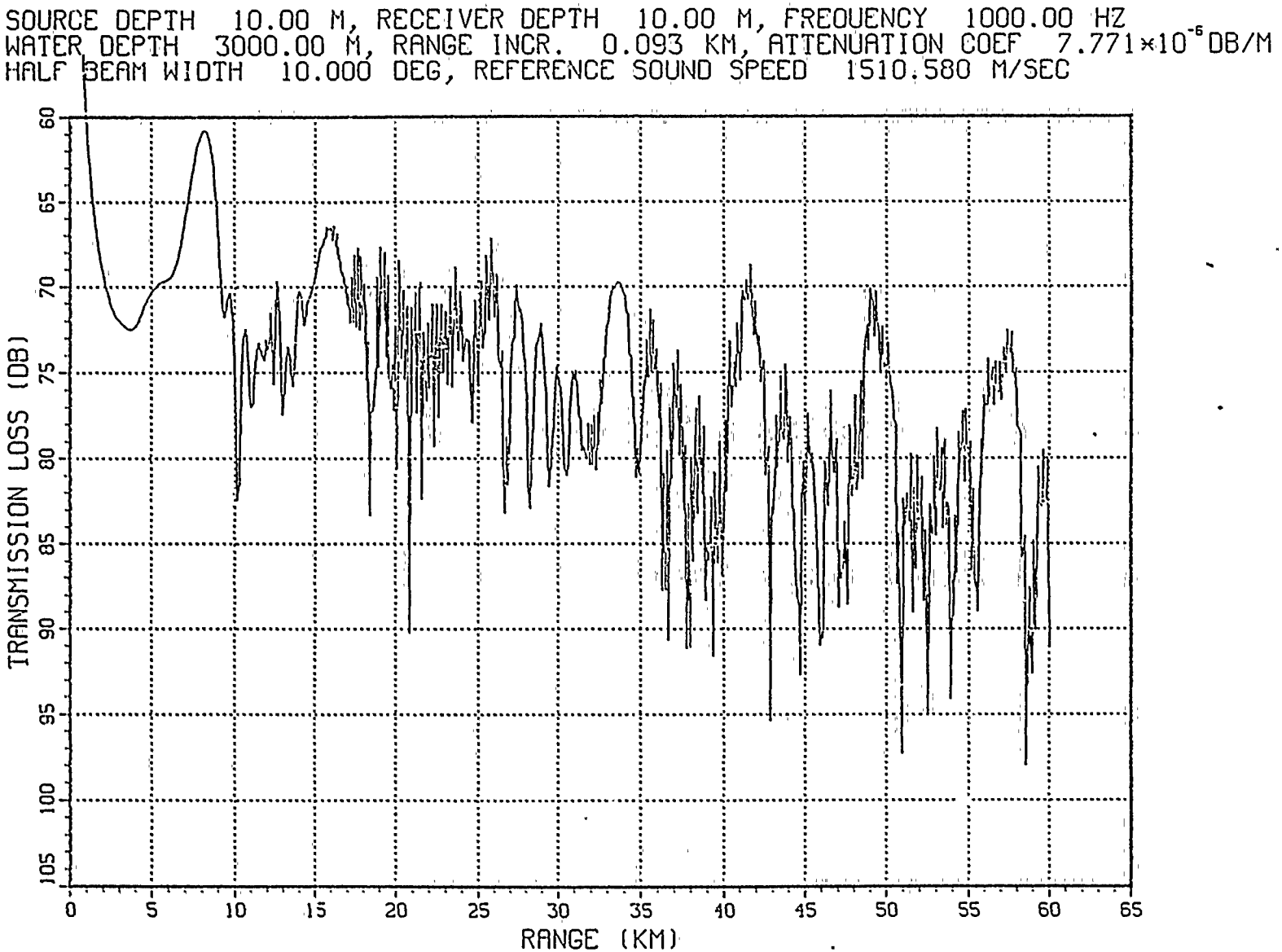

FIGURE A-16 TRANSMISSION LOSS ALONG PATH 4 IN WINTER

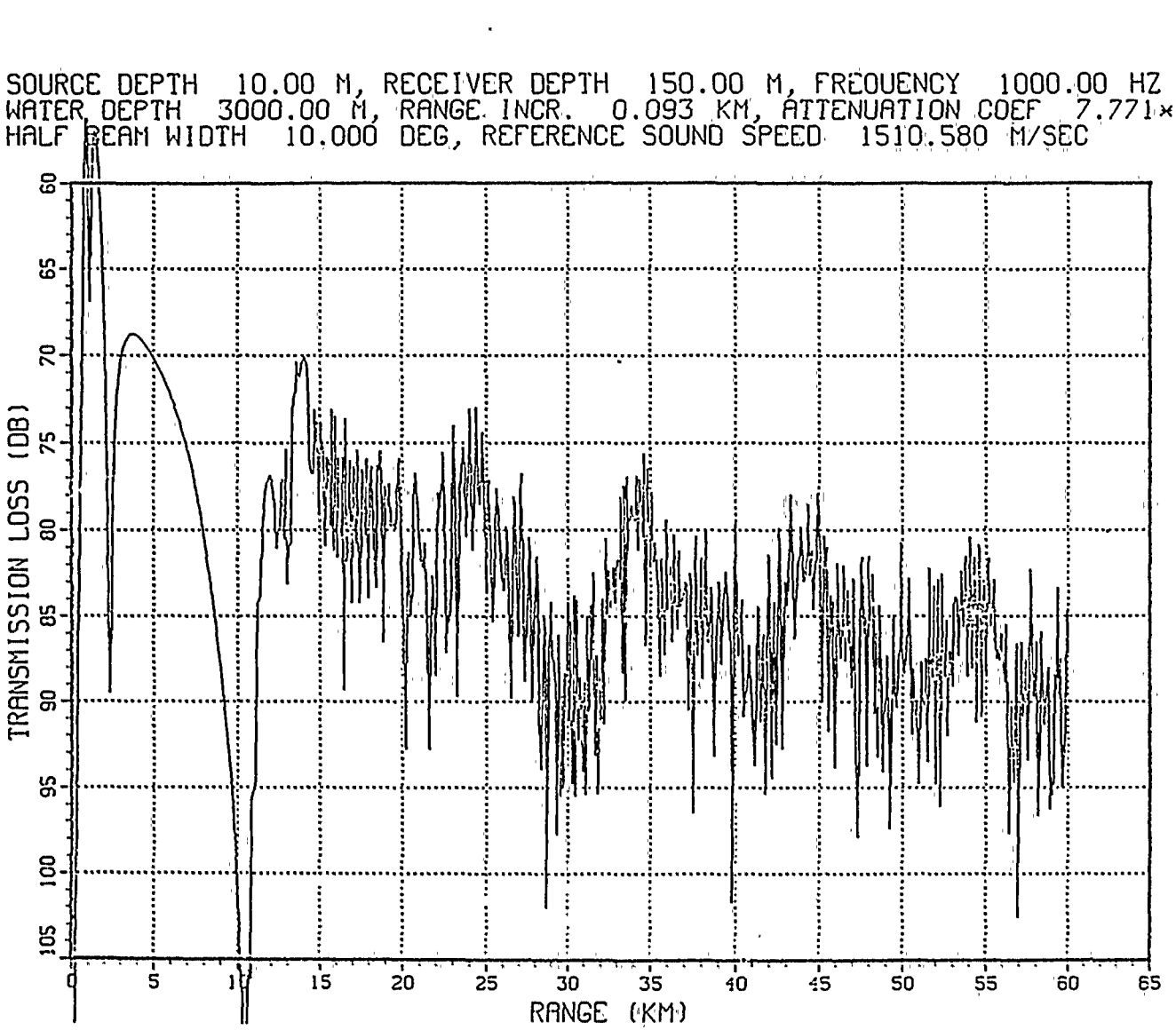

FIGURE A-17 TRANSMISSION LOSS ALONG PATH 4 IN WINTER

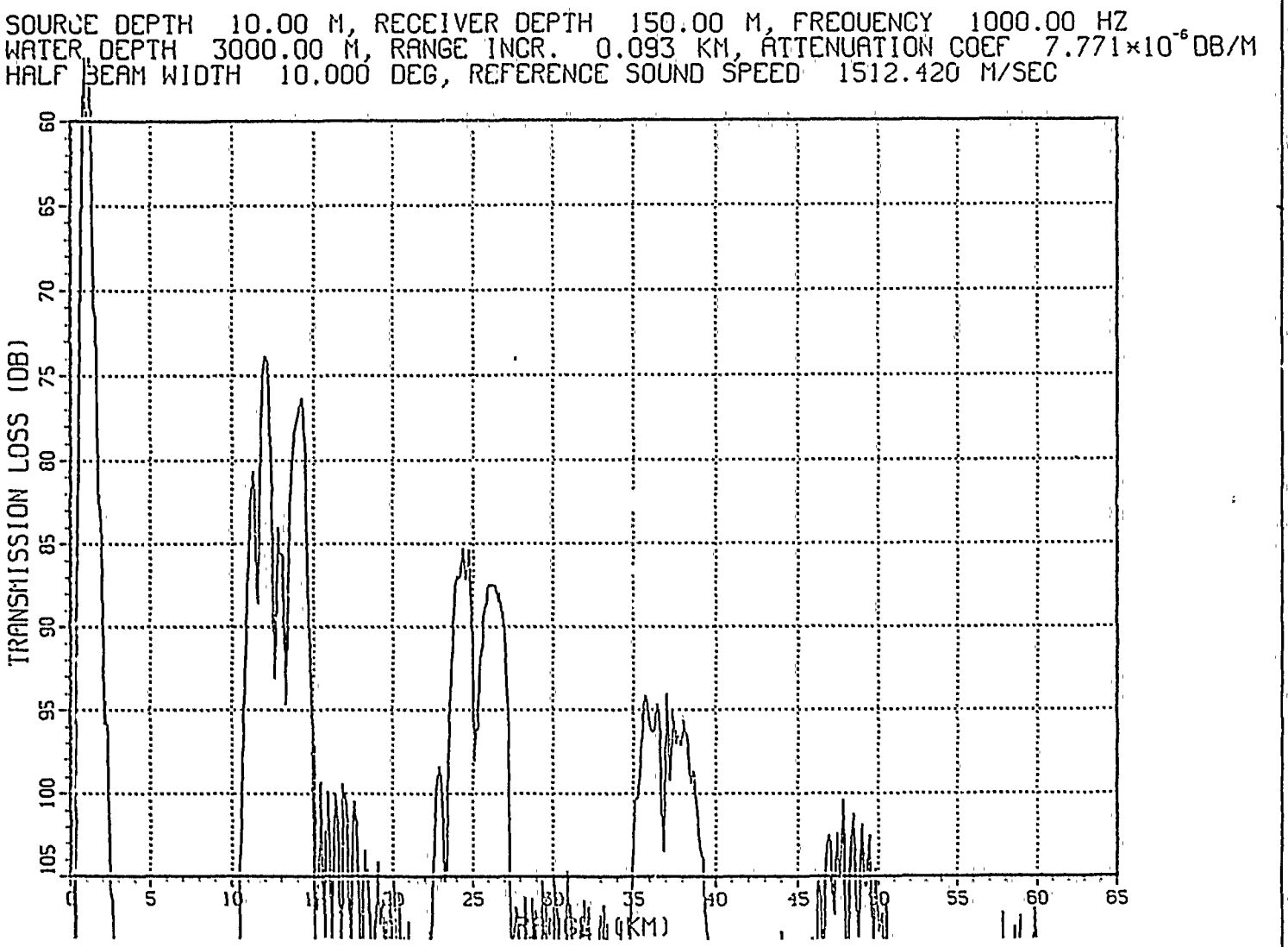

FIGURE A-18 TRANSMISSION LOSS ALONG PATH 4 IN SUMMER

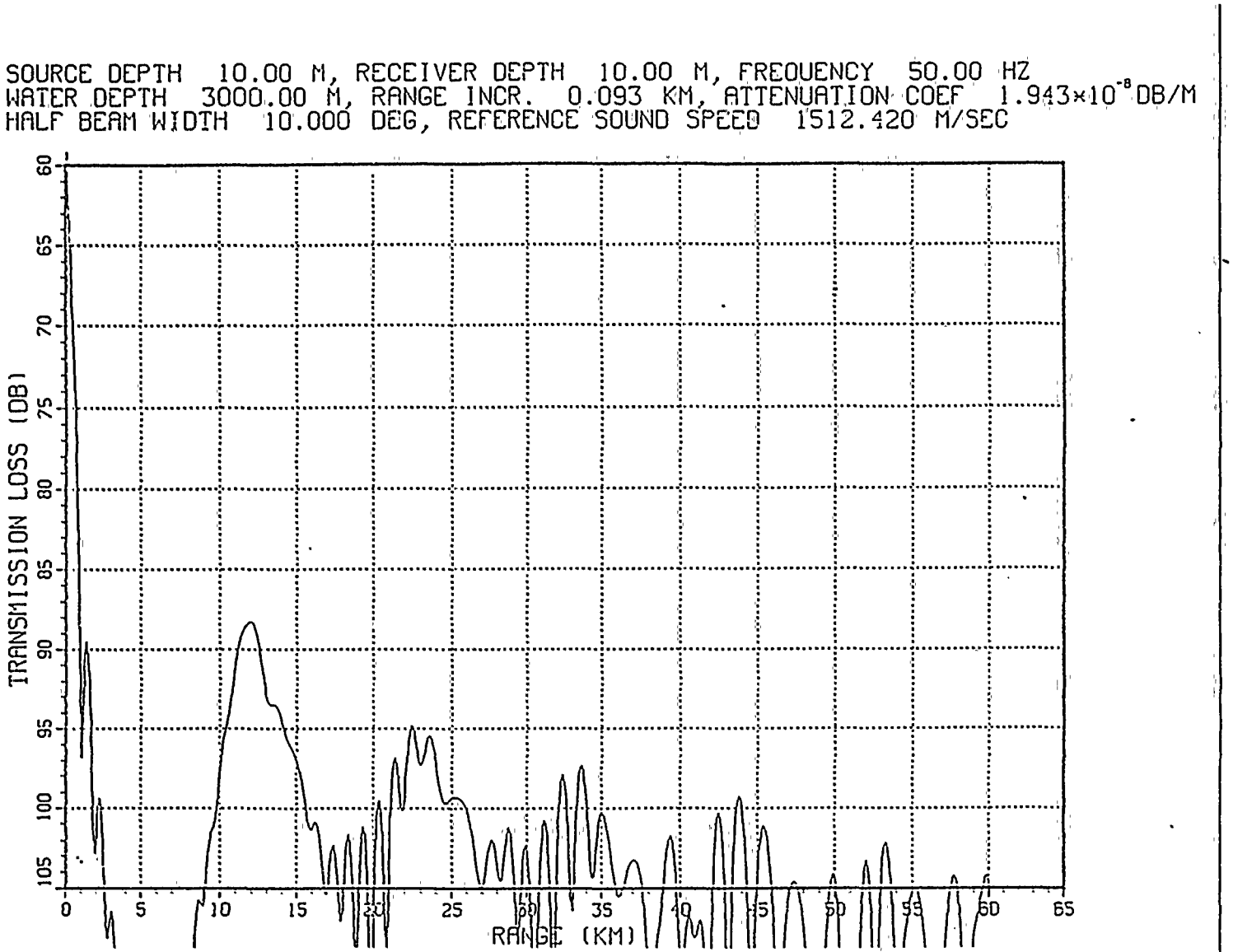

FIGURE A-19 TRANSMISSION LOSS ALONG PATH 4 IN SUMMER

SOURCE DEPTH 10.00 M, RECEIVER DEPTH 150.00 M, FREQUENCY 50.00 HZ
WATER DEPTH 3000.00 M, RANGE INCR. 0.093 KM, ATTENUATION COEF 1.943×10^{-8} DB/M
HALF BEAM WIDTH 10.000 DEG, REFERENCE SOUND SPEED 1512.420 M/SEC

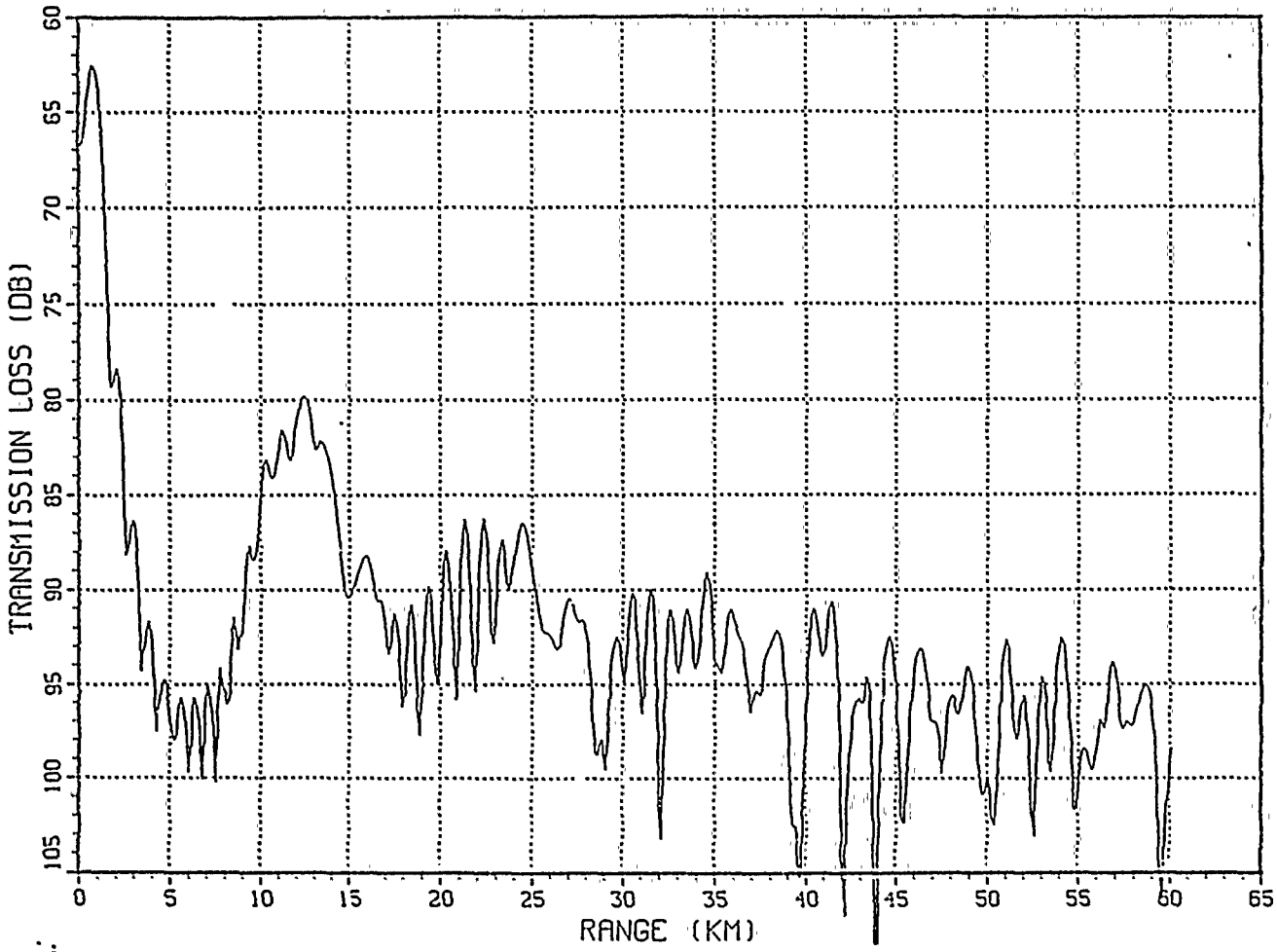

FIGURE A-20 TRANSMISSION LOSS ALONG PATH 4 IN SUMMER

LIST OF REFERENCES

1. J.P. Bethoux, *Budgets of the Mediterranean Sea. Their dependence on the local climate and on characteristics of the Atlantic waters,* Oceanologica Acta, Volume 2-2, p. 157-163, 1979.

2. J.P. Bethoux, *Mean water fluxes across sections in the Mediterranean Sea, evaluated on the basis of water and salt budgets and of observed salinities,* Oceanologica Acta, Volume 3-1, p.79-888, 1980.

3. M.A Biot, *Mechanics of deformation and acoustic propagation in porous media,* J.Appl. Phys. 33, p.1482-1498, 1962.

4. H.L. Bryden, H.M. Stommel, *Origin of the Mediterranean outflow,* J. Mar. Res., Supplement, p. 55-70, 1982.

5. J.Chen and I.J. Millero, *Sound speed in seawater,* J. Acoust.Soc.Am. 62, p.1129-1135, 1977.

6. A.Coppens, *An introduction to the parabolic equation for acoustic propagation* , Naval Postgraduate Shool, 1982.

7. A. H. El-Gindy and S. H. Sharaf El-Din, *Water masses and circulation patterns in the deep layer of the Eastern Mediterranean,* Oceanologica Acta, Volume 9-3, p. 239-248, Jul-Sep 1986.

8. R. Frasseto, *A study of the turbulent flow and character of the water masses over the Sicilian ridge in both summer and winter,* p. 9-10, SACLANTCEN TM-93, 1965.

9. E.L. Hamilton, *Prediction of in situ acoustics and elastic properties of marine sediments* , Geophysics 36, p.266-284, 1971.

10. E.L Hamilton, *Geoacoustic models of the sea floor* , Physics of Sound in Marine Sediments, p.181-221, Plenum, NY 1974.

11. F.D. Tappert and R.H. Hardin, *Applications of the Split Step Fourier method to the numerical solution on nonlinear and variable coefficient wave equations,* SIAM Review 15, p.423, 1973.

12. Hydrographic Service of the Hellenic Navy, Chart No 022 *Ionian Sea - Northern part,* 1982.

13. Hydrographic Service of the Hellenic Navy, Chart No 030 *South Ionian Sea,* 1988a.

14. Hydrographic Service of the Hellenic Navy, Chart No 065 *Ionian Sea,* 1983.

15. Hydrographic Service of the Hellenic Navy, *Pilot of the Hellenic Seas,* Volume A, p. 5-9 and 20-78, Athens, 1979.

16. Hydrographic Service of the Hellenic Navy, RESTRICTED Letter F:303/75/88 to Lt Rad. Fountoulakis, Subj. Station Data, 15 November 1988b.

17. Hydrographic Service of the Hellenic Navy. CONFIDENTIAL Letter F:334/19/89 to Lt Rad. Fountoulakis H.N., Subject: *Thesis at NPS,* 8 Aug 1989.

18. O.M. Johannessen, F. Strobel and C. Gehin *Observation of an oceanic frontal system east of Malta in May 1971,* Technical Memorandum No 169, SACLANTCEN 1971.

19. A.C. Kibblewhite, *Attenuation of sound in marine sediments : A review with emphasis on new low-frequency data,* J.Acoust.Soc.Am., 86, p.716-738, 1989.

20. L.A. Kinsler, A.R. Frey, A.B. Coppens, J.V. Sanders *Fundamentals of Acoustics* , 3rd edition, John Wiley & Sons, 1984.

21. H.Lacombe, P.Tchernia and G.Benoist *Contribution of Atlantic water in the Aegean Sea, seasonal and annually* , p. 454-468, Bull Inf. COECX 10, 1958.

22. H. Lacombe, P. Tchernia, *Quelques traits generaux de l'hydrologie Mediterranee,* in the Mediterranean : a natural Sedimentation Laboratory, edited by D.J. Stanley and others, Strodsburg, PA, 1960.

23. H. Lacombe, C. Richez, "The regimes of the straits of Gibraltar", in *Hydrodynamics of Semi- enclosed Seas,* p. 13-74, Amsterdam, 1982.

24. D. Lee and J.S. Papadakis, *Numerical solutions of underwater acoustic wave propagation problems* , NUSC technical report 5929, 1979.

25. D. Lee, G. Botseas and J.S. Papadakis *Finite- difference solution to the parabolic wave equation* , J. Acoust.Soc. Am. 70, p.795-800, 1981.

26. P. Malanotte-Rizzoli, A. Hecht, *Large scale properties of the Eastern Med: a review,* Oceanologica Acta ,volume 11-4, p.323-335, Oct-Dec 1988.

27. P. Malanotte-Rizzoli, P. Bergamasco, *Modeling of the circulation of the Eastern Med* , Part I, submitted to Oceanol. Acta, 1988.

28. Maury Center for Ocean Science, *Mediterranean Environmental Acoustic Summary,* Long Range Acoustic Propagation Project, Report 104, (CONFIDENTIAL), 1974.

29. R.C. Medeiros, *RAYMODE, Passive Propagation Loss Program,* New England Technical Services, p. 1 to 14, 15 July 1982.

30. R.C. Medeiros, *A Simplified Overview of the RAYMODE,* New England Technical Services, p. 2-18, 1 November 1985.

31. L.V. Moskalenko, *Steady-state wind- driven currents in the eastern half of the Mediterranean,* Oceanology, p. 494-496, 1974.

32. J. N. Nielsen, *Hydrography of the Mediterranean and adjacent waters,* Rep. Dan. Oceanogr. Expedition 1908-1910, 1912.

33. National Oceanographic Data Center, Letter to Rad. Fountoulakis, *Subj. Station Data,* 18 August 89.

34. NUSC, *Program Performance Specification for the 1985 baseline RAYMODE computer program,* NUSC, p. 1-1 to 3-14 and 3-100 to 3-240, May 1987.

35. I.M. Ovchinnikov, *The second (Mediterranean) trip of R/V Prof. Bogorov* , Oceanology Volume 18, p.165-168, 1978.

36. G.L. Pickard, W.J. Emery. *Descriptive Physical Oceanography,* 4th edition p.164-168. Pergamon, 1982.

37. E.M. Podeszwa, *Sound Speed Profiles for the Mediterranean,* NUSC, p.1-14 and 29-42, 1980.

38. M.J. Pollack, *The sources of deep water of the Eastern Mediterranean,* J. Mar. Res., Volume 10-1, p.128-152, 1951.

39. I.S. Robinson, *Satellite Oceanography* , p.240- 242, Halsted press, 1985.

40. W. Roether and others, *Transient tracer studies of the thermocline circulation of the Mediterranean,* MS for Mediterranean circulation, NATO Workshop, p.44, 1983.

41. R.D Stoll, *Theoretical aspects of sound transmission in sediments,* J.Acoust.Soc. Am., 68, p.1341-1350, 1980.

42. UNESCO Reports in Marine Science, *POEM : an overview and research plan* , Report No 30, p.16, 1984.

43. UNESCO Reports in Marine Science, *POEM, a research programme,* Report No 35, p.67, 1985.

44. UNESCO Reports in Marine Science, *POEM, Initial Results* , Report No 44, p.92, 1986.

45. R.J. Urick, *Principles of Underwater Sound* 3rd edition, McGraw-Hill, NY 1983.

46. U.S. Hydrographic Office, *ASW prediction areas* , Naval Warfare Planning Chart Base (NWPCB), NA8 p.2401, 1972.

47. G. Wust, *On the vertical circulation of the Mediterranean Sea,* J.Geophys. Res, p. 3261-3271, 1961.

48. Telephone conversations between D.W Collins, Oceanogr. Services Branch, NODC and the author, of 8/1, 8/2 and 8/4/89.

INITIAL DISTRIBUTION LIST

		No. Copies
1.	Defense Technical Information Center Cameron Station Alexandria, VA 22304-6145	2
2.	Library, Code 52 Naval Postgraduate School Monterey, CA 93943-5002	2
3.	Professor Robert H. Bourke Naval Postgraduate School, Code OCBf Monterey, CA 93943	1
4.	Professor Alan B. Coppens Naval Postgraduate School, Code PHCz Monterey, CA 93943	2
5.	Embassy of Greece Naval Attache 2228 Massachusetts Av., N.W. Washington D.C. 20008	2
6.	Lieutenant R. Fountoulakis Grigoriou Lampraki 15 18120 Kordalos, Athens Greece	2